Technical Report 1355
June 1990

Exploratory Evaluation of Alumina Ceramic Housings for Deep Submergence Service Fourth Generation Housings

J. D. Stachiw

NAVAL OCEAN SYSTEMS CENTER
San Diego, California 92152–5000

J. D. FONTANA, CAPT, USN
Commander

R. M. HILLYER
Technical Director

ADMINISTRATIVE INFORMATION

JG

SUMMARY

PROBLEM REQUIRING SOLUTION

Unmanned vehicles operating at depths in excess of 10,000 feet require for the optimization of their performance parameters (i.e., speed, range, payload, maneuverability) pressure hulls with a low weight-to-displacement ratio, preferably less than 0.5. Such low weight-to-displacement ratios cannot be achieved with metallic pressure hulls because of their low specific strengths (i.e., compressive strength/specific gravity). Other materials must be selected for this purpose (figure 1).*

SOLUTION

Aluminum oxide ceramics possess specific strength in the $82 \times 10^3 - 139 \times 10^3$ psi range, which is adequate for achieving a ≤ 0.5 weight-to-displacement ratio in pressure hulls fabricated from that material. The intrinsic cost of the material is low (less than $0.2/pound). The material is nonmagnetic, impervious to water, inert in seawater, a good conductor of heat, and possesses a high modulus of elasticity. Its major drawback is brittleness, which results in low point impact resistance. There appears to be also a limitation in the maximum size that can be fabricated by the present manufacturing process.

The fabrication process limitation for cylinders appears to be around 100 inches in diameter, but up to the initiation of this program the largest pressure housings fabricated were only 12 inches in diameter. The basic question that needed answering, however, was whether the physical properties of alumina ceramic decreased with an increase in wall thickness of pressure housing, as it is the case with metallic housings.

APPROACH

An experimental approach was chosen as a solution to the problem. A series of 20-inch-diameter, 94-percent composition alumina ceramic cylinders and hemispheres, patterned after the previously tested 6- and 12-inch housings, were to be fabricated, instrumented with strain gages, and pressure-tested. If the structural performance of the 20-inch housings was found to be identical to that of 6- and 12-inch housings, it could be postulated that the structural properties of 94-percent alumina ceramic are independent of the structures' dimensions (figure 2).

A total of three 20-inch OD $\times$ 18.64-inch ID $\times$ 30-inch L cylinders and two 19.66-inch OD $\times$ 18.98-inch ID hemispheres were fabricated by Coors Ceramic. The associated metallic components in the form of joint rings, stiffeners, and penetration inserts were machined from Ti-6 Aℓ-4 V alloy. In addition, a series of handling and test fixtures were fabricated in aluminum for the handling of the individual ceramic components and of the assembled housings during pressure testing. Polyurethane jackets protected the ceramic components against point impacts during assembly and handling of the housings.

The testing of the housing took place in the 30-inch-diameter pressure vessel of the Southwest Research Institute. Testing was first performed on individual cylinders capped by hemispheres and, subsequently, on assemblies made up of two cylinders joined by a ring stiffener and closed off at the ends with hemispheres. Testing consisted of pressurizing each cylinder test assembly once to the test

---

* Figures and tables are placed at the end of the text.

i

pressure of 10,000 psi, followed by 10 pressurizations to design pressure of 9,000 psi. The two-cylinder test assembly was subjected once to test pressure, followed by 100 pressurizations to design pressure. Strains were recorded during the testing.

CONCLUSION

The 94-percent alumina, 20-inch-diameter ceramic pressure housings performed structurally under external pressure in the same manner as the 4-, 6-, and 12-inch pressure housings tested at NOSC in prior year (Stachiw, 1964, 1968, 1984; Stachiw and Snyder, 1965). This indicates that small alumina ceramic housings can be scaled up to large dimensions without a noticeable decrease in physical properties. Based on this finding, one can expect that even very large alumina ceramic pressure housing will provide the unmanned vehicles with a 0.5 weight-to-displacement ratio.

The joint on 20-inch-diameter ceramic cylinders, using epoxy adhesive as a bearing gasket, performs reliably for a minimum of 50 pressure cycles to a 9,000-psi design depth before some debonding and spalling of ceramic bearing surfaces takes place. A redesigned joint with larger radial bearing surface can withstand a minimum of 250 pressure cycles to design depth.

It appears then that the only limit to the use of ceramic pressure hulls is the imagination of the designer and capability of the ceramic industry to produce large ceramic components. In 1989, it appeared that the ceramic fabricators were able to produce 94-percent alumina ceramic pressure hull sections *routinely* to 20 inches in diameter and 20 inches in length and, on a *experimental* basis, to 50 inches in diameter and 20 inches in length. This size could be further extended by funding research and development programs at major U.S. ceramic fabricators.

RECOMMENDATION

Alumina ceramic of 94-percent composition should be seriously considered for construction of cylindrical and spherical pressure housings in the 4- to 50-inch-diameter range with a 0.5 weight-to-displacement ratio for deep submergence service. At the present time, a safety factor of 2 based on compressive strength of material and elastic instability of the structural shape is considered adequate for alumina pressure housings with a 20,000-feet design depth. The safety factor can be decreased to 1.5 for pressure housings in noncritical application (i.e., implosion of housing will not result in loss of life). Because of the lower safety factor, the weight-to-displacement ratio of such housings will decrease to 0.375.

Further work should to be done to increase the structural fatigue life of mechanical joints between ceramic components of the housings to a minimum of 1000 dives to design depth. It appears that this can be accomplished economically by optimizing the existing design in which epoxy resin serves as the bearing gasket material between the ceramic components and metal joint rings.

CONTENTS

FIGURES

FIGURES (continued)

FIGURES (continued)

FIGURES (continued)

FIGURES (continued)

FIGURES (continued)

TABLES

INTRODUCTION

All remotely operated vehicles (ROVs) for undersea operation require pressure-resistant housings that protect the electrical equipment aboard the vehicle from contact with seawater. These housings not only must be watertight, but also pressure resistant. These objectives are easy to achieve as long as the housing is not required also to provide positive buoyancy for the vehicle (i.e., keep the vehicle afloat) at depths in excess of 10,000 feet. To achieve this requires pressure housings with a weight-to-displacement ratio of at least 0.5, otherwise, the vehicle will be severely limited in its performance (i.e., its speed and operational range will be restricted).

If pressure housings are used whose weight-to-displacement ratios are above 0.5, additional buoyancy is provided by means of syntactic foam (glass microballoons imbedded in a plastic matrix) applied to the exterior of the pressure housing. The lightest available syntactic foam with a 20,000-foot depth service rating provides only 1 pound of buoyancy for each pound of foam. For this reason, the overall weight of the vehicle increases twice as fast as that of the pressure housing (i.e., for each additional pound of housing weight, the vehicle weight increases by 2 pounds). The added foam increases also the volume of the vehicle by about 54 cubic inches for each pound of buoyancy, which in turn increase its hydrodynamic drag. Thus, it appears to be very desirable from the operational view to minimize weight-to-displacement ratio of the pressure housings so that syntactic foam need not be added to the vehicle structure.

There are only three classes of structural materials from which pressure housings with 0.5 weight-to-displacement ratio are feasible for operation in the 0- to 20,000-foot depth range. These three classes of materials are fiber-reinforced plastic composites, ceramics, and glass (table 1, figure 1).* Experimental pressure housings have been built from these materials with different levels of success. This report addresses only ceramic pressure housings fabricated from alumina ceramic.

BACKGROUND DISCUSSION

Numerous experimental ceramic pressure housings have been fabricated from 99.5-percent alumina, 94-percent alumina, 99.5-beryllia, and 9606 Pyroceram. The housings were either of spherical or cylindrical shape, and their diameters varied from 2 to 16 inches. The successful ones were generally seamless spheres or single rib stiffened cylinders closed up with flat metallic bulkheads. The early ambitious attempt to assemble a long cylindrical pressure housing from several short cylinders joined by metallic joints failed due to excessive dimensional tolerances on flatness and angularity of bearing surfaces at the joints (Stachiw, 1964, 1968; Stachiw and Snyder, 1965).

Spurred by its interest in deep diving ROVs, the Naval Ocean Systems Center (NOSC) since 1980 has pursued a low-level exploratory development program of cylindrical pressure housings with a 20,000-foot depth capability. The objective of the program was to develop experimentally proven designs of ceramic housings that could serve as pressure housings for electrical equipment aboard ROVs. The program was to focus on techniques for construction of long, large-diameter ceramic housings from short monocoque cylinders, or rings, as this would *minimize* the fabrication cost and *maximize* the useful internal space for the payload. The NOSC ceramic housing program was conducted in three phases (figure 2).

---

* Figures and tables are placed at the end of the text.

1

NOSC CERAMIC HOUSING PROGRAM

FIRST PHASE

The *first phase* of the program used beryllia as construction material because of its excellent strength-to-weight ratio and heat transfer capability (Stachiw, 1984). However, beryllia was soon replaced by 99.5-percent and, subsequently, by 94-percent alumina, as the contemplated construction of large housings from beryllia appeared to be economically unacceptable. The designs of the cylinders and joining techniques were validated by fabricating and, subsequently, hydrostatic testing of 6-inch-diameter housings with L/D_0 ratios in the 1.5 to 6.0 range. End closures in each case served titanium hemispheres (Stachiw and Held, 1987).

The findings of the preliminary studies using *6-inch-diameter* scale models are (Stachiw, 1984, 1988) as follows:

1. Long monocoque cylinders of 94-percent alumina can be economically fabricated by assembling them from rings joined together by brazing. The structural performance of brazed monocoque cylinders is identical to that of monolithic cylinders.

2. Monocoque cylinders of 94-percent alumina ceramic with $t/D_0 = 0.034$ slenderness ratio and $t/D_0 = 1.5$ unsupported length ratio possess a short-term critical pressure of 17,000 psi and a cyclic fatigue life in excess of 1,000 pressure cycles at 9,000 psi. Maximum compressive stresses in ceramic and titanium were 137,000 and 100,000 at 10,000 psi proof-test pressure.

3. I-shaped ring stiffeners machined from 6 Aℓ-4 V titanium alloy or 7075-T6 aluminum alloy provide adequate radial support to the ends of monocoque ceramic cylinders to prevent buckling at design pressure.

4. Titanium hemispherical end closures provide adequate radial support to the ends of ceramic cylinders. The radial contraction of the titanium hemisphere matches rather well the contraction of the ceramic cylinder when the ratio between hoop stresses in ceramic cylinders and in the flanges on titanium hemispheres or I-ring joint stiffeners is approximately 2.67.

5. Unprotected ceramic bearing surfaces between adjoining cylinders, or hemispheres, will fret during pressurization of the housing assembly, causing the assembly to fail in less than 50 pressure cycles to design pressure of 9,000 psi.

6. The fretting of radial and plane bearing surfaces on the ceramic cylinder has been reduced by encasing the ends of cylinder in 6 Aℓ-4 V titanium, or 7075-T6 aluminum, alloy U-shaped caps filled with epoxy. The cyclic fatigue life of protected bearing surfaces on cylinders exceeds 1000 cycles at 9000-psi pressure, generating a bearing stress of 60,000-psi magnitude on the plane bearing surface.

7. The cyclic fatigue life of 6 Aℓ-4 V titanium alloy U-shaped caps, I-joint rings stiffeners, and hemispherical bulkheads exceeds 1,000 cycles at 9,000 psi pressure. The short-term critical pressure of titanium hemispheres is in the 11,250- to 12,000-psi range.

8. The lowest weight-to-displacement ratio achieved with a single 6-inch-diameter, 94-percent alumina cylinder equipped with titanium end closures and joint hardware was 0.55. This ratio decreased to 0.65 when three cylindrical sections were joined together with titanium joint stiffeners and closed off at the ends with titanium hemispheres.

Based on the findings of these preliminary studies with model scale 6-inch-diameter cylindrical housings, it appeared worthwhile to apply the validated designs to larger ceramic housings. If it could be shown that larger housings perform in the same structural manner as the model scale housing, the designers of ceramic housings would be less hesitant to scale up proven designs of model scale housings to functionally useful sizes.

SECOND PHASE

The second phase of the ceramic housing program at NOSC focused on ceramic housings with external diameters of 12 inches.

The *objectives* of this study were to show that model scale ceramic pressure housings can be scaled up directly without incurring any significant penalty in structural performance and that titanium hemispheres can be replaced with ceramic hemispheres incorporating penetrations.

The *scope* of the study was limited to a single diameter and design. The external diameter of housing chosen for this study was 12 inches, approximately twice the size of the model scale housing. A scale factor of 2 was considered to be sufficiently large to show the presence, or absence, of degradation in structural performance between the model scale and full scale ceramic housings.

The *test specimens* served four 94-percent alumina ceramic cylinders with 12-inch OD, 18-inch L, and 0.416-inch wall thickness, two titanium hemispherical end closures, two titanium joint rings, eight titanium end caps, four aluminum clamps, and four ceramic hemispherical end closures. The design of the ceramic end closures was not based on any model scale components, but on general structural considerations.

The findings of the studies using a *12-inch-diameter* test model are (Stachiw, 1988, 1990):

1. The short-term implosion pressure of 12-inch cylinders is in the same range as 6-inch cylinders with identical L/D_0 and t/D_0 ratios.

2. The short-term implosion pressure of ceramic hemispheres exceeds that of titanium hemispheres of equal weight.

3. Penetrations have been successfully incorporated into hemispheres, providing that a removable metallic insert with plastic bearing pad is introduced into the penetration to prevent direct contact between metallic bulkhead, connectors, and the ceramic surfaces of the hemisphere. Plastic bulkhead connectors can be mated directly with the ceramic hemisphere, eliminating the need for metallic inserts.

4. The number of penetrations that can be incorporated into the ceramic hemisphere is a function of penetration diameter and safe spacing between edges of penetrations. The hemispheres tested in this program had one, four, and five penetrations, whose diameters ranged from 2.0 to 2.25 inches.

5. The depth of the annular cavity in the metallic end caps for ceramic cylinders and hemispheres and the thickness of bond line between ceramic surfaces and metallic end caps are important factors in the cyclic fatigue life of bonded joints.

6. Split wedge bands provide a satisfactory approach to the joining of cylinders and hemispheres.

7. Cyclic fatigue fractures originate on the plane ceramic bearing surfaces of cylinders and hemispheres inside the metallic caps.

8. The cyclic fatigue life of 12-inch ceramic cylinders fitted with Mod 0 metallic end caps is an order of magnitude less than that of 6-inch cylinders (i.e., 50 versus 1,000 cycles). However,

3

there are insufficient data to determine whether the lower cyclic fatigue life is a function of end cap design or of scaled up wall thickness.

9. The ceramic shells of cylinders and spheres contained a small number of randomly distributed voids. The number of voids and their magnitude varied from one specimen to another. The largest void observed in one of the cylinders was a 0.095-inch diameter. These voids were not sufficiently large to initiate fractures during proof testing, or pressure cycling of the ceramic housings during which membrane stresses of 130,000- to 140,000-psi magnitude were generated. The data generated during testing of 12-inch ceramic cylinders and hemispheres were encouraging enough to warrant the initiation of the third phase of the ceramic housing program, which would focus on some of the issues not resolved or raised by the second phase of the program.

The issues that required further resolution were as follows:

1. Problems associated with fabrication of cylinders and hemispheres in operationally useful sizes.

2. Mounting of payload components.

3. Operational handling of cylindrical housings assembled from several cylindrical sections that cannot be lifted by hand due to their weight.

4. Protection of ceramic components against point impacts.

5. It is not known whether it was the increase in cross section, thicker bond line, or a too shallow end cap that caused cyclic fatigue cracks to initiate after approximately 50 pressure cycles.

It was thought that those issues could be resolved by fabrication and testing of ceramic housing components approximately twice as large in size as the 12-inch housings evaluated in phase 2 of the program. After investigating the size limitation of the existing isostatic pressing equipment at Coors Ceramic Corporation, 20 inches was selected as the diameter of the ceramic housings for evaluation in phase 3 of the ceramic housing program at NOSC. The diameter of the isostatic press would have allowed pressing cylinders of up to 24 inches in diameter, but the length of the press was insufficient to form cylinders longer than 30 inches. Since the 6- and 12-inch-diameter cylinders tested in phases 1 and 2 of the housing program were of 1.5 D_0 in length, the cylinders in phase 3 had to be 20 inches in diameter so the $L/D_0 = 1.5$ aspect ratio could be retained. Although the 20-inch diameter was less than the desired 24-inch size, it was close enough to the scale factor of 2 to be useful and it was chosen for phase 3 of the ceramic housing program.

STUDY OUTLINE

Phase 2 of the ceramic housing program focused on the design, fabrication, and evaluation of *20-inch-diameter ceramic housings*. All facets of the study were oriented towards making the ceramic pressure housings acceptable as the primary pressure hull of an inexpensive deep submergence diving system. This was particularly reflected in the design, fabrication, and assembly/handling procedures of the housing components prior to testing.

DESIGN

Ceramic Cylinders

The 20-inch-diameter ceramic cylinders were designed by scaling up the appropriate dimensions of the 12-inch-diameter cylinders. The were fabricated and tested in the second phase of the NOSC

ceramic housing program (Stachiw, 1990). There were several reasons for choosing this design approach. The most important one was to study further the effect of scaling up on the structural performance of ceramic components. Other reasons for selecting this monocoque design of the cylinder were the uniformity of the stress field, low fabrication cost, and conservative magnitude of design stresses at proof-test pressure.

The principal *design stresses* in the 20 OD $\times$ 18.63 in 1D $\times$ 30-inch-long ceramic cylinder (figures 3 and 4) were not to exceed 130,000 psi in the hoop and 65,000 psi in the axial orientation at 10,000 psi proof-test pressure. These are rather low values, and even the higher hoop stress represents a *nominal* safety factor of approximately 2.7. At first glance, this safety factor may appear to be too conservative for an unmanned vehicle application, as small, high-quality alumina ceramic pressure housings have been shown to tolerate compressive stresses of 300,000 psi under short-term pressurization.

Experience has shown, however, that to duplicate the same quality in large castings would require a quality assurance (QA) program patterned after aerospace industry. Such QA program would require absence of inclusions over 0.020 inch in diameter at the expense of doubling or tripling the fabrication cost. In effect, a stringent QA program would move the casting of ceramic housings from production practice for components used in the chemical industry (for example, crucibles, pipes, grinding balls, etc.) to production practices for components used in the aerospace industry (for example, missile noses, ablative shields, rocket nozzles, etc.). Since at the present time the ROV and autonomous underwater vehicle (AUV) programs that could benefit from the use of ceramic housings are not funded at the aerospace level, it was decided to keep the design stresses low and the QA programs to the minimum.

Because of the low design stresses, the ceramic components can tolerate much larger inclusions (for example, voids) than would be the case if the design stresses were above 150,000 psi. This supposition has been substantiated during pressure testing of 12-inch ceramic components in the second phase of the ceramic housing program at NOSC. There it was shown that, at design stress levels in the 130,000- to 150,000-psi stress range, the ceramic cylinders with 0.42-inch-thick walls can tolerate inclusions of 0.095-inch magnitude under sustained pressurizations without cracking at those locations (Stachiw, 1990). This is explained by the fact that with a safety factor of 2.7, based on the ultimate compressive strength of ceramics, the structure can contain stress risers with a stress concentration factor of 2 and still perform satisfactorily.

The *elastic stability* of the 20-inch cylinder was designed, like the 6- and 12-inch cylinders tested previously, to exceed the design test pressure by a factor of 1.8 (i.e., to implode by buckling at 18,000 psi). To attain this safety margin, the monocoque cylinders had to be of finite length and radially supported at the ends. For cylinders with $t/D_0 = 0.034$ ratio, the critical pressure of 18,000 psi required the radial supports to be spaced 1.5 D_0 apart (Stachiw, 1968). Thus, the length of 20-inch OD cylinders was chosen to be 30 inches. This length could be extended to 40 inches if the critical pressure due to buckling was reduced to just 12,500 psi, representing a safety factor or 1.38.

Ceramic Hemispheres

The 20-inch-diameter ceramic hemispheres were also designed by scaling up the 12-inch hemispheres used in phase 2 of the ceramic housing program (Stachiw, 1990). The two hemispheres fabricated for the 20-inch housings differed only in the number of penetrations (figures 5 through 12). Mod III hemisphere contained only one polar penetration with a 3.25-inch diameter, while Mod II contained four of them, equally spaced at 45 degrees latitude. The polar penetration was surrounded by a spot-faced plane surface while the four penetrations on Mod II sphere were without plane spot

5

faces. The Mod 0 and Mod 1 hemispheres are also scaled-up versions of the 12-inch hemispheres tested in phase 2 of the program (Stachiw, 1990).

The *design stresses* at 10,000-psi proof pressure in the hemispheres were in the same range as the design stresses in the 20-inch ceramic cylinders. To achieve this without adding substantially to the weight of the hemispheres, their thickness varied from 0.340 inch at the equator to 0.680 inch at the edges of penetrations. In this manner, the 100-percent increase in hoop stress associated with a penetration would be compensated for by a 100-percent increase in wall thickness at the penetration.

The *elastic stability* of the 20-inch diameter hemispheres exceeded the proof-test pressure of 10,000 psi by a factor of 5. Because of this outstanding elastic stability, it can serve as a radial support for the monocoque ceramic cylinder without any additional hoop stiffener at the joint.

End Caps

Both the ceramic cylinders and hemispheres were equipped with metallic end caps, whose purpose was to protect the plane and curved bearing surfaces from contacting directly the mating surfaces of adjoining ceramic, or metallic, components of the housings (figures 5 through 18).

For proper functioning, the metallic end cap was designed to be filled with epoxy resin and the end of the ceramic cylinder, or hemisphere, immersed in it until it came to rest upon the bottom of the cap. To prevent total displacement or resin from between the mating plane surfaces, 0.5 × 3.0 × 0.010-inch-thick cardboard spacers were placed at 3.5-inch intervals inside the cap prior to filling the cap with resin. The resin displaced by the ceramic poured over the edges of the cap and was, subsequently, wiped off.

To function properly, the cap has to fit snugly over the edge of the ceramic component so the thickness of the epoxy layer between the curved walls of the cap and the curved surfaces of the ceramic components is minimized. A thick layer would tend to displace under axial bearing stress of approximately 70,000-psi magnitude when the housing is pressurized to 10,000-psi proof pressure. Experience with end caps for 6-inch-diameter cylinders has shown (Stachiw and Held, 1987) that a 0.005-inch-thick epoxy layer in the annular spaces did not extrude even after several proof tests to 10,000 psi, and over 3,000 pressure cycles to 9,000-psi design pressure.

This kind of tight clearance was impossible to achieve with *standard* machine shop practices for components with 20-inch diameters and still insure interchangeability between components for all the cylinders. To retain interchangeability, without resorting to expensive model making fabrication procedures, the dimensional tolerances on end caps and ceramic components were relaxed to allow for the clearance to range from 0.01 to 0.03 inch. If after assembly the actual clearance was found to be ≥ 0.015 inch, a 0.010-inch-thick steel shim was inserted into the annular space between the surfaces of the ceramic component and the metallic end cap. A similar approach was used previously in the fitting of end caps on 12-inch ceramic cylinders.

The depth of the annular cavity in the end cap for 20-inch cylinders was only approximately 40 percent deeper than on caps for 6-inch cylinders and only 25 percent deeper than on caps for 12-inch cylinder built previously. Linear scaling was not applied to the depth of the caps as this was not thought to be necessary and, furthermore, linear scaling of this dimension would increase significantly the weight of the end caps.

The end caps for the ceramic hemispheres were patterned after the end caps for cylinders, except the depth of the annular cavity was somewhat greater to compensate for the greater annular clearance between the spherical ceramic surfaces and the cylindrical metallic surfaces (figures 17 and 18).

Penetrator Inserts

The penetrations in the ceramic hemispheres were protected by titanium inserts (figures 19 through 22). The function of the inserts was to protect the ceramic surfaces of the hemisphere at the penetration from point loading by a commercial metallic bulkhead penetrator with radial and axial O-ring seals. This was achieved by having the bulkhead penetrator thread into and seal against the metallic insert and not the ceramic surfaces of the hemisphere (figure 20). The insert in turn was designed not to exert high bearing pressures against the ceramic surfaces.

The *axial* contact between the metallic insert and the exterior surface of the ceramic hemisphere was eliminated by a cloth reinforced phenolic plastic pad that served as a bearing gasket and retainer for the facial O-ring seal (figure 20). The *radial* contact between the penetrator insert and the ceramic surface of the penetration was reduced to a minimum by providing a 0.002-inch clearance between the metallic insert and the ceramic edge of the opening. Because of this clearance, the radial bearing stress was totally eliminated at lower pressure and significantly reduced at design pressure when the metal penetrator finally contacted the ceramic surface. The closing up on the radial clearance at high pressures also kept the O-ring seal from extruding through the clearance between the insert and the hemisphere.

The maximum size of penetration incorporated into the ceramic hemispheres was 3.250 inches, which after placement of the penetration insert allowed mounting of commercial bulkhead penetrators with 2.5-inch diameters (figures 23 through 26). There was one penetration in hemisphere Mod III and four in hemisphere Mod II. Hemispheres Mod 0 and Mod 1 with five penetrations were designed (figure 13), but not fabricated or tested, although 12-inch hemispheres with five penetrations were fabricated and tested in phase I of the ceramic housing program (Stachiw, 1990). But even this does not represent the maximum number of penetrations that could be incorporated into a 20-inch ceramic hemisphere if the operational requirements called for it.

The number of penetrations that can be incorporated into a spherical shell is a function of the penetration diameter, the location of penetrations, and their spacing. A definitive answer to this question cannot be stated at this time; however, the following findings, experimentally validated, bearing upon this question are listed below:

1. The diameter of penetrations $\leq 0.165 D_0$.

2. The thickness of hemisphere at the edge of penetration $0.166 pD \times 10^{-5} \leq t \leq 0.33 pD \times 10^{-5}$.

3. The spacing between edges of adjacent penetrations $\geq$ diameter of larger penetration.

4. The center of penetration shall not be placed closer to the equator than 45° latitude.

Metallic penetrator inserts can be eliminated by using plastic bulkhead penetrators that seal directly against the ceramic surface of the hemisphere. Substitution of plastic bulkhead penetrators for metallic bulkhead penetrators and the subsequent elimination of metallic penetration inserts can reduce the weight of a 20-inch ceramic hemisphere assembly (equipment with five steel bulkhead penetrators and the associated titanium penetrators inserts) by 20 pounds. Since large-diameter plastic bulkhead penetrators are not available commercially, the use of plastic bulkhead penetrators would require the incorporation of many small penetrations into the ceramic hemispheres instead of a few ones, as in this test program. Although the drilling of more penetrations would increase the cost of the hemisphere substantially (approximately $1000/hole), the elimination of the few large metallic penetration inserts (approximately $2000 per insert) would recoup the cost of drilling the additional penetrations.

7

Joint Stiffeners

Joint stiffeners are structural components pioneered by NOSC for extending the overall length of a cylindrical monocoque ceramic housing without reducing its critical buckling pressure. A joint stiffener is best described as a removable ring stiffener inserted between two adjoining cylinders that simultaneously aligns and provides radial support to the ends of the cylinder (figures 27 through 30). To *maximize the stability*, while at the same time *minimizing the weight*, the joint stiffener has the cross section of the capital letter I.

The stiffener can be fabricated from any material that is readily available, easy to machine, economical, and exhibits good mechanical properties. In practice, this eliminates from consideration all materials except titanium and aluminum. Titanium is always chosen for housings that will be continuously submerged in seawater for long periods of time, while aluminum finds application in housings submerged in seawater only for short periods of time, followed by rinsing with tap water (figure 30).

To function properly, the design of the joint stiffener must satisfy two opposing structural objectives. On one hand, the design must *maximize the elastic stability* of the stiffener so it can provide the radial support to the end of the monocoque ceramic cylinder needed to raise its elastic stability to the specified critical pressure, which in this case was 18,000 psi. On the other hand, the design must *minimize* the radial stiffness of the stiffener so its radial compliance under radially applied loading approaches that of the ceramic monocoque cylinder. The closer one can match the radial compliance of the joint stiffener to that of the cylinder, the smaller the bending moment will be in the shell of the monocoque cylinder near the stiffener.

Both design objectives can be achieved in the design of a stiffener if the material selected for its fabrication has a Young's Modulus that is significantly smaller than of the cylinder. Both titanium and aluminum meet this requirement with their Young's Moduli of 16.4×10^7 psi and 10×10^6 psi respectively.

The joint ring stiffeners for the 20-inch cylinders were scaled-up versions of the stiffeners designed for the 6- and 12-inch cylinders and validated during the second phase of the NOSC ceramic housing program (Stachiw, 1990). The only major difference was the absence of lightening holes in the web of the stiffener. The function of these holes, besides reducing the weight of the stiffener by approximately 2 percent, is to serve as passageways for electrical cables and hydraulic lines joining electrical and hydraulic equipment components placed at different locations in the ceramic housing. Since the 20-inch ceramic housings tested in this study did not contain any functional electrical or hydraulic equipment, the joint stiffeners were not provided with any holes (figure 27), even though a stiffener design with lightening holes was also generated (figure 29).

Another joint stiffener design generated for the 20-inch cylinders, but not used, was the dry joint stiffener. It differed from the other (wet) joint stiffener design in that *none* of the stiffener surfaces was ever exposed to external pressure, or to axial bearing stresses (figure 31). Because of these two features, the joint stiffener can be machined from materials that are not resistant to seawater corrosion or whose compressive yield strength is ≈40,000 psi, as it does not have to withstand axial bearing stresses of 75,000 psi magnitude. This joint stiffener design was not used in this study for two reasons: it would require the re-design of end caps on cylinder, and it was not evaluated previously on 6- or 12-inch pressure housing, thus presenting a higher risk in application to 20-inch housings than the wet joint stiffener previously evaluated successfully on the 6- and 12-inch diameter housings.

INTERNAL ATTACHMENTS

All external pressure housings must be equipped with internal attachments for the mounting of payload components. In metallic housings, these attachments generally take the form of brackets

welded to the internal surface of the cylinder, or to the internal diameter of the ring stiffeners. In plastic or fiber-reinforced plastic housings, the mounting brackets are generally bonded to the interior surface of the cylinder.

The same approach could have been applied to ceramic housings by bonding the metallic brackets to the internal surface of the monocoque ceramic cylinder with elastomeric adhesive that would compensate for the larger difference in strains between the metallic bracket and the ceramic cylinder at design depth. This approach was, however, discarded because of the propensity of elastomeric adhesive to fail under relatively low tensile or shear stresses applied for long periods of time by dead weight of the payload components, regardless of whether the housing was in storage or on a submerged operational vehicle.

The approach chosen for mounting the payload components inside the ceramic cylinders was to bolt eight metallic channels to the metallic end caps on both ends of the cylinder and to use them subsequently as rails on which shelves with payload components could slide in or out as desired (figures 32 and 33). One very attractive feature of this approach for mounting of payload components inside the cylinder was that the metallic channels also served as pretensioned mechanical tie rods holding both end caps together. This feature was particularly attractive, as it relieved the epoxy bonds between the end caps and the ceramic cylinder from tensile stresses generated by lifting the cylinder during assembly and handling of the housing. By judicious pretensioning of the channels the whole ceramic cylinder could be precompressed, so that during lifting of the housing, the ceramic would not be exposed to any tensile strains.

The channels in 20-inch cylinders were fabricated from 6061-T6 aluminum to minimize their weight and cost. Their weight, however, could be further reduced if instead of aluminum they were fabricated from a magnesium or beryllium alloy; however, their cost would increase significantly. One further reduction in weight could be achieved by eliminating one set of rails and using only three instead of four sets of rails. A 0.125-inch-thick strip of neoprene was placed between the rails and cylinder to preclude any contact between the metallic rails and the ceramic cylinder during radial contraction of the cylinder under external pressure loading. The use of rails for mounting the cage with payload components inside the cylinder is not new, it was used previously on cylindrical housings fabricated from either plastic or metallic materials. Its most recent application was in the Advanced Unmanned Deep-Ocean Search System (AAUS) vehicle hull where the rails were used for supporting a cage-like frame work inside the 30.75-inch OD $\times$ 25.75-inch ID $\times$ 65.0-inch L carbon fiber reinforced plastic hull, to which all the payload components were fastened (Stachiw and Frame, 1988). The operational advantages for such an arrangement are obvious: by mounting all the payload components to a movable cage the mounting and replacement of these components was significantly simplified.

SHELVES FOR PAYLOAD COMPONENTS

The shelves for mounting payload components were fabricated from aluminum honeycomb panels arranged in a cruciform configuration. Each of the shelves was supported at one edge by the rail and on the other side by the other shelves (figures 36 and 37). To simulate payload components, 18.75 $\times$ 5 $\times$ 2 inch aluminum blocks weighing 18.5 pounds were bolted on each side of the shelves. The shelves themselves were bolted to the rails to prevent sliding during handling of the housing (figures 38 and 39).

The cruciform shelves do not act as stiffeners for the ceramic shell, since the long slender rails to which the shelves are mounted can deflect over 0.050 inch without applying any significant radial loading to the ceramic shell by the compressed neoprene gasket underneath the rails.

9

WEDGE CLAMPS

The cylindrical and hemispherical shell assemblies (figures 34 and 23) were fastened together by metallic wedge clamps (figures 40 and 41). These wedge clamps were scaled-up versions of the wedge clamp evaluated previously on 12-inch diameter housings. The wedge clamps were fabricated from 6 Al-4 V titanium alloy to resist corrosion and to withstand stresses generated in them during lifting of housing assemblies composed of three or more cylindrical shells. Significant weight savings could have been achieved if the wedge clamps were molded from plastic composite instead of being machined from metal. This option was not exploited because of the high tooling cost associated with molding the composite wedge clamps. Composite wedge clamps are cost-effective only if a large production run is being considered.

JACKETS

Although the alumina ceramic from which the cylindrical and spherical shells are fabricated can withstand a point impact of at least a 50-pound-inch magnitude, steps were taken to improve its impact resistance by covering the exterior surfaces of ceramic shells with elastomeric jackets. Neoprene and polyether urethane sheets with 65A hardness and 0.375-inch thickness were used for construction of jackets. Both the hardness and thickness of these jackets were thought to be adequate for protection of the ceramic shells against impacts they may encounter in industrial environment during handling associated with assembly, lifting, and pressure testing of the ceramic housing assembly.

The jackets for cylindrical shells were molded as seamless tubes from polyether urethane (figures 42 and 43). These tubes were later slipped over the ceramic cylinders and were held in place by the metallic end caps bonded to the end of cylinders. The jackets for spherical shells were fabricated from pre-cut neoprene segments bonded with rubber contact cement to the ceramic surfaces (figures 44 through 45).

INSTRUMENTATION

All ceramic cylinders and hemispheres were instrumented with electric resistance strain gages Type M&M CEA-06-125WT-350. They were bonded to ceramic surfaces with methyl cyanoacrylate cement at locations where peak stresses were expected. As instrumentation leads, served vinyl-insulated flat cables Type Micro Measurements Division 426 DFV with four stranded copper conductors. After soldering the conductors to copper tabs on each strain gage, were waterproofed with the polysulphide compound (figure 46). The other end of the instrumentation cable was terminated with a multipin plug for rapid plugging and unplugging with the bulkhead penetrator. A neoprene-jacketed, 40-conductor cable, in turn, plugged at one end into the bulkhead penetrator on the ceramic hemisphere and, at the other end, plugged into an identical bulkhead penetrator on the pressure vessel end closure (figure 47). The bulkhead penetrator in the pressure vessel and closure was, in turn, connected by a cable to a computer-controlled strain recording unit. The strain data were recorded during the pressure testing on a magnetic disc from which it was later retreived in digital and graphic format.

TEST SETUP

All the testing was performed on two 20-inch-diameter ceramic cylinders and two 20-inch-diameter hemispheres equipped with appropriate end caps, penetration inserts, joint stiffener, and wedge clamp bands. These components were assembled into the following test configuration:

Test Assembly A

    Cylinder 1 capped at both ends with ceramic hemispheres Mods II and III (figure 48).

Test Assembly B

    Cylinder 2 capped at both ends with ceramic hemispheres Mods II and III.

Test Assembly C

    Cylinders 1 and 2 joined with titanium joint stiffener and capped at the ends with ceramic hemispheres Mod II and III (figure 49).

Test Assemblies A and B were put together by lifting manually each hemisphere and fitting them into the ends of a cylinder resting in a cradle (figures 50 and 51). After assembly, two nylon slings were placed around the cylinder and attached to a short strongback fabricated for this purpose (figure 52). The test assembly was then lifted by an overhead crane and transported into the immediate vicinity of the pressure vessel, where it was placed horizontally on a cushioned pad on the concrete floor (figures 53 and 54).

The next step was the placement of the upper cage fixture over the test assembly (figure 55). Once the upper cage fixture was securely positioned over the test assembly, the pneumatic radial actuators located inside the flanges in the fixture were inflated, gripping securely the housing assembly along its whole length. Once the housing assembly was securely gripped by the pneumatic actuators, it could be lifted from the ground and placed on the lower half cage fixture (figure 56). After bolting the lower cage fixture to the upper cage fixture, the whole cage could be rotated to a vertical position and the air supply to the pneumatic actuators could be disconnected (figure 57). The cage could be lowered then into the pressure vessel, and the instrumentation cable could be connected to the bulkhead penetrator in the pressure vessel end closure (figure 59).

Test Assembly C was assembled from two cylinders, two hemispheres, and a joint stiffener. The assembly procedure consisted of taking two cylinders (figure 60), placing them on skids located on a roller conveyor, inserting the appropriate ballast into each cylinder, closing off each cylinder with hemisphere, and joining them with a joint stiffener (figures 61 and 62). The joining of cylinders was facilitated by rollers underneath the skids, which allowed the cylinders to be moved readily toward each other.

The completed assembly then was lifted with four nylon straps attached to a strongback (figure 63) and was placed in the lower half of the cage fixture. After the upper half of the cage fixture was lowered over the housing assembly and bolted to the lower half of the cage fixture (figure 64), the whole cage fixture was lifted by crane and moved to the pressure vessel test area (figure 65). At the vessel, the cage fixture was rotated into a vertical position and lowered into the vessel (figure 66). Attachment of the instrumentation cable to the vessel end closure completed the preparation of the housing assembly for pressure testing.

PRESSURE TESTING

Pressure testing consisted of individually pressurizing Test Assemblies A, B, and C repeatedly with tap water at 600- to 1,000-psi/minute rate to the desired maximum pressures.

The pressurization schedule for each test assembly consisted of a single pressurization to *design test pressure* of 10,000 psi followed by 10 pressurizations to *design pressure* of 9,000 psi. During the pressurization to design test pressure, strain readings were recorded at 1,000-psi intervals. After the 10 pressure cycles to design pressure, the test assemblies were taken apart and inspected for damage.

11

Test Assembly C was subsequently subjected to an additional 100 pressure cycles to design pressure. Since Test Assembly C was made up of cylinders and hemispheres that previously constituted Assemblies A and B, the total number of pressurizations to which each housing component was subjected would differ:

Hemispheres 1 and 2
    3 pressurizations to 10,000 psi
    120 pressurizations to 9,000 psi

Cylinders 1 and 2
    2 pressurizations to 10,000 psi
    110 pressurizations to 9,000 psi

TEST OBSERVATIONS

ASSEMBLY OF HOUSINGS

The ceramic pressure housings were assembled without any particular difficulty as the radial clearances between mating components were in the 0.002- to −0.005-inch range. Two observations, however, were made that should to be implemented before larger ceramic housings are fabricated and assembled for testing. These observations are as follows:

1. The mating of housing components during assembly requires a set of level, parallel rails supporting movable dollies equipped with precise level adjustments.

2. The hemispherical bulkhead must be mounted either into a cylindrical fairing prior to placement onto the dolly, or the dolly itself must be equipped with a special fixture that holds the hemisphere with its axis of revolution in horizontal position.

Some minor difficulties were encountered during disassembly of the housings after pressure testing. The difficulties consisted of sticking between mating titanium parts that had to be overcome by pulling apart the dollies on which the mating housing components rested. Based on this observation, the following action should be taken:

Fixtures should be incorporated into the dollies for attachments of hydraulic actuators that would be used to move the dollies along on the rails during mating or separation of cylinders from hemispheres and the central joint stiffener.

HANDLING OF HOUSINGS

The cage-like fixture (appendix A) used for handling assembled housings performed satisfactorily. Some permanent deformation of the cage took place when the pneumatic pressure inside the air-operated, inflatable actuators exceeded 40 psi. Based on this observation, the pneumatic pressure applied to the inflatable actuators should not exceed 20 psi, unless the cage fixture described in appendix A is substantially reinforced.

The mechanically fastened cage closure has been found to be absolutely necessary for holding the housing assembly in place during the removal of the cage from the pressure vessel after pressure testing. During pressure testing, the pneumatically operated inflatable actuators became deflated, and

without the mechanically fastened cage closure, the ceramic housing assembly would have fallen out of the cage into the pressure vessel interior.

TESTING OF HOUSINGS

The two housing assemblies, made up of a single cylinder and two hemispheres, successfully withstood a single proof-test to 10,000 psi and 10 pressure cycles to design pressure of 9,000 psi. After this series of tests, the housing assemblies were disassembled and visually inspected for cracks. The inspection did not reveal any cracks in the two cylinders or hemispherical end closures.

Upon completion of this preliminary series of tests, the two cylinders and hemispheres were mated together to form a long housing. This housing successfully withstood a single proof-test to 10,000 psi and 10 pressure cycles to design pressure of 9,000 psi. After this series of tests, the housing was disassembled and visually inspected for cracks. The inspection did not reveal any cracks in the two cylinders and hemispheres.

Upon completion of this inspection, the two cylinders and hemispherical closures were reassembled into a long housing and pressure-cycled to design pressure of 9,000 psi. The pressure cycling was terminated by implosion during the 100th pressure cycle.

Inspection of ceramic fragments and deformed metallic components revealed there were many origins of fractures, one of them triggering the implosion (figures 67 through 72). All of the fractures originated on the plane bearing surfaces of the ceramic cylinders, inside the metallic end caps. These fractures propagated into the body of the cylinder at a right angle to the plane bearing surface. These fractures penetrated through the exterior surface of the cylinder approximately 2 to 3 inches away from the end. Upon breaking through the cylindrical surface, the resulting sliver of ceramic would separate from the cylinder. When the thickness of the cylinder decreased to the point where the stresses in the cylinder exceeded the compressive strength of the ceramic catastrophic, failure took place.

Inspection of the ceramic fragments still retained by the metallic end caps disclosed that significant extrusion of the epoxy adhesive had taken place from inside the annular space between the exterior surface of the ceramic cylinder and the metallic end cap. It is not known at what point during pressure cycling the extrusion originated; it is only certain that the appearance of extrusion either preceded, or coincided, with the appearance of spalling. This statement is supported by observations made during pressure testing of 12-inch pressure housings in phase 2 of the ceramic housing program (Stachiw, 1990). In those tests, the epoxy adhesive began to extrude several pressure cycles prior to the appearance of spalling (figure 73), which in turn was preceded by at least a 50- to 100-cycle catastrophic failure.

STRAINS

The strains generated in ceramic components by pressure testing were linear from 0 to 10,000 psi pressure loading (tables 3, 4, and 5, figures 74 through 81) and were identical in character and magnitude to those previously observed during pressure testing of the 12-inch-diameter ceramic housings (Stachiw, 1990). In cylinders, all strains were compressive, and the magnitude of hoop and axial strains varied with the distance from the ends. Maximum hoop and axial strains were recorded at midbay; their magnitude at midbay was approximately 3 percent higher than at the ends for hoop strains and 19 percent higher for axial strains. The rather large difference in the magnitude of axial strains indicated that significant bending of the shell took place at the ends of the cylinders due to the difference in radial compliance between the cylinder providing radial support to the ends of the cylinder and the hemispheres.

13

In ceramic hemispheres on Mod II and Mod III, all strains were compressive. The hoop strains at the joint were about 12 percent lower than the hoop strains on the ends of cylinders, confirming the previous observation that the radial compliance of the hemispheres was somewhat less than of the cylinders. The highest strains on the Mod II hemisphere were observed at the apex, and the lowest strains at the center of the reinforcing pad. On hemisphere Mod III, the highest strain was in hoop direction at the base of the pad around the penetration, and the lowest strain was in the axial direction at the same location, indicating that significant bending of the shell was occurring at that location.

The strains on the titanium stiffener (table 6, figures 82 through 84) were also linear from 0- to 10,000-psi external pressure loading, indicating that the stiffener was elastically stable at that pressure and the material was within the elastic range of deformation.

STRESSES

The magnitude and character of stresses were identical to those observed on 12-inch-diameter ceramic housings during pressure testing in phase 2 of the this program (Stachiw, 1990). The stresses were all negative (tables 7, 8, and 9; figures 85 through 92) and of magnitude predicted by the finite element analysis performed previously for the 12-inch housings. The range of stresses found in the cylinder at 10,000-psi external pressure loading was –125,370 to –137,143 psi in the hoop and –55,181 to –68,323 psi in the axial direction. In the hemispheres, the range of stresses was –84,633 psi to –157,473 psi for Mod II and –94,670 to –140,708 psi for Mod III.

The magnitude of stresses in the titanium stiffener (table 10, figures 93 through 95) did not exceed 30 percent of the materials' yield strength. The highest recorded compressive stress of –40,000 psi at proof-test pressure was in the web of the stiffener. Actually, the highest compressive stress was applied to the lip of the stiffener by adjoining end caps on cylinders. Its magnitude has been calculated to be in the range of –60,000 to –70,000 psi.

DISCUSSION OF TEST OBSERVATIONS

STRESSES

The wide range of stresses in the ceramic hemispheres indicates that the design is not optimized and that significant weight savings can be achieved by redesigning the buildup of material around penetrations so that all stresses are in the –145,000- to –155,000-psi range when the housing is pressurized to 10,000 psi. The thickness of the cylinders can be reduced by approximately 15 percent to raise the magnitude of stresses to the same range of values. By doing this, the *actual* safety factor for material failure would be brought in line with the *design* safety factor of 2.

The reduction in thickness would reduce the calculated elastic buckling critical pressure of cylinders from 18,000 to 13,500 psi, thus decreasing the design safety factor for buckling from 2 to 1.5. The reduced value of the safety factor for buckling of the cylinder is acceptable, however. The monocoque configuration of the cylinder with less than 0.1 percent deviation from ideal curvature and perfectly elastic nature of the ceramic make the calculated and experimental values of critical pressure at which buckling occurs differ by less than 5 percent.

CYCLIC FATIGUE LIFE

The appearance of spalling at the ends of 20-inch cylinders after only 50 pressure cycles to 9,000 psi and the occurrence of catastrophic failure after only 110 cycles is acceptable only if the housings are incorporated into diving systems with a projected operational life of <50 dives to 9,000 psi, or <10 dives to 10,000 psi interspersed with <100 dives to lesser depths. Since the operational life of many diving systems calls for up to 100 dives to 9,000 psi interspersed with at least 1000 dives to lesser depth, the cyclic fatigue life of the bearing surfaces on cylinders and hemispheres evaluated in this series of tests must be increased to meet this operational requirement.

The extended operational requirement can be met by a bearing surface encapsulation that provides the ceramic components of the housing with a minimum fatigue life of 250 cycles to 9,000 psi without spalling of ceramic surfaces on the ends of ceramic housing components. A short-term solution to this problem has been already developed (figure 96) and experimentally evaluated on 12-inch-diameter ceramic cylinders (figure 97).

The redesigned end caps Mod 1 for encapsulation of bearing surfaces incorporate two significant changes to Mod 0 end cap configuration; the depth of the seat is increased by 300 percent, and an elastomeric seal is placed between the epoxy adhesive and the pressurizing medium (figure 99). Both changes aim at (1) providing radial restraint to the edge of ceramic component, (2) protecting epoxy from the marine environment, and (3) restraining epoxy from extruding between the metallic end cap and the curved ceramic surfaces during hydrostatic loading to the housing. If so desired, the elastomeric seal could be replaced by an O-ring held in place by a retaining ring.

The experimental results obtained to date during pressure cycling of the 12-inch-diameter housings with Mod 1 end caps were impressive and appear to confirm the reasoning underlying the modifications to Mod 0 end cap for the 20-inch-diameter cylinder. With Mod 1 end caps, spalling did not occur on the 12-inch cylinder even after 500 pressure cycles to 9,000 psi. With Mod 0 end caps, spalling always appeared after only 30 to 50 cycles, regardless of whether the end caps were machined from 7075-T6 aluminum or 6 Aℓ-4 V titanium alloys (Stachiw, 1990). Based on these encouraging results, a Mod 1 end cap design was generated for 20-inch cylinders that will be experimentally evaluated in the near future and a 20-inch ceramic housing (figures 99 to 101).

STIFFENER PERFORMANCE

The low stresses measured in the titanium stiffener (figures 27 and 28) during proof testing to 10,000 psi indicate that the configuration of the stiffener is not optimized for minimum weight. Minor weight reduction can be achieved by incorporating holes into the web of the stiffener (figure 29). Large weight reductions can be achieved only by a very detailed finite element stress and elastic stability analysis that pinpoints where some material can be removed from the stiffener.

Additional weight and cost savings can be achieved by removing the lip from the exterior of the stiffener, so the end caps on the ends of cylinders butt directly against each other. In this arrangement, the stiffener is neither subjected to axial bearing stresses nor exposed to seawater and for this reason does not have to be fabricated from expensive titanium (figure 102).

15

FINDINGS

1. Distribution and magnitude of stresses in 20-inch-diameter alumina ceramic cylinders and hemispheres are the same as in previously tested 12- and 6-inch-diameter cylinders and hemispheres. Since all dimensions on 20-inch housings were scaled linearly form 12- and 6-inch-diameter housings, it indicates that the modulus of elasticity remains constant in spite of a large variation in ceramic mass of structural components.

2. Inclusions of various sizes have been found in the ceramic components. Their origin is not known at the present time, although it is hypothesized that they are due to the presence of combustible impurities in the green castings, or insufficient compaction during isostatic pressing of the green castings.

3. Inclusions in the wall of ceramic components with dimensions less than 0.050 inches in diameter and that represent less than 10 percent of wall thickness do not serve as crack originators when the nominal compressive stresses in 94-percent alumina ceramic do not exceed 150,000 psi.

4. The locations of inclusions, their shape, and size can be determined by acoustical C-scans and scanning acoustic microscopy with equipment of appropriate sensitivity.

5. The calculated and experimentally obtained critical pressure at which buckling occurs agree rather well; the calculated values being approximately 5 percent higher. For this reason, the design safety factor of 2, based on calculated critical pressure for buckling, may be reduced to 1.5 in future designs without compromising the structural performance of ceramic cylindrical housings.

6. The 0.375-inch-thick polyurethane jackets of 65A Rockwell hardness provide adequate protection against point impacts with 100 foot-pounds of energy to which ceramic housings may be accidentally subjected during handling.

7. The Mod 0 end caps provide the 20-inch-diameter ceramic housing components with a cyclic fatigue life of 100 pressurizations to design pressure of 9,000 psi. The Mod 1 end caps design, based on performance of 12-inch-diameter ceramic housings, is expected to extend the cyclic fatigue life of 20-inch housings beyond 500 pressure cycles.

8. Rails fastened to end caps on both ends of the cylinder provide adequate support to a cage on which payload components are mounted. The insertion and removal of the payload components from the interior of the cylinder is accomplished by sliding out the cage from inside the cylinder.

9. The external wedge bands provide adequate clamping force to hold the sections of the housing together during handling and lifting of the whole housing.

10. The metallic penetration inserts with plastic bearing pads provide adequate protection to the ceramic bearing surfaces at the edges of penetrations through the ceramic hemispherical end closures. Neither cracks nor spalling were observed on these surface after 200 pressure cycles. The metallic penetration inserts can be eliminated if bulkhead penetrators with plastic instead of metallic bodies are used for penetrations through ceramic hemispheres.

11. The metallic joint ring stiffeners perform satisfactorily by providing the ceramic monocoque cylinders with sufficient radial support to raise their critical pressure to 17,000 psi. Lightening holes may be machined in the web of the stiffeners to reduce their weight and to act as raceways for electric cables and hydraulic lines connecting payload components in adjoining cylinders.

REFERENCES

Stachiw, J.D. 1964. "Solid Glass and Ceramic External Pressure Vessels," External Report No. 63-0209C, Pennsylvania State University, Ordnance Research Laboratory.

Stachiw, J.D. 1968. "Hulls for Deep Submergence Capsules," *American Ceramic Society Bulletin*, vol. 47, no. 2, February 7.

Stachiw, J.D. 1984. "Exploratory Beryllia Ceramic Cylindrical Housing for Deep Submergence Service," NOSC TR 951, Naval Ocean Systems Center, San Diego, CA.

Stachiw, J.D. 1988. "Pressure Resistant Ceramic Housings for Deep Submergence Systems," NOSC TD 1294, Naval Ocean Systems Center, San Diego, CA.

Stachiw, J.D. 1990. "Ceramic Housings for Deep Submergence Applications," *Proceedings of the Marine Technology Society, Annual Intervention 1990 Conference*, pp 313–321.

Stachiw, J.D. 1990. "Exploratory Evaluation of Alumina Ceramic Cylindrical Housings for Deep Submergence Service: The Third Generation NOSC Ceramic Housings," NOSC TR 1314, Naval Ocean Systems Center, San Diego, CA.

Stachiw, J.D., and B. Frame. 1988. "Graphite-Fiber Reinforced Plastic Hull Mod 2 for Advanced Unmanned Search System Vehicle," NOSC TR 1245, Naval Ocean Systems Center, San Diego, CA.

Stachiw, J.D., and J.L. Held. 1987. "Exploratory Evaluation of Alumina Ceramic Cylindrical Housings for Deep Submergence Service: The Second Generation NOSC Ceramic Housings," NOSC TR 1176, Naval Ocean Systems Center, San Diego, CA.

Stachiw, J.D., and R.F. Snyder. 1965. "The Design and Fabrication of Glass and Ceramic Deep Submergence Free-Diving Instrumentation Capsules." Paper 65-UNT-1, American Society of Mechanical Engineers, National Underwater Technology Conference.
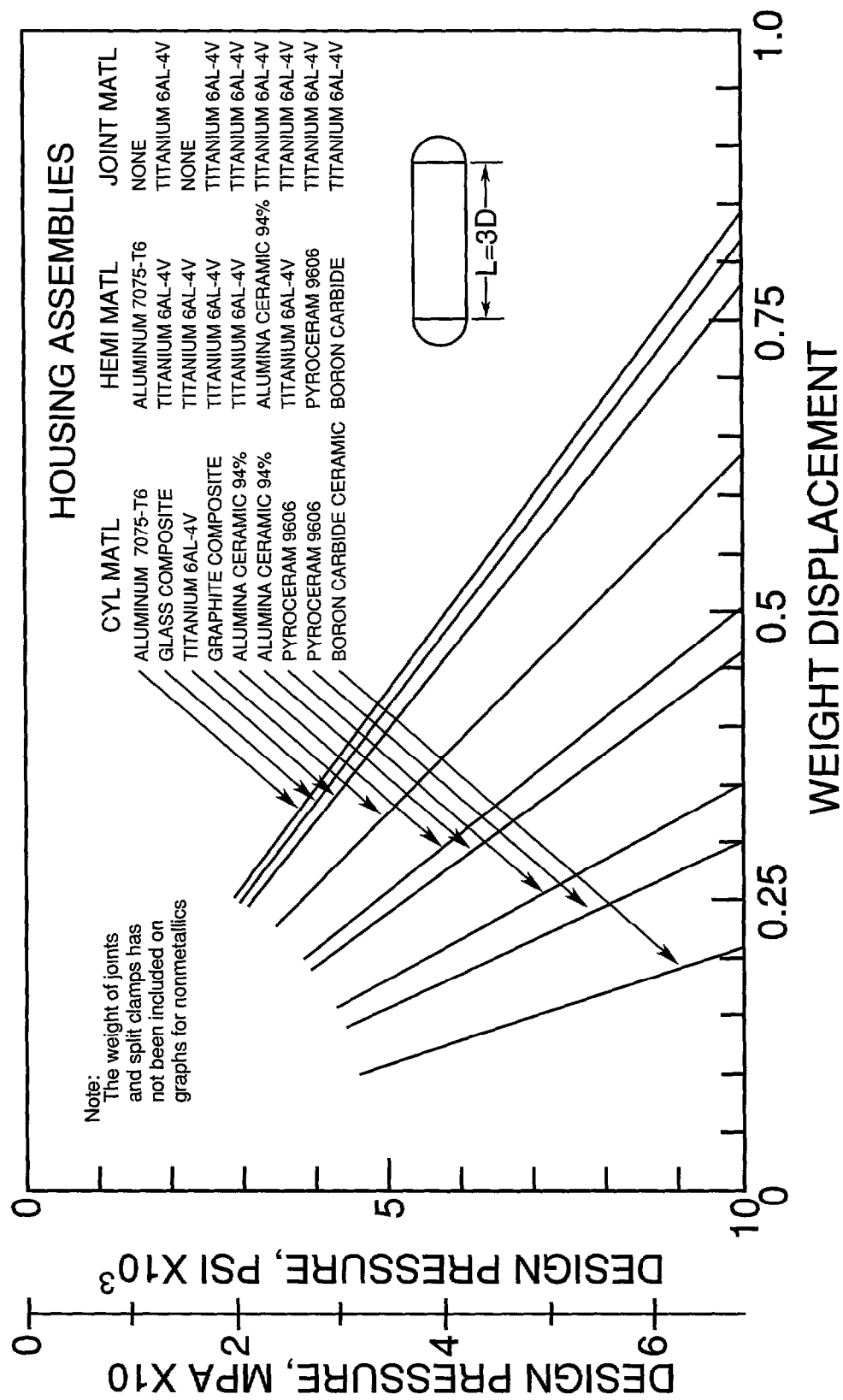
Figure 1. Weight-to-displacement of housing assemblies fabricated from different materials.

Figure 2. Cylindrical shells of 94-percent alumina ceramic used in the NOSC ceramic housing program. Phase 1 of the program focused on 6-inch, Phase 2 on 12-inch, and Phase 3 on 20-inch-diameter cylinders.

19

NOTES:

1. MATERIAL: ALUMINA CERAMIC, COORS AD94
   OR EQUIVALENT.

2. MATERIAL REQUIREMENTS:
   CERAMIC COMPOSITION $\geq 94\% \ Al_2O_3$
   ⓔ MODULUS OF ELASTICITY $\geq 40 \times 10^6$ PSI
   ⓔ COMPRESSIVE STRENGTH $> 300,000$ PSI
   ⓔ MODULUS OF RUPTURE $> 50,000$ PSI
   POISSON'S RATIO   0.21
   SHEAR MODULUS $\geq 17 \times 10^6$ PSI
   BULK MODULUS $\geq 24 \times 10^6$ PSI
   SPECIFIC GRAVITY   3.62
   COEFFICIENT OF THERMAL
   EXPANSION AT 70°F $2 \times 10^{-6}/°F$

3. THE CRITICAL MECHANICAL PROPERTIES ⓔ OF
   THE MATERIAL SHALL BE VERIFIED BY THE
   FABRICATOR ON TEST SPECIMENS PREPARED
   FROM MATERIAL COUPONS THAT WERE
   PRESSED AND FIRED AT THE SAME TIME
   AS THE PART.

4. THE FINISHED PART SHALL BE FREE OF
   DEFECTS IN THE FORM OF NICKS, CHIPS,
   DINGS, SCRATCHES, CRACKS, SEPARATIONS OR
   FOREIGN INCLUSIONS VISIBLE WITH UNAIDED EYE.

5. ALL DIMENSIONS AND SURFACE FINISHES
   ON THE PART SHALL BE INSPECTED FOR
   CONFORMANCE TO THE DRAWING.

6. ALL SURFACES SHALL BE INSPECTED FOR
   CRACKS AND SEPARATIONS BY DYE
   PENETRANT METHOD.

7. THE FABRICATOR SHALL PROVIDE WITH EACH
   PART A SUMMARY OF INSPECTION AND
   TESTING RESULTS.

.685 WALL
.675

CHAM .02 X 45°
BOTH ENDS

30.02
30.00

Ø 20.01
20.00

NAVAL OCEAN SYSTEMS CENTER
SAN DIEGO CA 92152-5000

CYLINDER,
CERAMIC HULL

SIZE D   FSCM NUMBER 55910   DRAWING NUMBER 0121758

SCALE 1/2   SHEET 1 OF 1

Figure 3. Dimensional specification for 20-inch-diameter alumina cylinder.
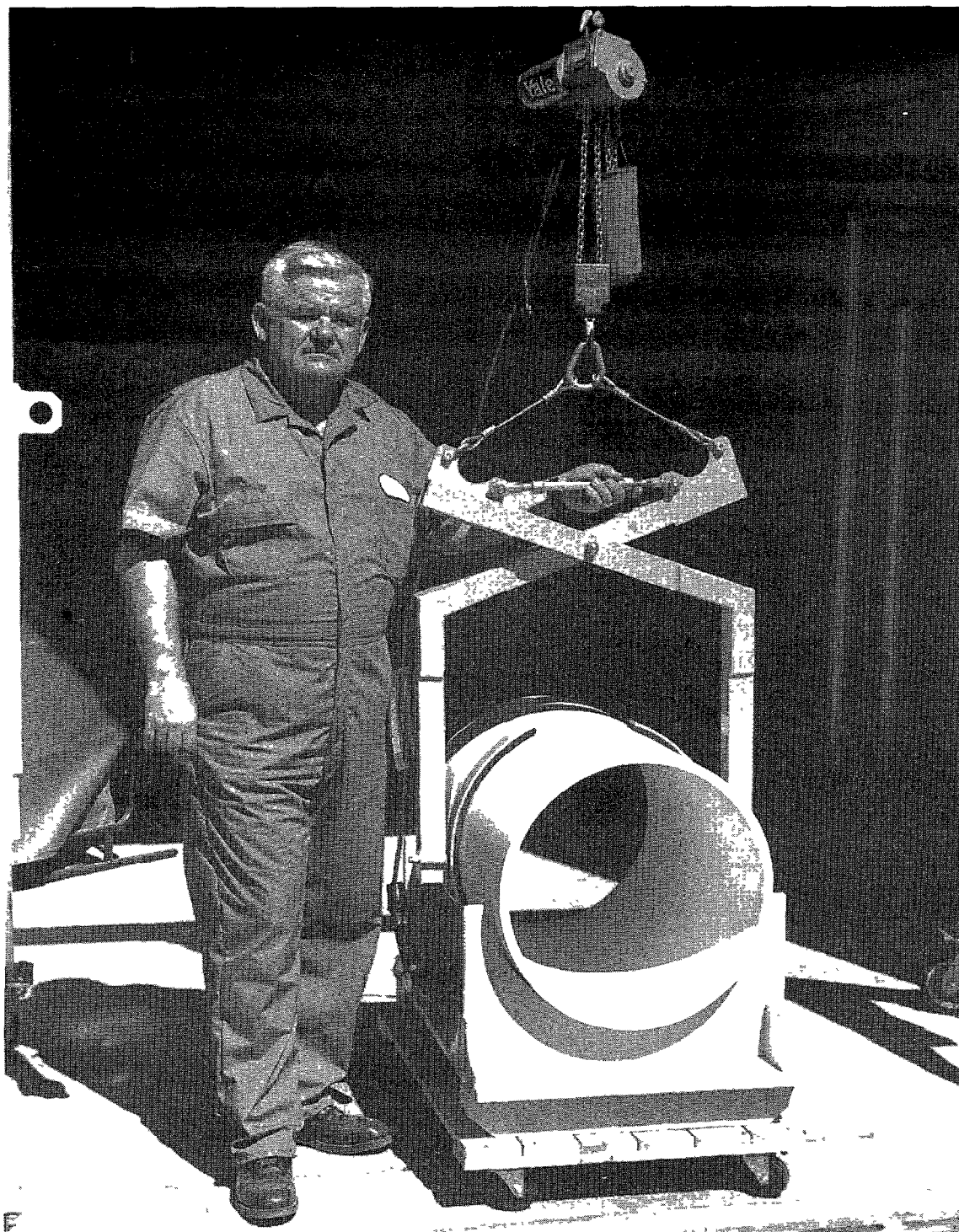
Figure 4. The 20-inch-diameter alumina cylinder and the fixture for handling it during installation of metallic end caps.
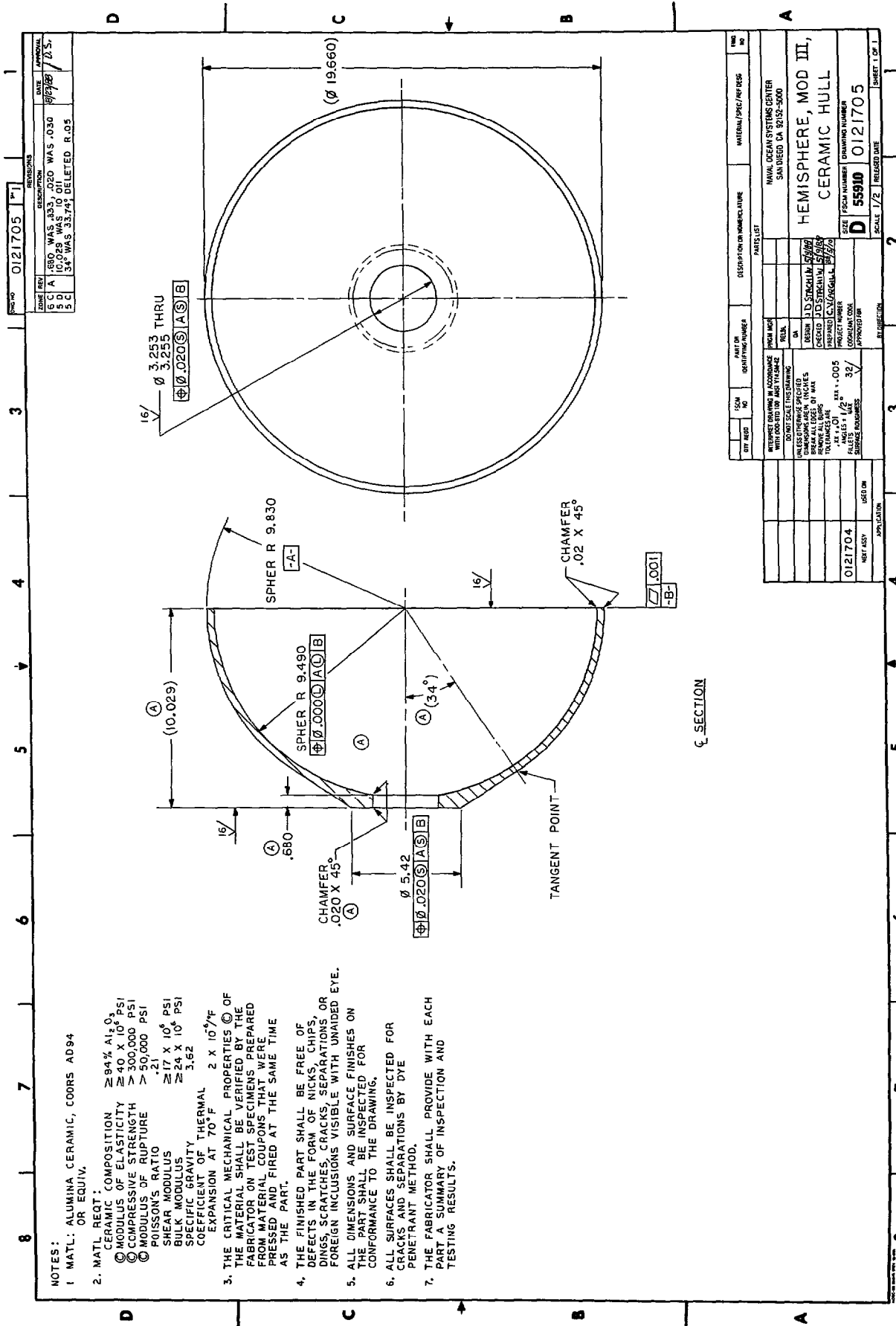
Figure 5. The dimensional specification for 20-inch-diameter alumina hemisphere Mod III with a single polar penetration. Note the increase in shell thickness near penetration to reduce the magnitude of stresses at that location.
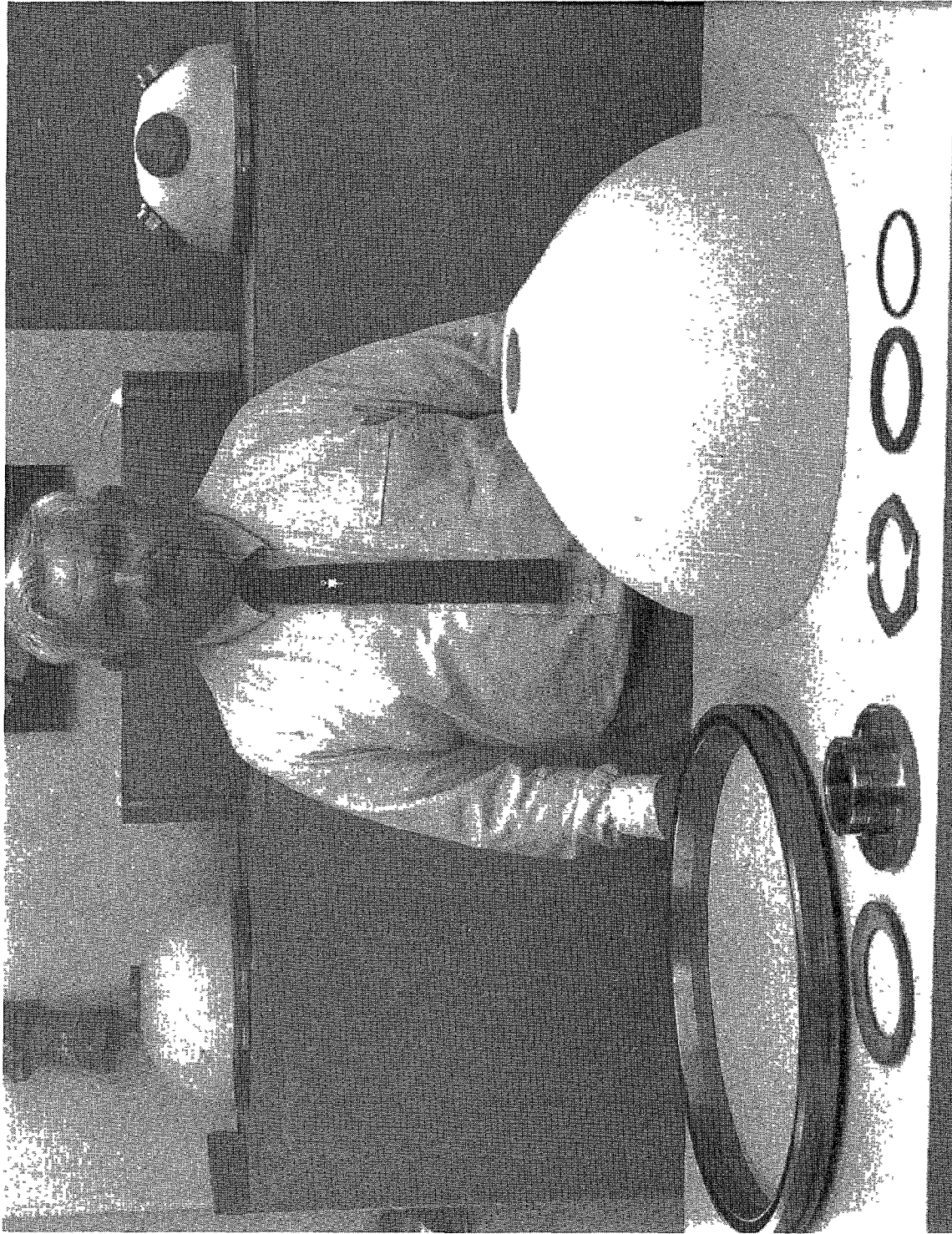
Figure 6. Components of the hemispherical Mod III ceramic end closure for 20-inch-diameter housing. In the background can be seen hemispherical ceramic end closures for 12-inch-diameter housing tested in Phase 2 of the NOSC ceramic housing program.

23
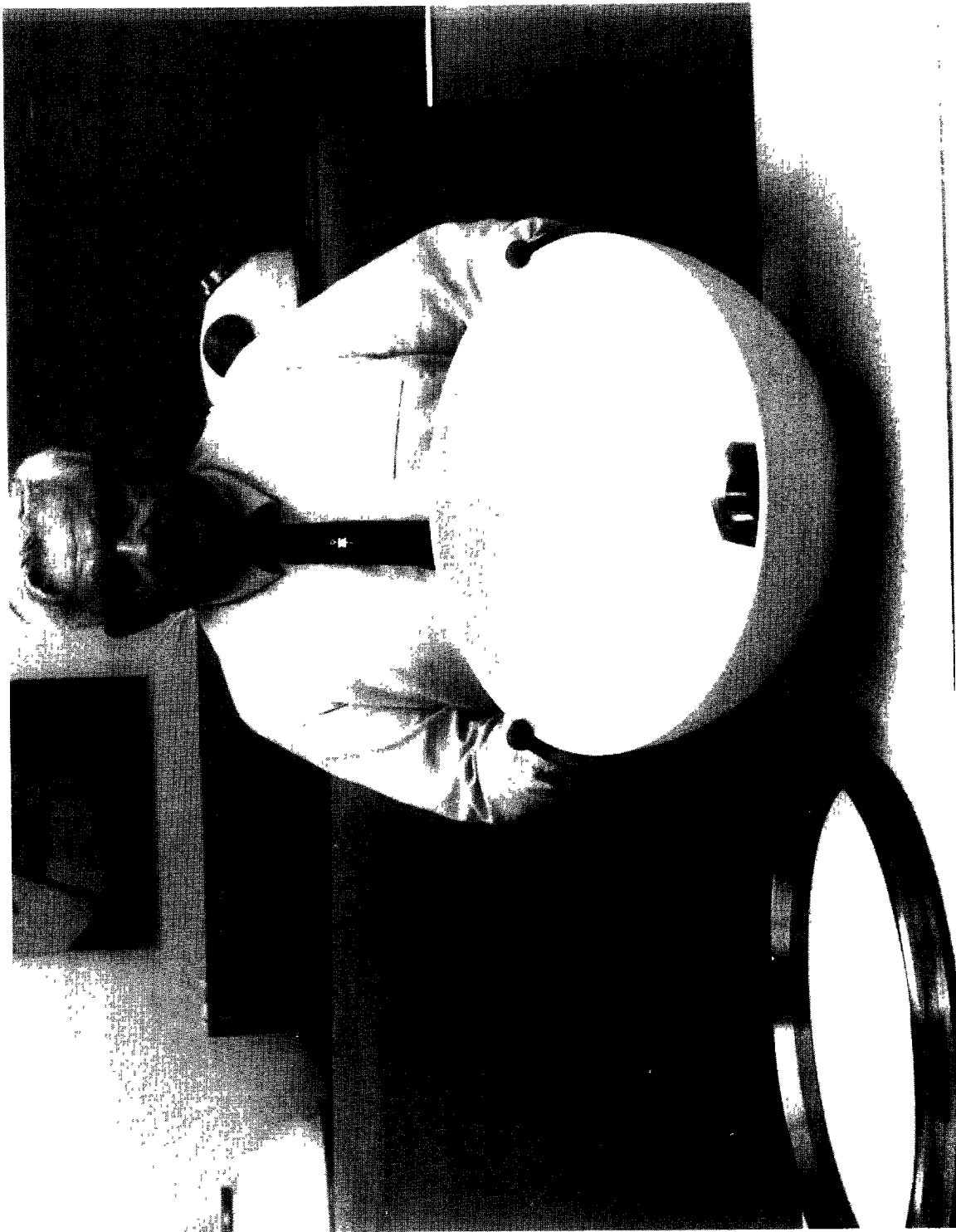
Figure 7 Mod III ceramic hemisphere with penetration insert in place

Figure 8. Assembled Mod III hemispherical end closure for 20-inch-diameter ceramic housing.

25

NOTES:
1. MATL: ALUMINA CERAMIC, CCORS AD94 OR EQUIV.
2. MATL REQT:

CERAMIC COMPOSITION	94% Al₂O₃
MODULUS OF ELASTICITY	41 X 10⁶ PSI
COMPRESSIVE STRENGTH	>300,000 PSI
FLEXURAL STRENGTH	>50,000 PSI
POISSON'S RATIO	.21
SHEAR MODULUS	17 X 10⁶ PSI
BULK MODULUS	24 X 10⁶ PSI
SPECIFIC GRAVITY	3.62
COEFFICIENT OF THERMAL EXPANSION AT 70°F	2 X 10⁻⁶/°F

REVISIONS
DWG NO. 0121954

ZONE	REV	DESCRIPTION	DATE	APPROVAL
4 D	A	.020 WAS .025 19.660 WAS 19.66		J.D.S
6 C				

NAVAL OCEAN SYSTEMS CENTER
SAN DIEGO CA 92152-5000

HEMISPHERE, MOD II, CERAMIC HULL

SIZE D   FSCM NUMBER 55910   DRAWING NUMBER 0121954
SCALE 6/10   SHEET 1 OF 1

₵ SECTION

ø 3.253 THRU
  3.255
4 PL EQUALLY SPACED
⊕ ∅.028 Ⓢ A Ⓢ B
CHAM .020 X 45°   Ⓐ 4 PL

9.490 SPHER R -A-

9.830 SPHER R
⊕ ∅.000 Ⓜ A Ⓛ B

10.170 SPHER R
⊕ ∅.000 Ⓜ A Ⓛ B

19.660 SPHER ∅ Ⓐ
⊕ ∅.000 Ⓜ A Ⓛ B

CHAM .020 X 45°

TANGENT POINT

Figure 9. The dimensional specification for the 20-inch-diameter alumina hemisphere Mod II with four penetrations.
Note the increasing shell thickness near penetrations to reduce the magnitude of stresses at that location.

Figure 10. Interior view of the Mod II alumina hemisphere.
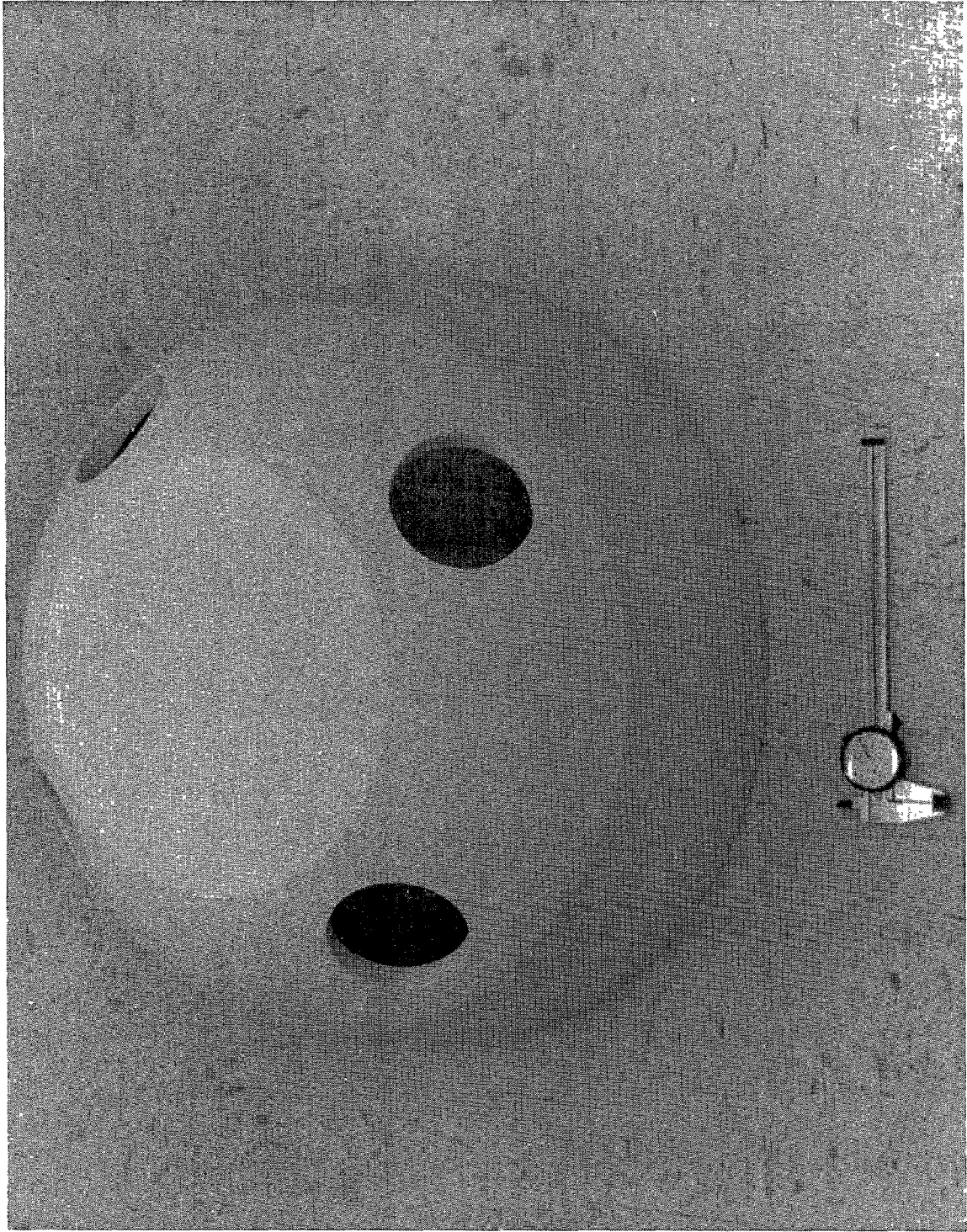
Figure 11. Exterior view of the Mod II alumina hemisphere.
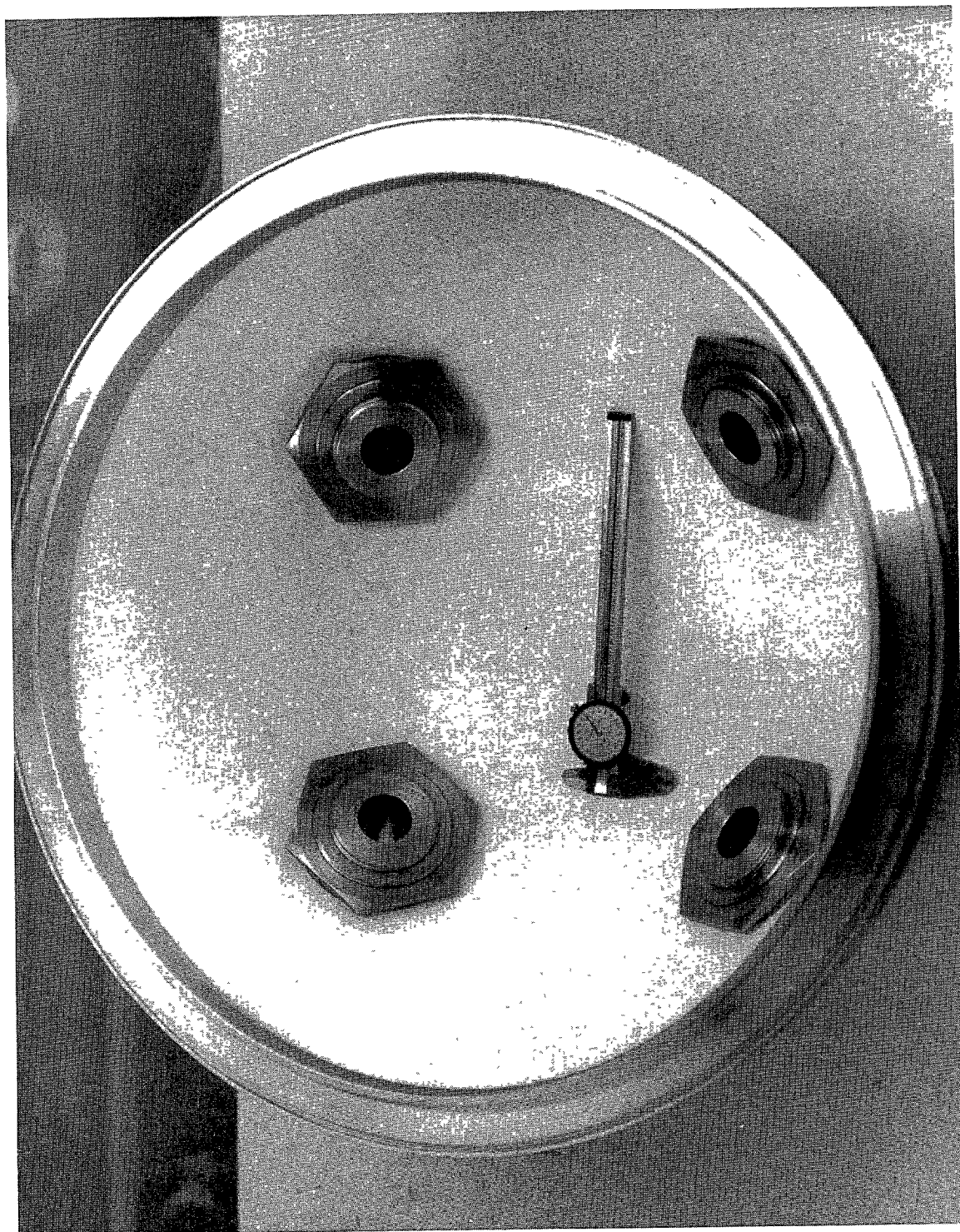
Figure 12. Interior view of the assembled Mod II hemispherical end closure for the 20-inch ceramic housing.

Figure 13. Dimensional specification for the 20-inch-diameter alumina hemisphere Mod I with five penetrations. This hemisphere was not fabricated due to lack of funding; a 12-inch-diameter ceramic scale model, however, was fabricated and successfully tested in Phase 2 of the program.

30
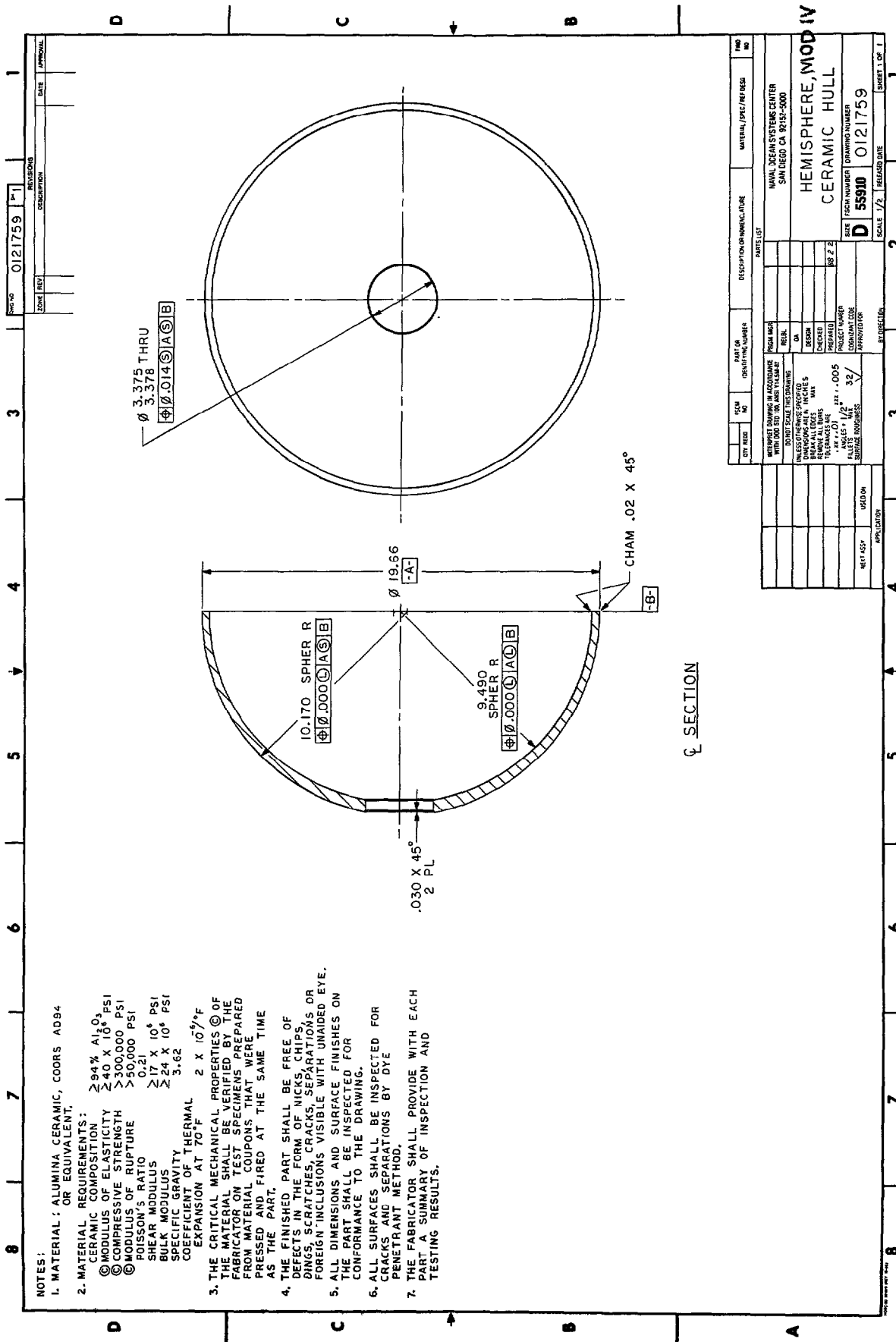
Figure 14. Dimensional specification for the 20-inch-diameter alumina hemisphere Mod 0 with a single penetration. This hemisphere was not fabricated due to lack of funding; a 12-inch-diameter ceramic scale model, however, was fabricated and successfully tested in Phase 2 of the program. Note the gradual buildup in shell thickness from the equator to the polar opening.

31
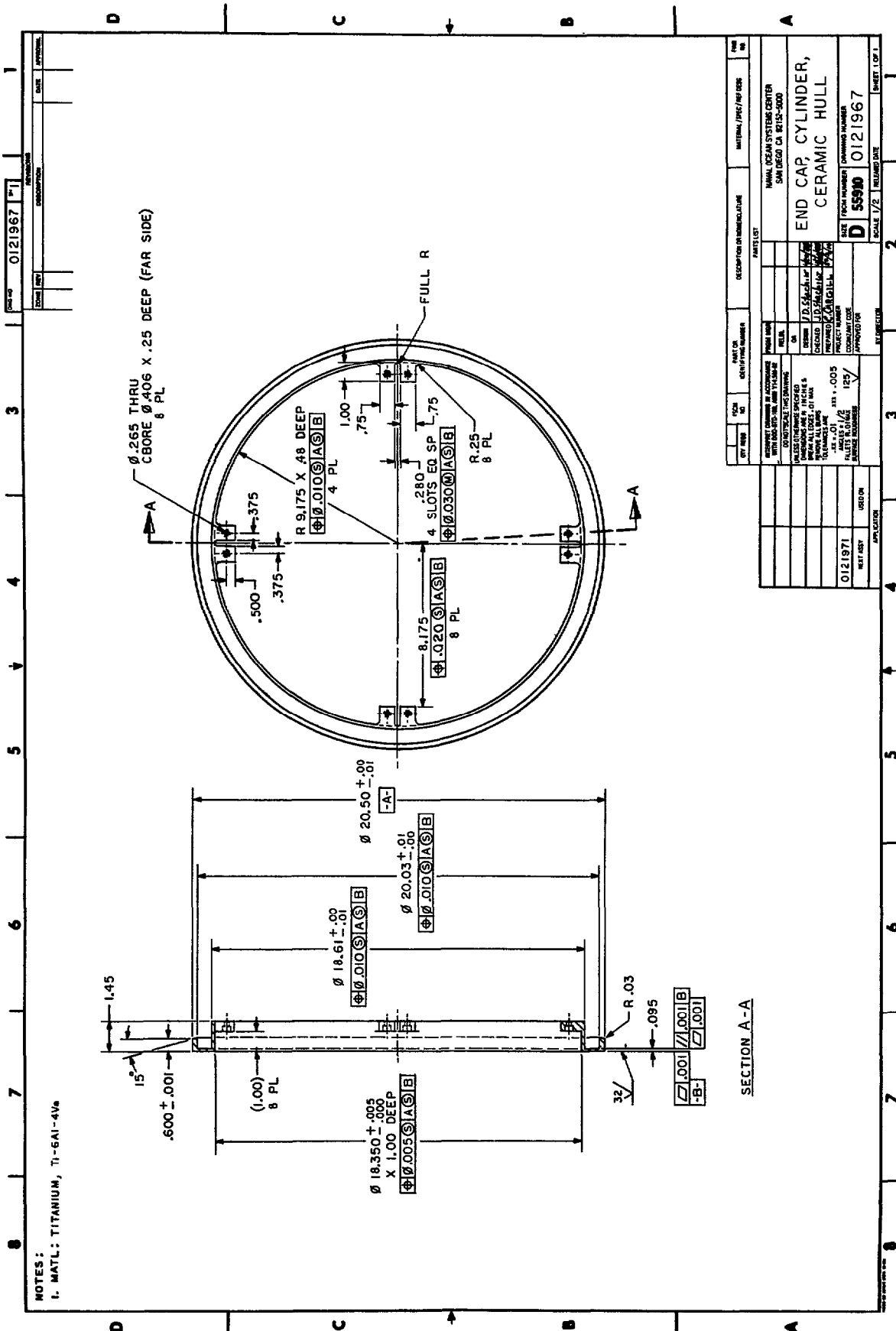
Figure 15. Fabrication drawing of Mod 0 end cap for 20-inch ceramic cylinders.
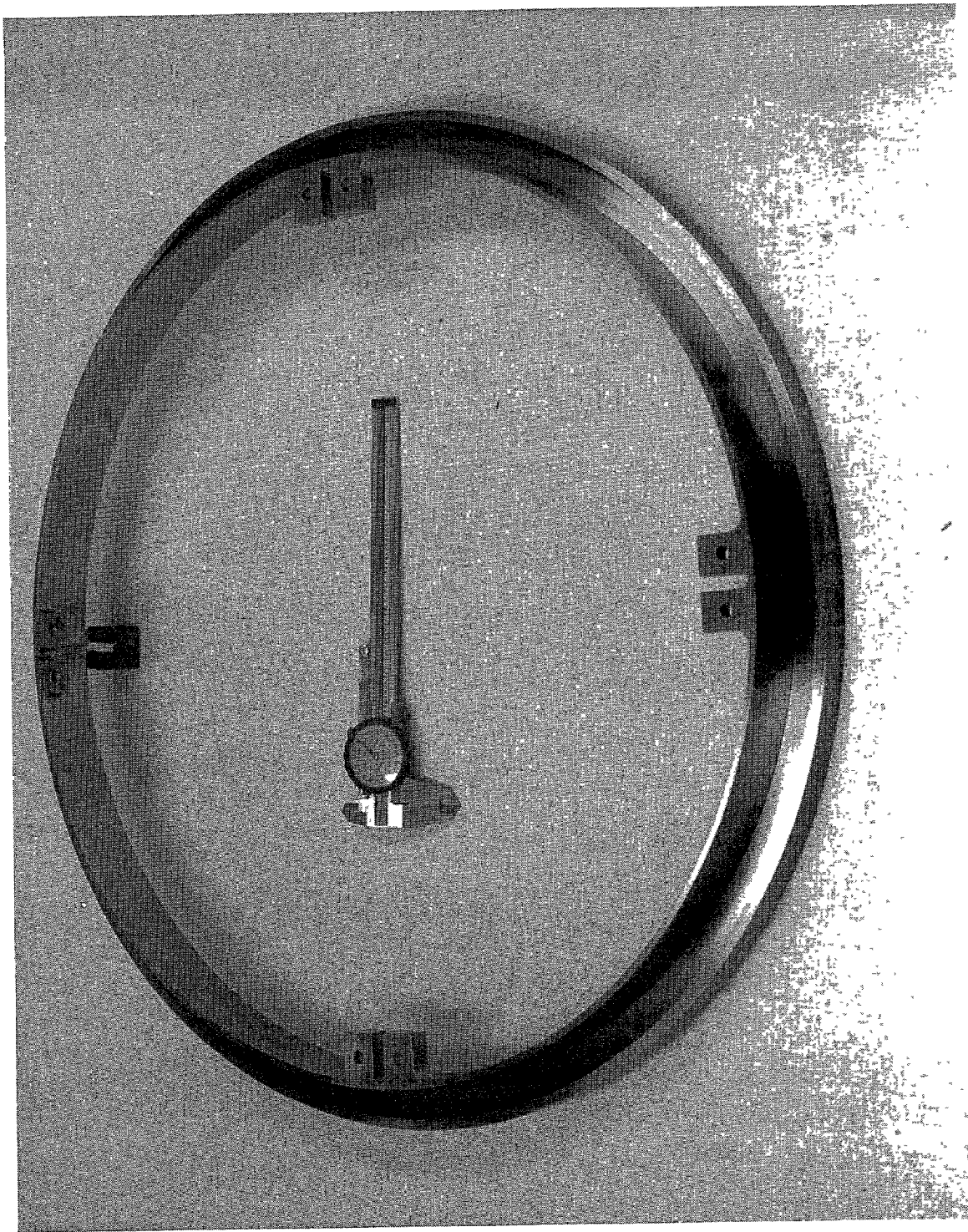
Figure 16. Interior view of the Mod 0 end cap for 20-inch ceramic cylinders.
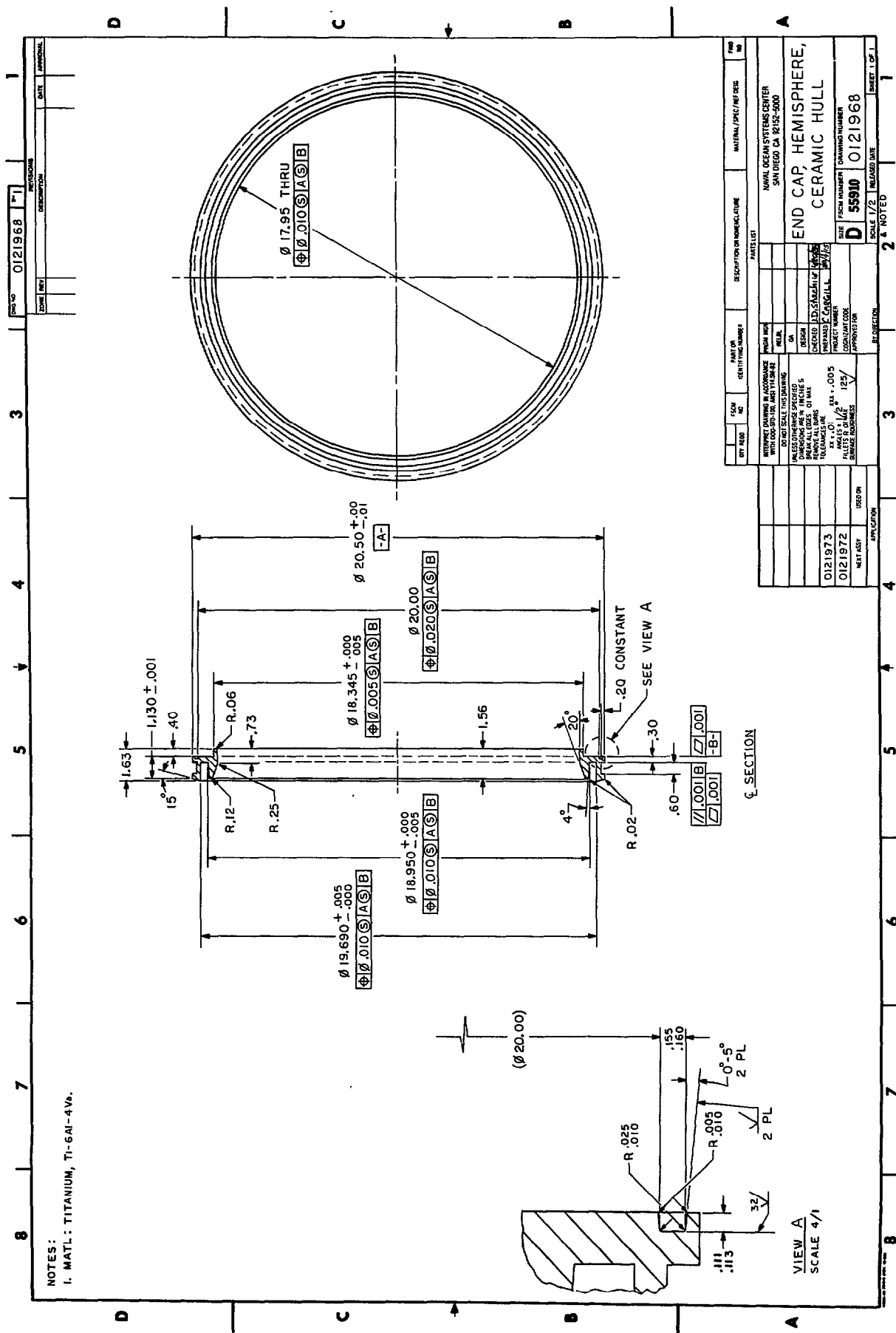
Figure 17. Fabrication drawing of Mod 0 end cap for 20-inch ceramic hemispheres.

34
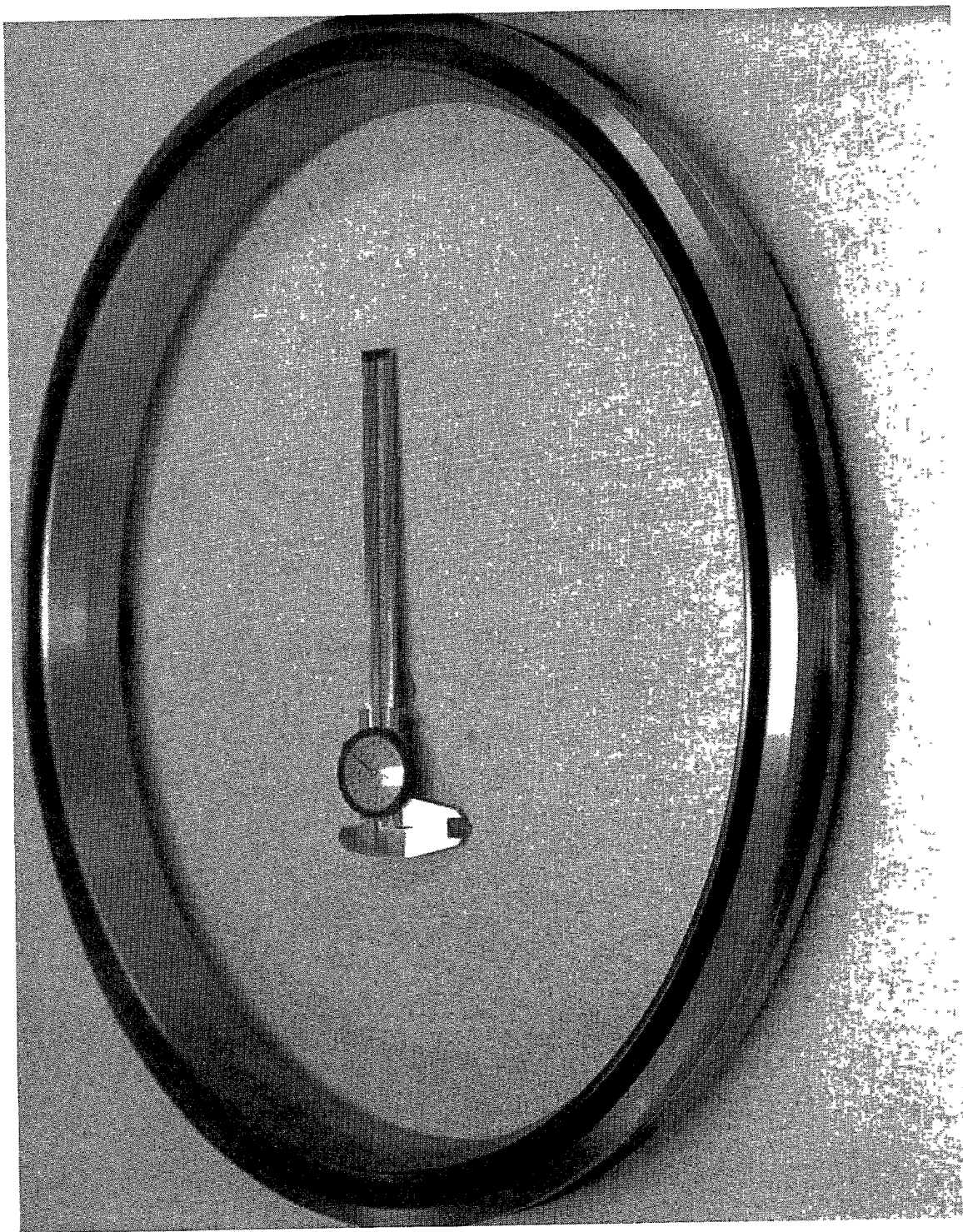
Figure 18. Interior view of the Mod 0 end cap for 20-inch ceramic hemispheres.

Figure 19a. Fabrication drawing of 2-inch-diameter penetration inserts for 20-inch-diameter ceramic hemispheres; they were not used in the housing assembly.

Figure 19b. Fabrication drawing of 3.25-inch-diameter penetration inserts for 20-inch-diameter ceramic hemisphere.

37
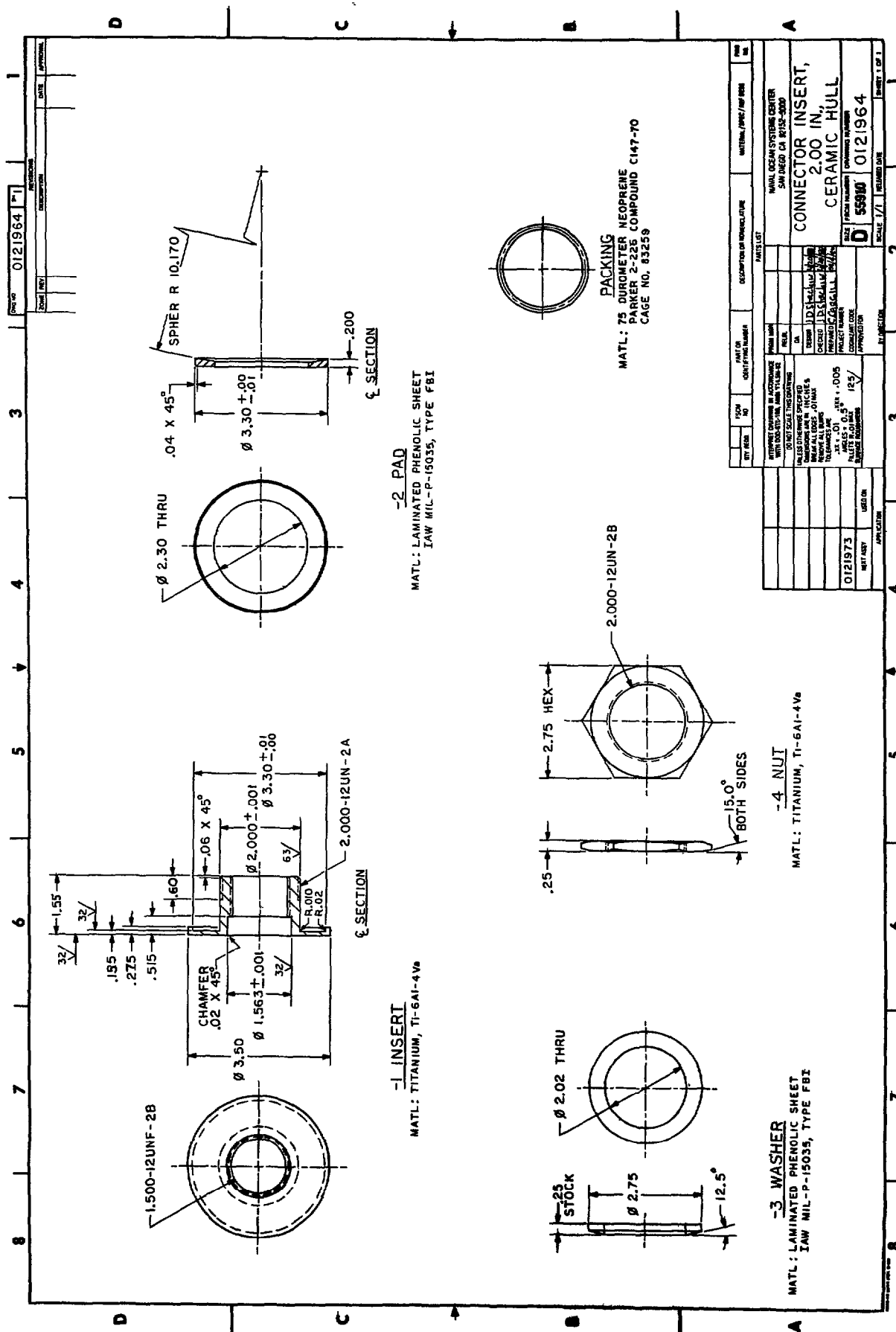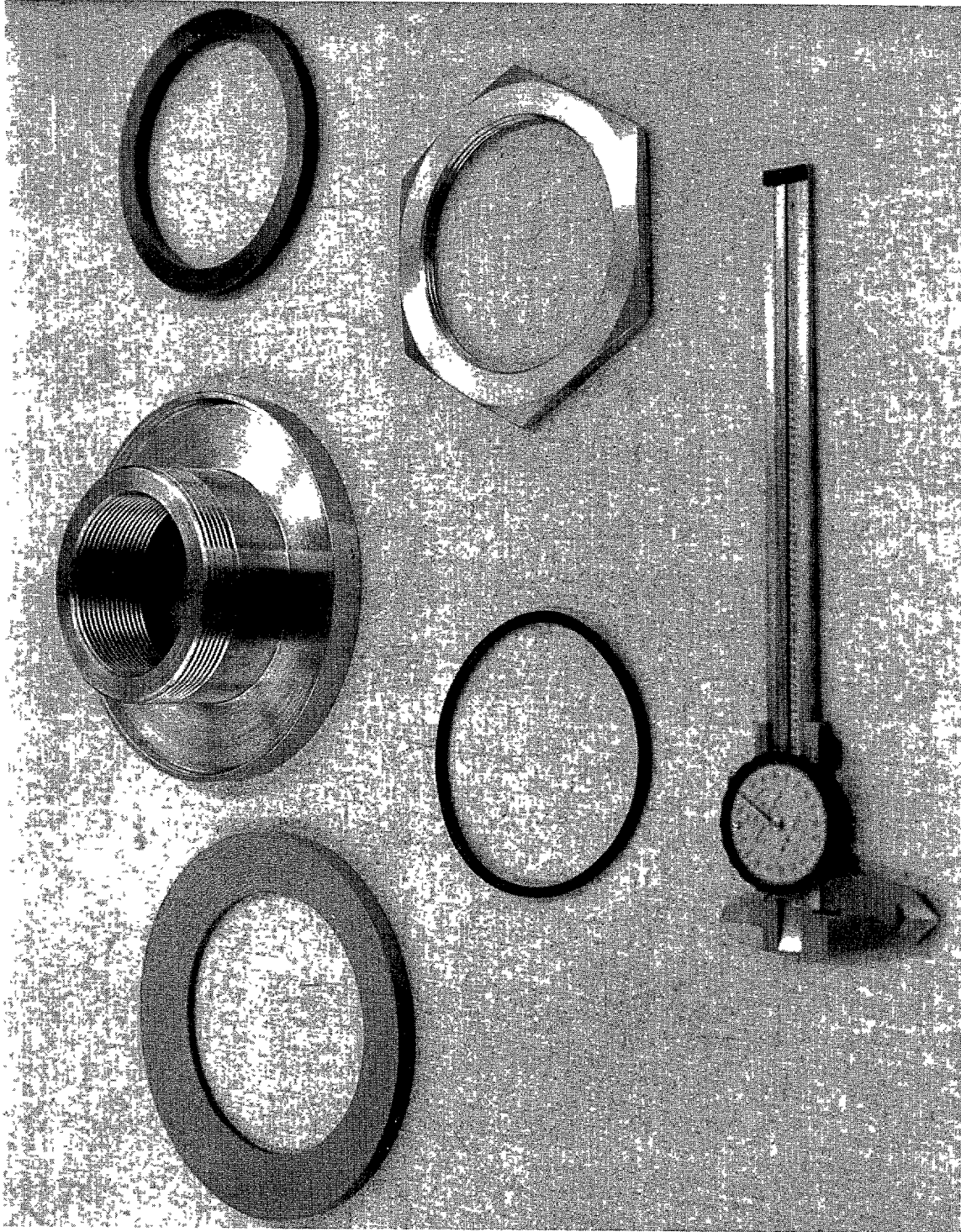
Figure 20a. Components of the 3.25-inch-diameter penetration insert. Note the phenolic, plastic glass reinforced bearing pad, and washer.

Figure 20b. The 2-inch-diameter bulkhead penetrator used for instrumentation leads during pressure testing of ceramic housing.

NOTES:
1. MATL: 303 CRES IAW QQ-S-764.

THD RELIEF
Ø 2.37 X .25
WIDE WITH .03
FILLET R

.06 X 45°

Ø 2.747
2.745

2.500-12UN-2A

2.50
1.50
.20
.495

Ø 2.505
2.500

Ø 3.25

Ø 3.80

B

A

₵ SECTION

(Ø 2.747)
2.745

R .015

R .005
.010

(.20)

.180

63/

2 PL

0°-5°
2 PL

32/

(Ø 2.505)
2.500

VIEW B
SCALE 4/1

2.00

1.00

Ø .187 X .25 DEEP
2 PL

VIEW A
SCALE 4/1

(Ø 3.25)

.175

0°-5°
2 PL

R .005
.010

63/
2 PL

R .015

.111
.113

32/

Figure 22. Dummy plug.

Figure 23. Mod III hemisphere assembly.

NOTES:
COAT PACKING WITH THIN FILM OF SILICONE COMPOUND
IAW MIL-S-8660 BEFORE INSTALLING.

EPOXY
ALL AROUND

HEMISPHERE ASSY,
MOD III,
CERAMIC HULL

NAVAL OCEAN SYSTEMS CENTER
SAN DIEGO, CA 92152-5000

SIZE F   CAGE NUMBER 55910   DRAWING NUMBER 0121704

SCALE   SHEET 1 OF 1

QTY REQD	PART OR IDENTIFYING NUMBER	DESCRIPTION OR NOMENCLATURE	
1	83259|2-236 C147-70	O-RING	
1	0121968	END CAP	
1	0121963-6	PAD	
1	0121963-5	INSERT	
1	0121963-4	NUT	
1	0121963-3	WASHER	
1	0121705	HEMISPHERE	

PARKER

PARTS LIST

Figure 24. Mod II hemisphere assembly.
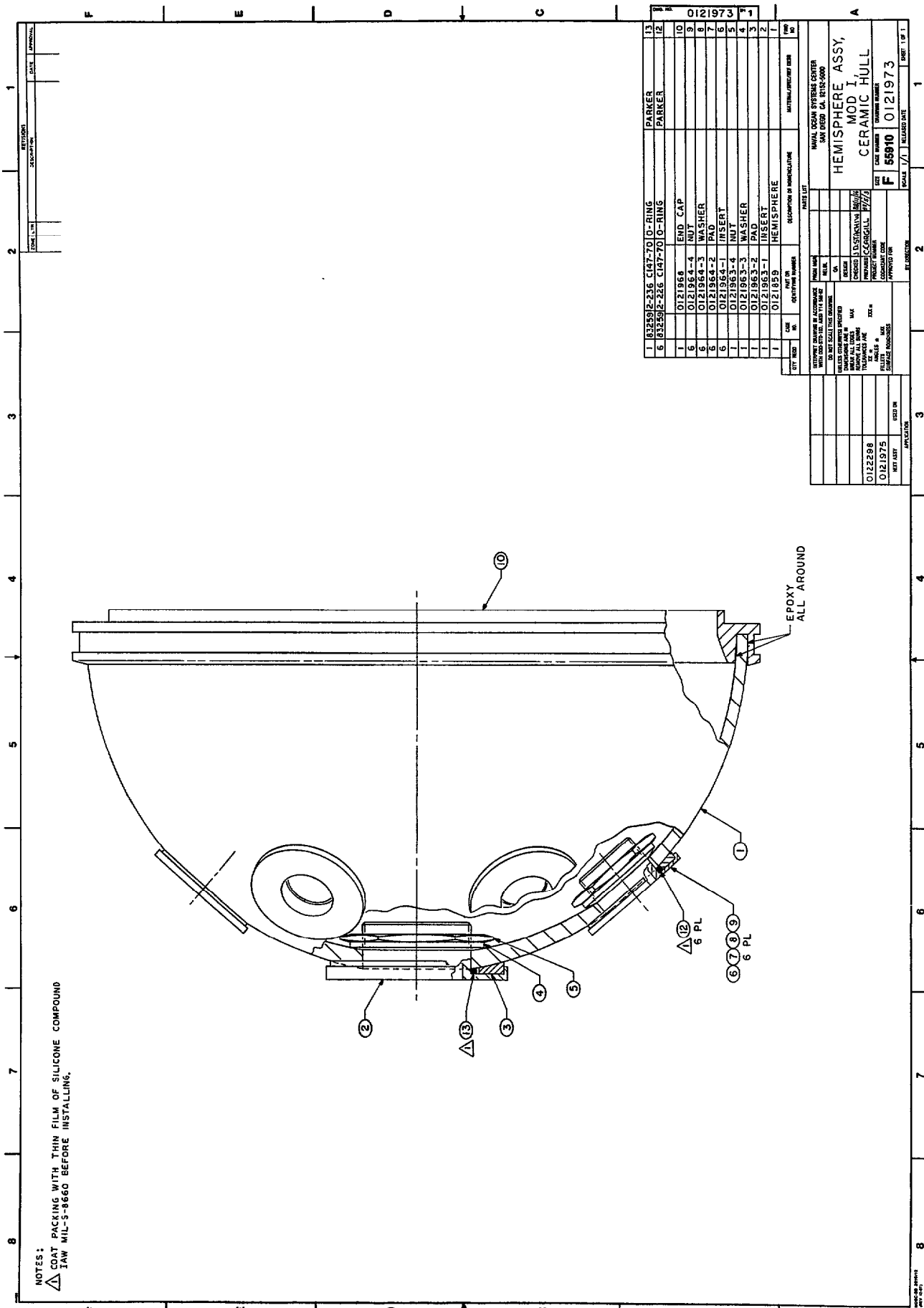
Figure 25. Mod I hemisphere assembly.
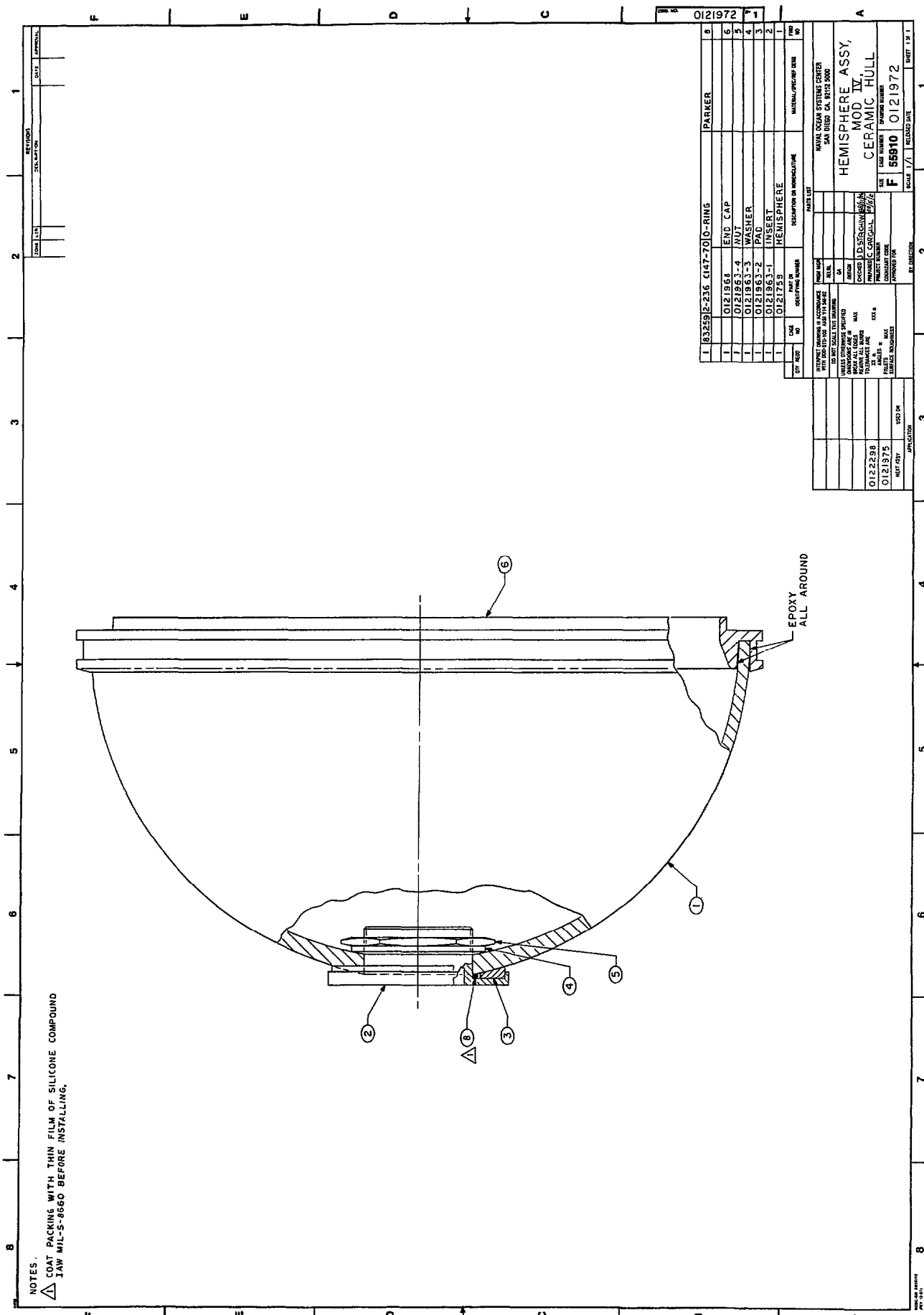
Figure 26. Mod IV hemisphere assembly.

NOTES:
⚠ COAT PACKING WITH THIN FILM OF SILICONE COMPOUND
IAW MIL-S-8660 BEFORE INSTALLING.

EPOXY ALL AROUND

HEMISPHERE ASSY,
MOD IV,
CERAMIC HULL

NAVAL OCEAN SYSTEMS CENTER
SAN DIEGO, CA 92152 5000

PARKER

8	83259	2-236	C147-7010-RING
6		0121968	END CAP
5		0121963-4	NUT
4		0121963-3	WASHER
3		0121963-2	PAD
2		0121963-1	INSERT
1		0121759	HEMISPHERE

SIZE F   CAGE NUMBER 55910   DRAWING NUMBER 0121972

SCALE 1/1   SHEET 1 OF 1

Figure 27. Fabrication drawing of titanium joint stiffener for 20-inch-diameter ceramic housing.

Figure 28. Titanium joint stiffener for 20-inch-diameter ceramic housing.
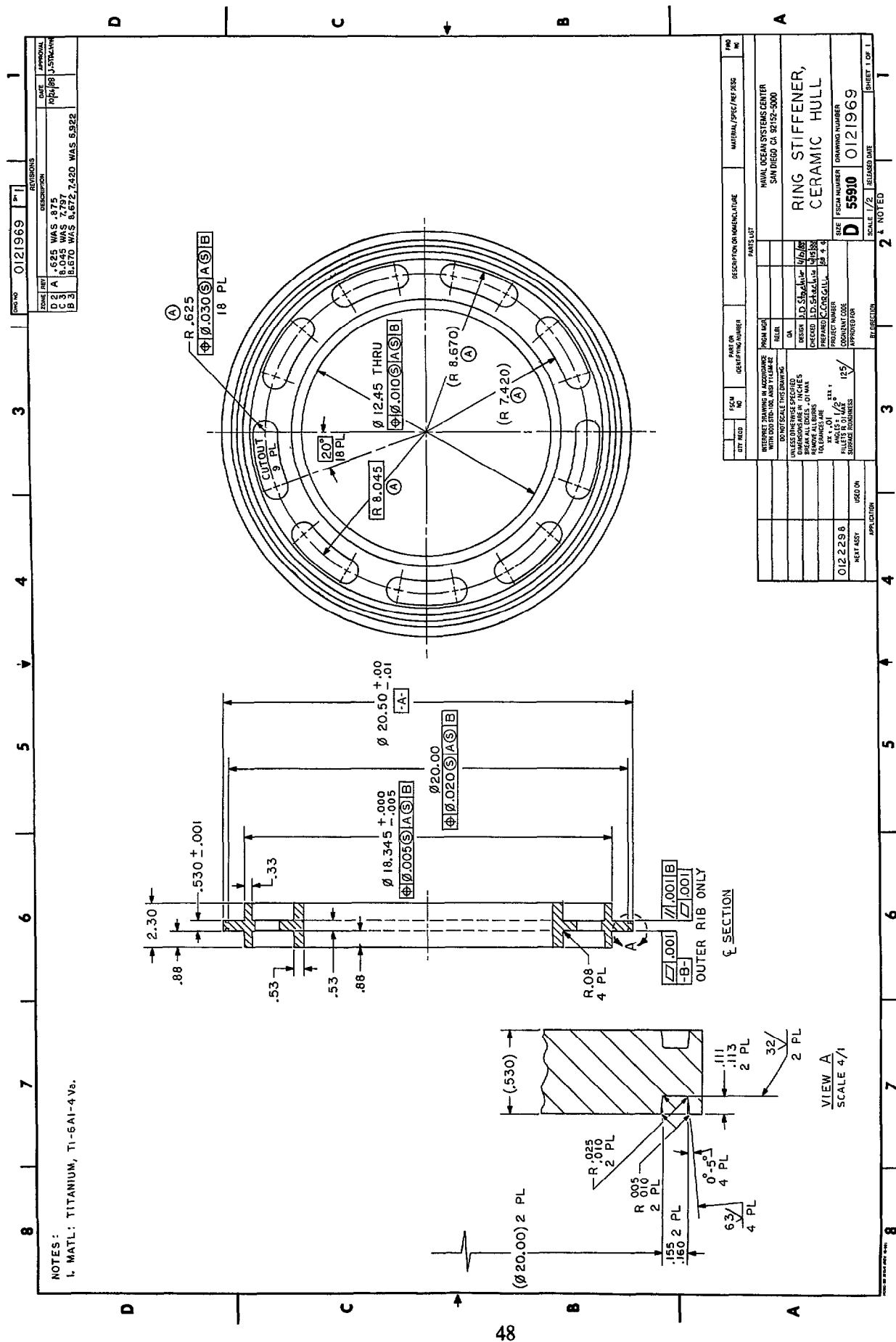
Figure 29. Fabrication drawing of titanium joint stiffener with lightening holes for 20-inch-diameter ceramic housing. This stiffener was not fabricated due to lack of funding.

48

Figure 30. Fabrication drawing of aluminum joint stiffener for 20-inch-diameter ceramic housing. This stiffener was not fabricated due to potential corrosion problems in service.

WEDGE CLAMP BAND

O-RING SEALS

END CAPS

JOINT RING
STIFFENER

WETTED JOINT RING STIFFENER
CONFIGURATION

O-RING
SEAL

DRY JOINT RING STIFFENER
CONFIGURATION
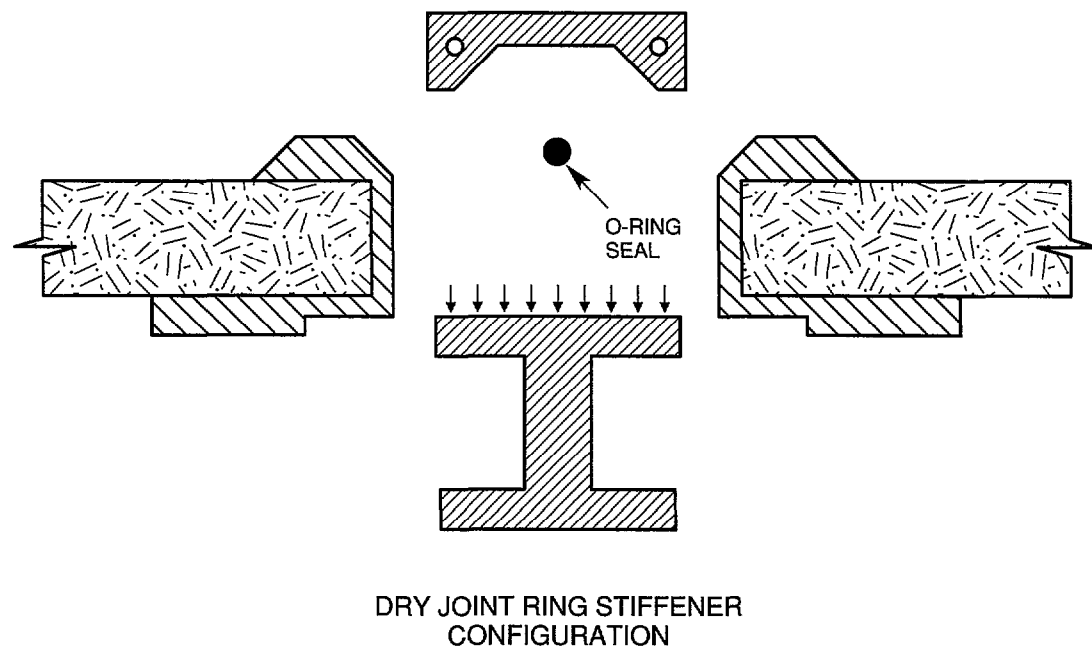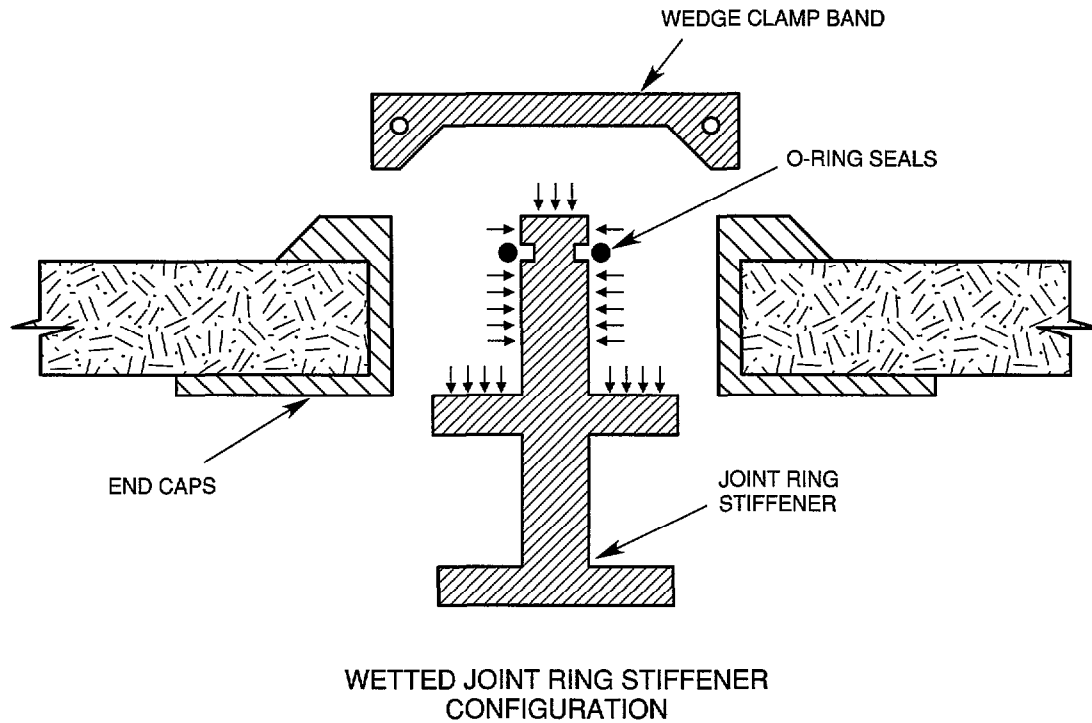
Figure 31. Proposed dry joint stiffener for ceramic housings. This design eliminates any contact between seawater and the stiffener, making it feasible to use for construction of joint stiffeners of inexpensive lightweight materials that otherwise would corrode if contacted by seawater.
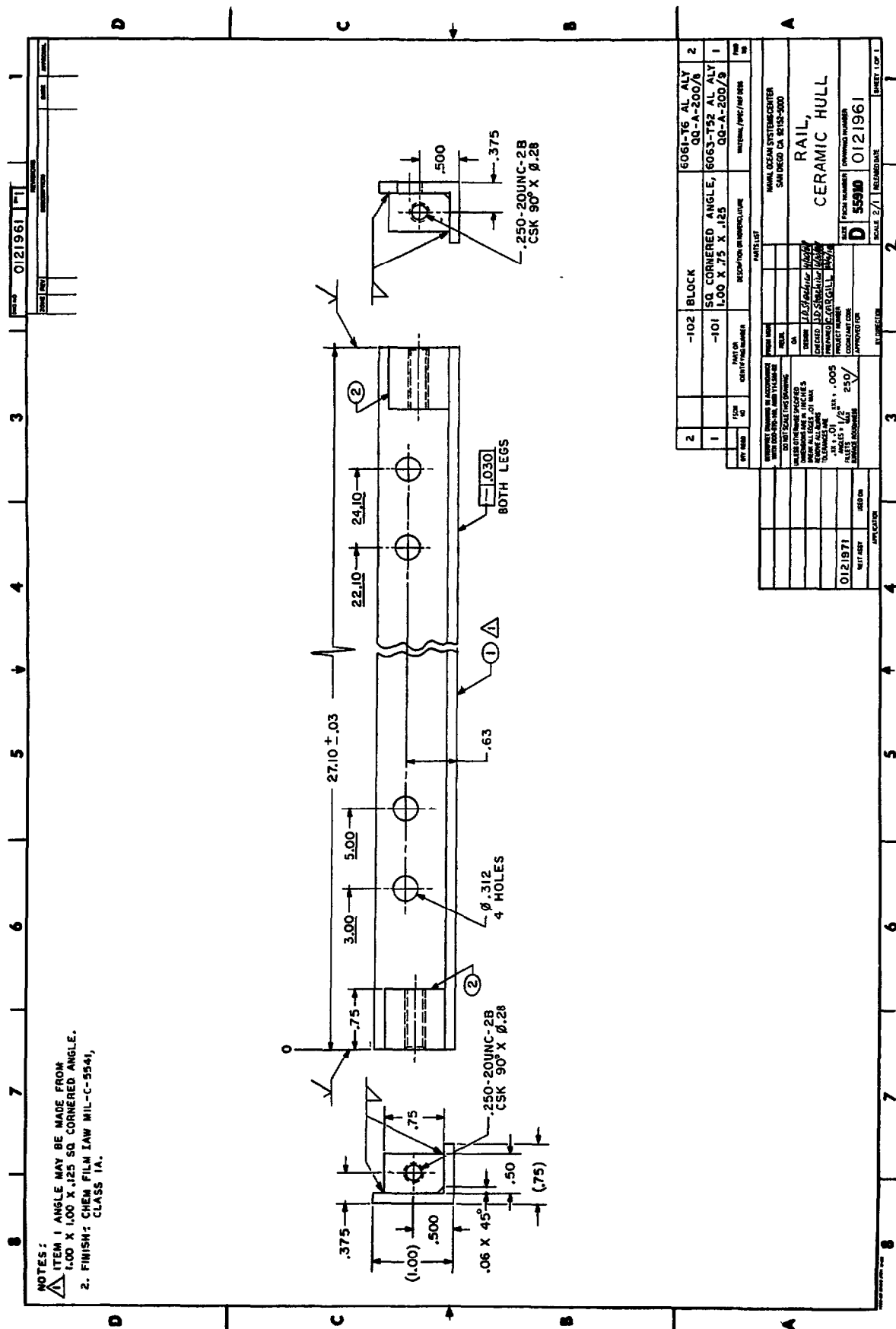
Figure 32. Fabrication drawing of mounting rails for equipment shelves inside the 20-inch-diameter ceramic housing.
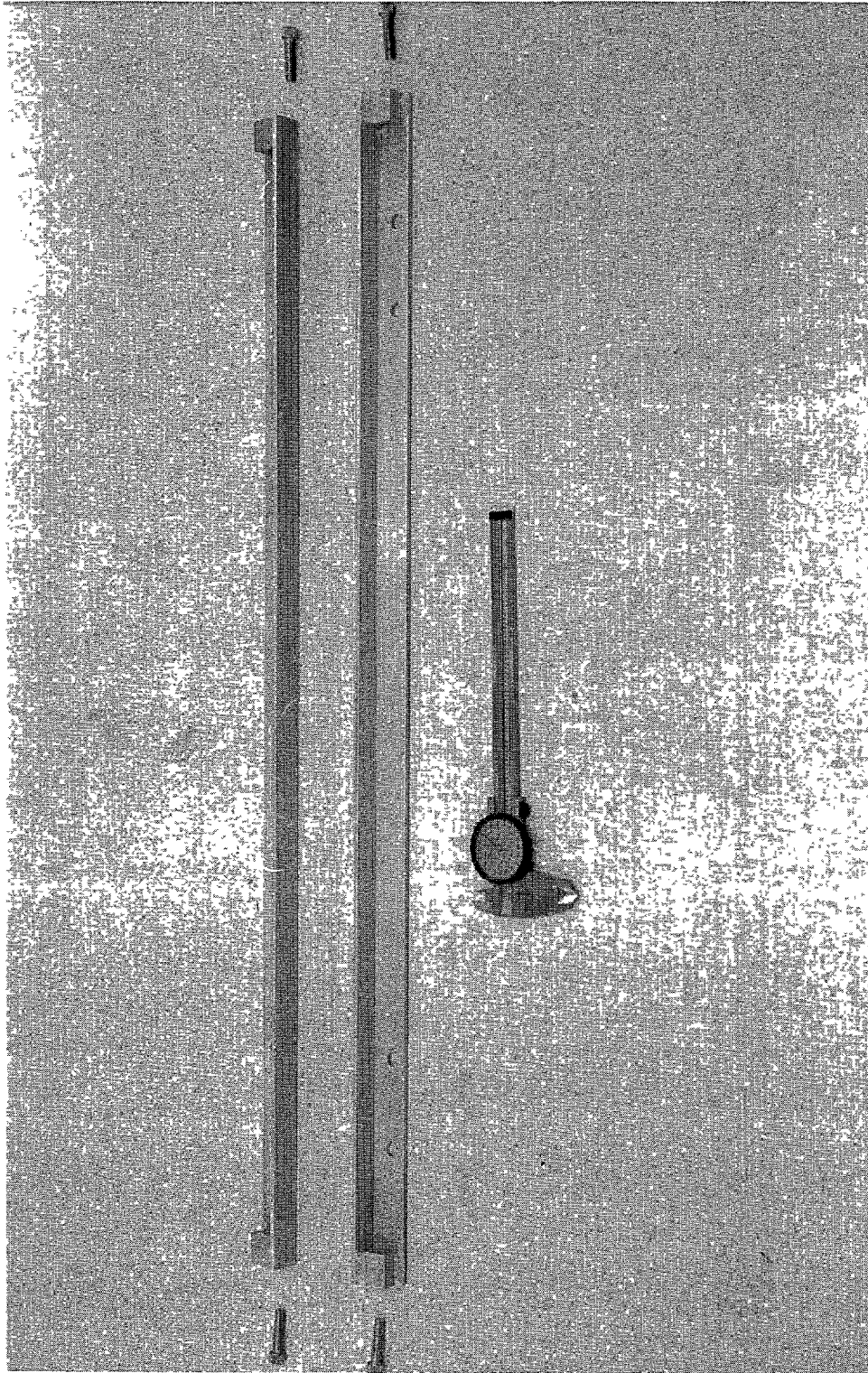
Figure 33. Rails for mounting equipment shelves inside 20-inch-diameter ceramic housing.

EPOXY TO
ITEM 2 CYLINDER
4 PL

VIEW A-A

.87

3
REF

1

5

4

3 2 REQD
6 8 PL

1 REF

EPOXY ALL AROUND
BOTH ENDS

2

5

1.000

.100

TABS TO BE IN LINE
WITH OPP END CAP
TABS WITHIN .030 T.I.R.

A

A

PARTS LIST

16		MS16995-52	SOC HEAD CAP SCREW, .250-20UNC-2A X 1.00 L, CRES		6
2		0121967	END CAP		5
1		0121965	JACKET		4
8		0121961	RAIL		3
1		0121758	CYLINDER		2
4		-101	CUSHION, .125 X 1.75 X 27.30 LONG	CHLOROPRENE 25-35, AMS 3207	1
QTY REQD	FSCM NO	PART OR IDENTIFYING NUMBER	DESCRIPTION OR NOMENCLATURE	MATERIAL/SPEC./REF DESG	FIND NO

INTERPRET DRAWING IN ACCORDANCE WITH DOD STD 100 ANSI Y14.5M-82
DO NOT SCALE THIS DRAWING
UNLESS OTHERWISE SPECIFIED
DIMENSIONS ARE IN INCHES
BREAK ALL EDGES
REMOVE ALL BURRS .005 MAX
TOLERANCES ARE
.XX ± .03   .XXX ± .015
ANGLES ± 1/2°
FILLETS & RADII
SURFACE ROUGHNESS

PRGM MGR
R&R
QA
DESIGN
CHECKED   D. Peters 4/27/88
PREPARED   CVC   8/24/88
PROJECT NUMBER
COGNIZANT CODE
APPROVED FOR

NAVAL OCEAN SYSTEMS CENTER
SAN DIEGO, CA 92152-5000

CYLINDER ASSY,
CERAMIC HULL

FSCM NUMBER 55910   DRAWING NUMBER 0121971

SIZE D   SCALE 1/2   RELEASED DATE   SHEET 1 OF 1

0122298
0121975
NEXT ASSY   USED ON
APPLICATION

REVISIONS
ZONE REV   DESCRIPTION   DATE   APPROVAL

DWG NO 0121971 REV

53

Figure 34. Assembly drawing for the 20-inch-diameter cylindrical section.
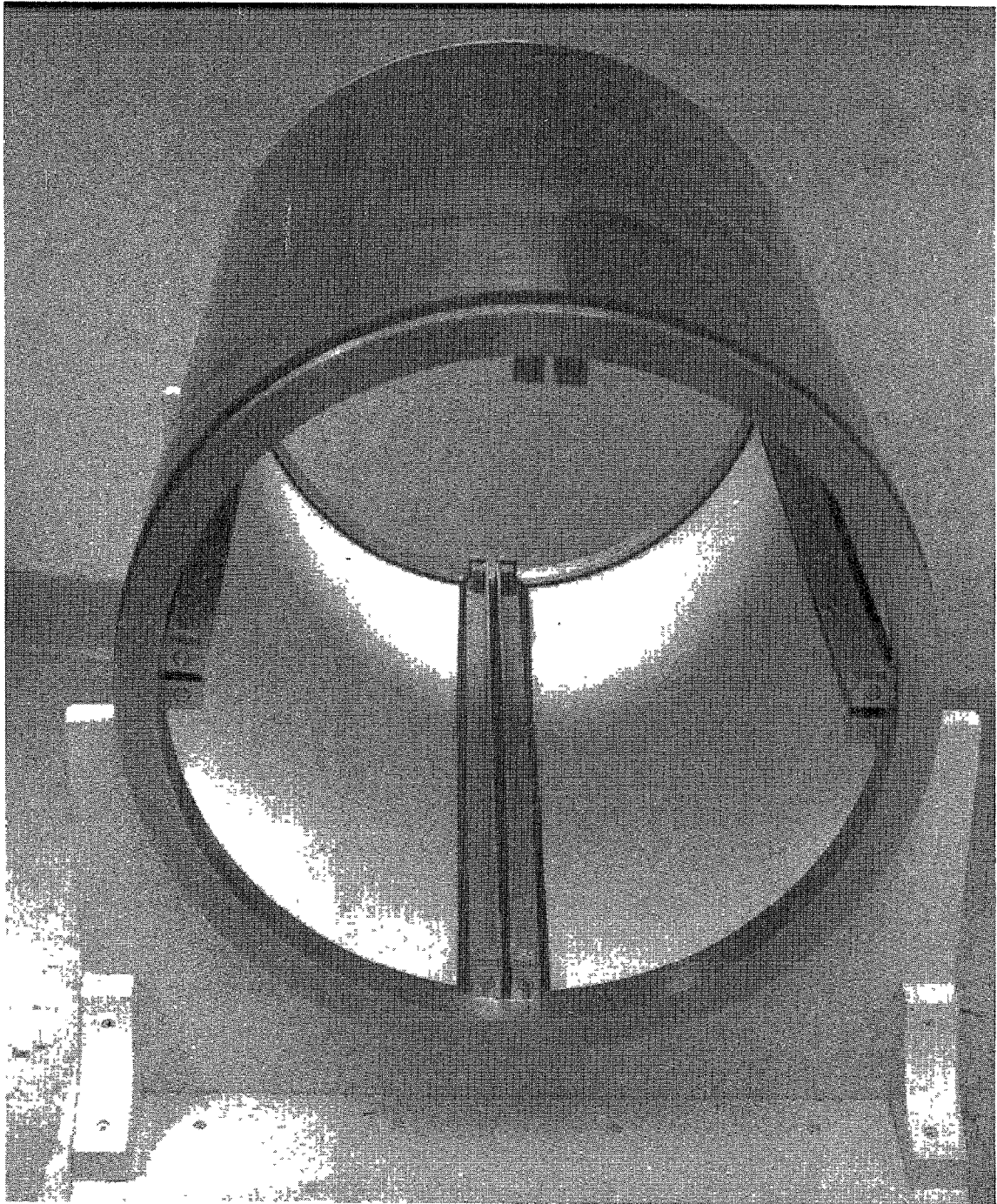
Figure 35. Inside view of the 20-inch-diameter cylindrical section. Note the rails for equipment shelves.
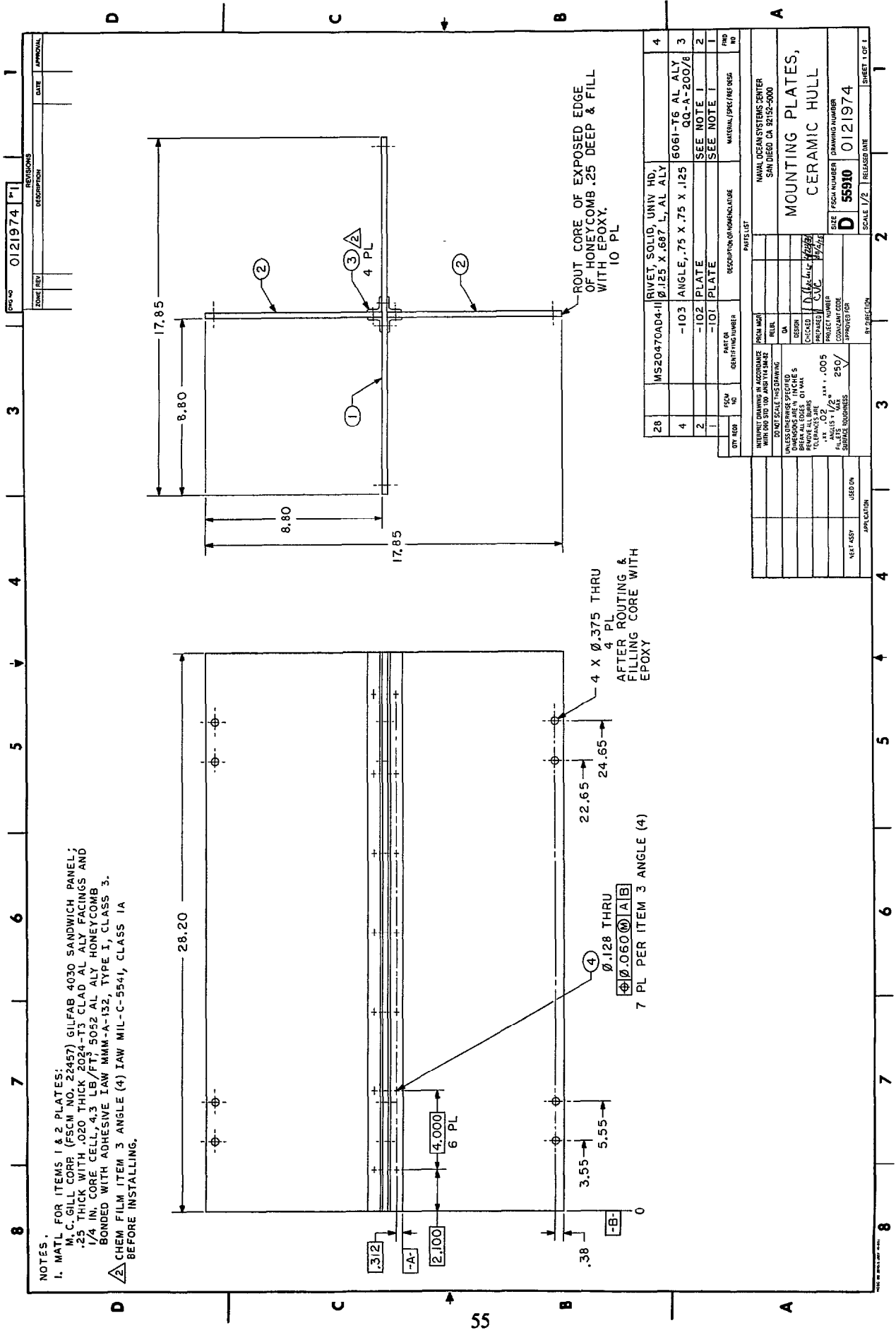
Figure 36. Drawing of shelves for mounting of equipment inside the cylindrical section of the housing.
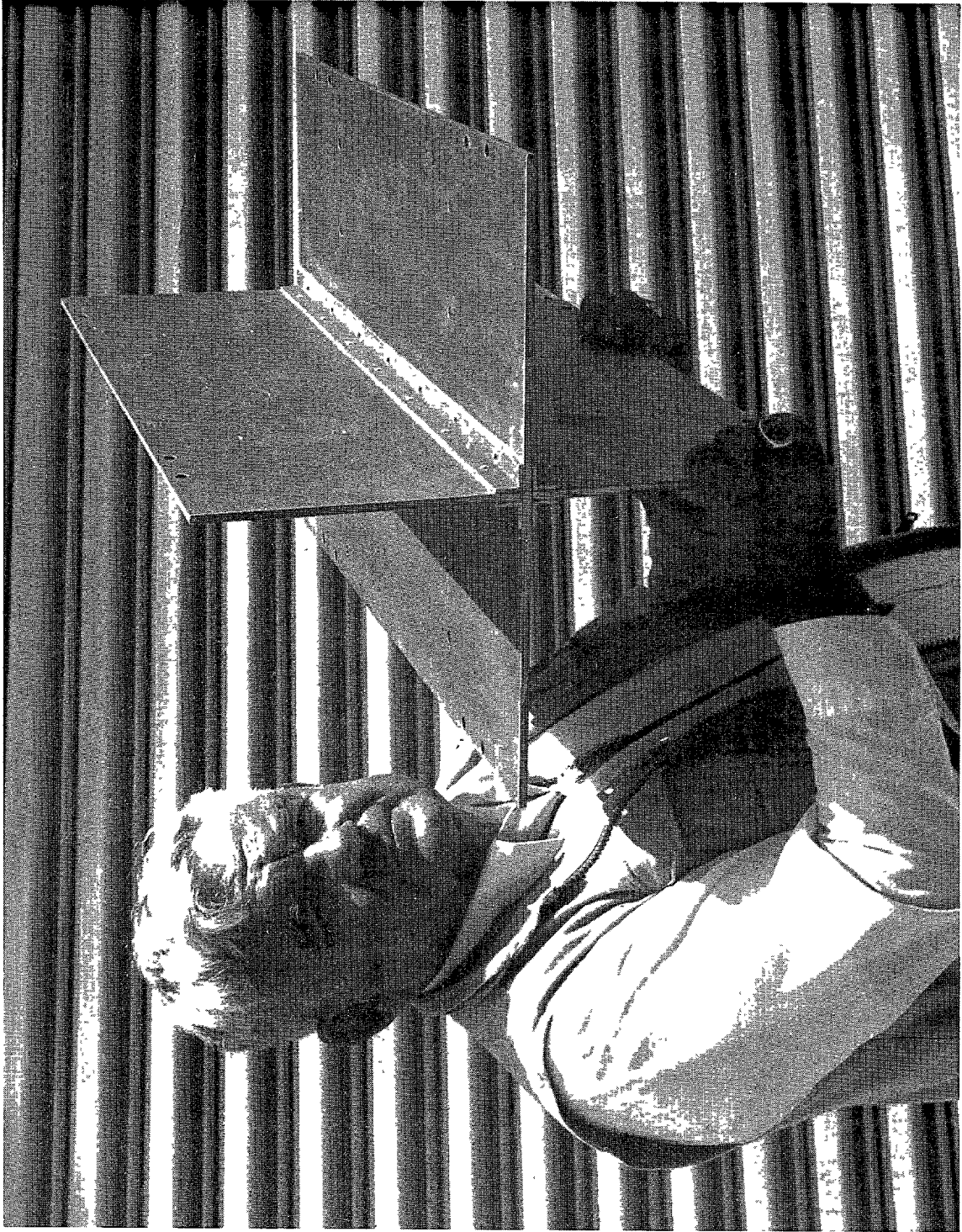
Figure 37. Shelf assembly for the 20-inch-diameter ceramic cylinders.

56
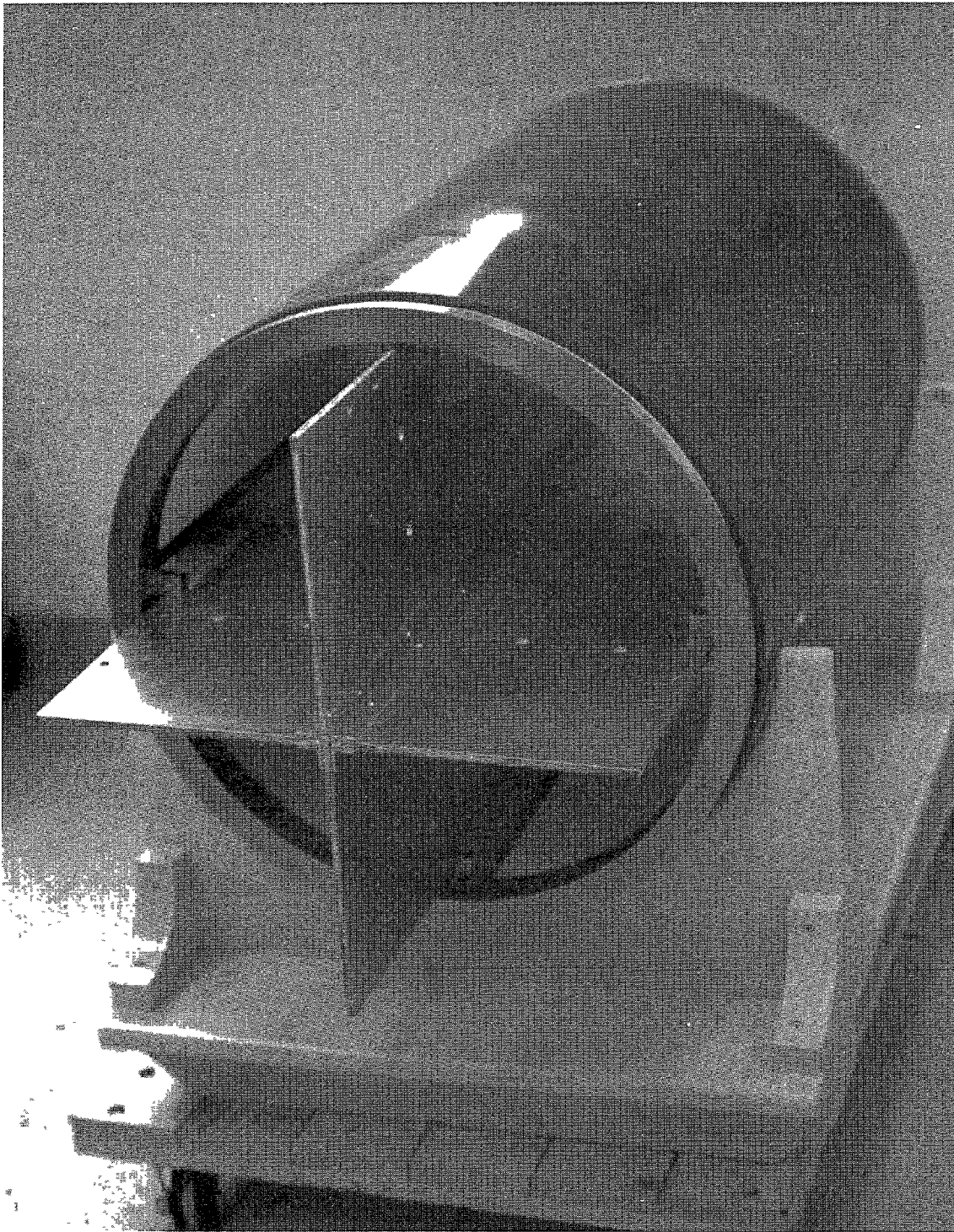
Figure 38. Shelf assembly partially inserted into the 20-inch-diameter ceramic cylinder.
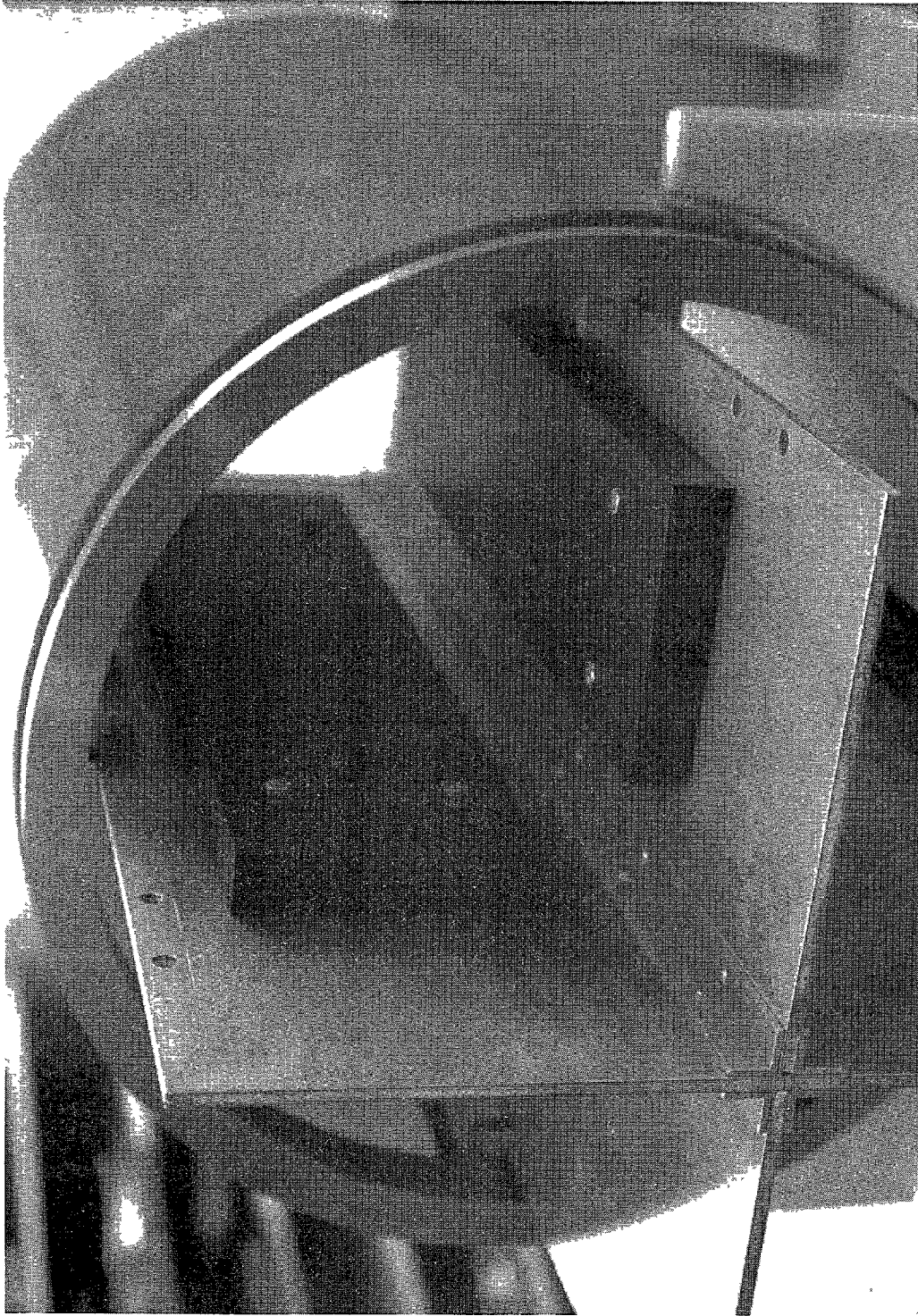
Figure 39. Shelf assembly with mounted blocks of aluminum simulating the weight of equipment.

Figure 40. Fabrication drawing of wedge clamp bands for locking together cylindrical and spherical sections of the 20-inch-diameter housing.

59
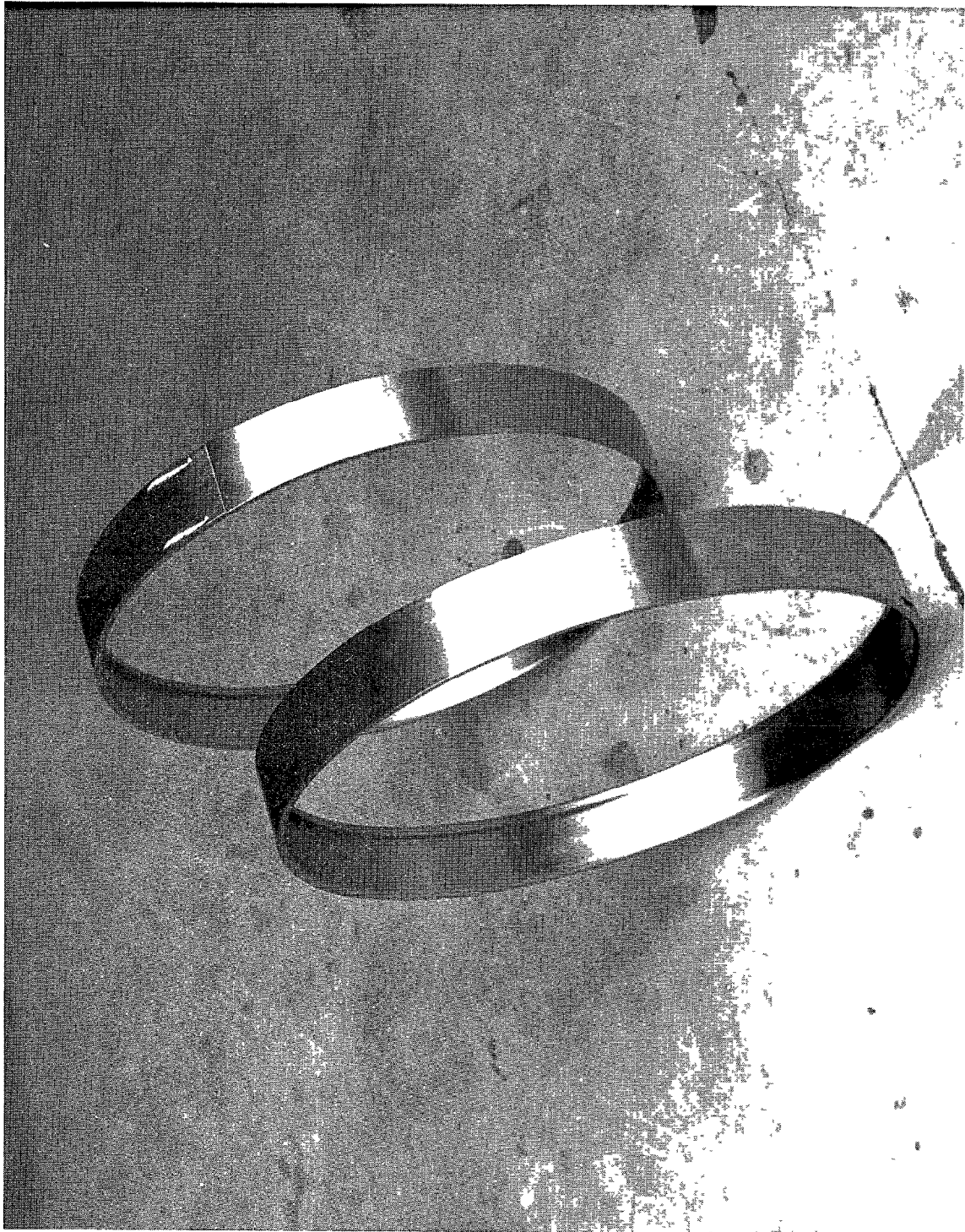
Figure 41. Wedge clamp bands assemblies.
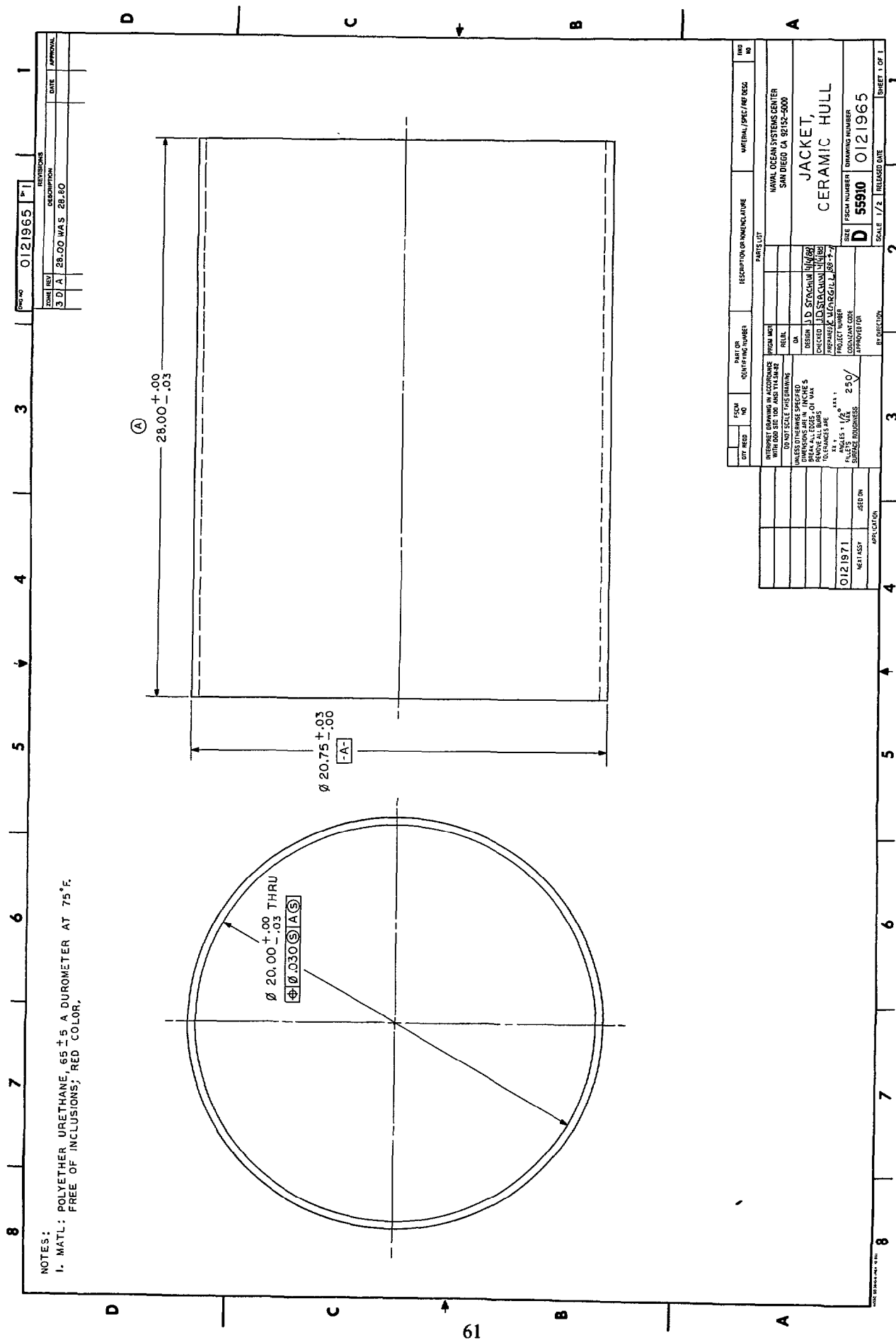
Figure 42. Fabrication drawing of elastomeric jacket for 20-inch-diameter ceramic cylinders.

61
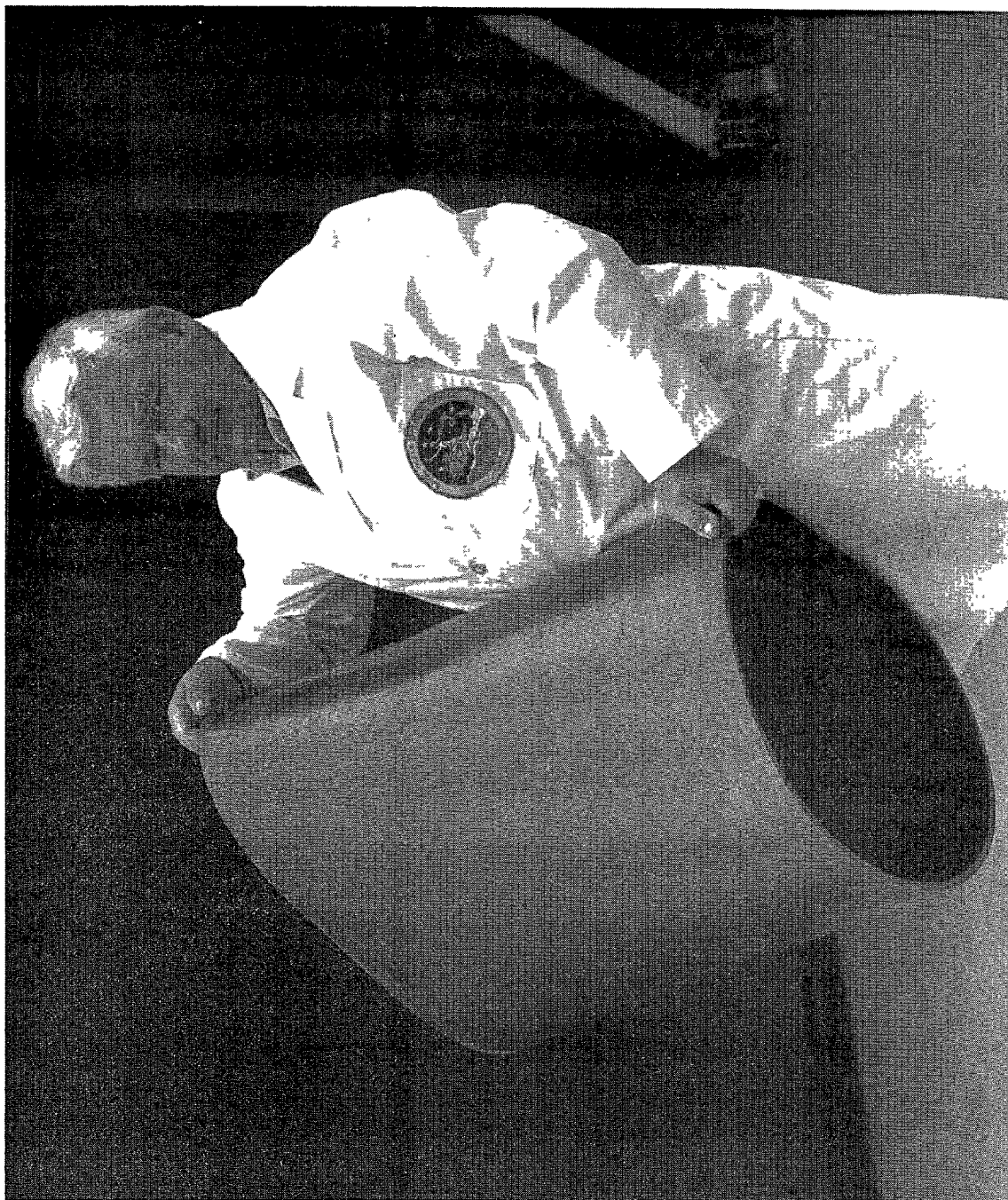
Figure 43. Elastomeric jacket for ceramic cylinders.
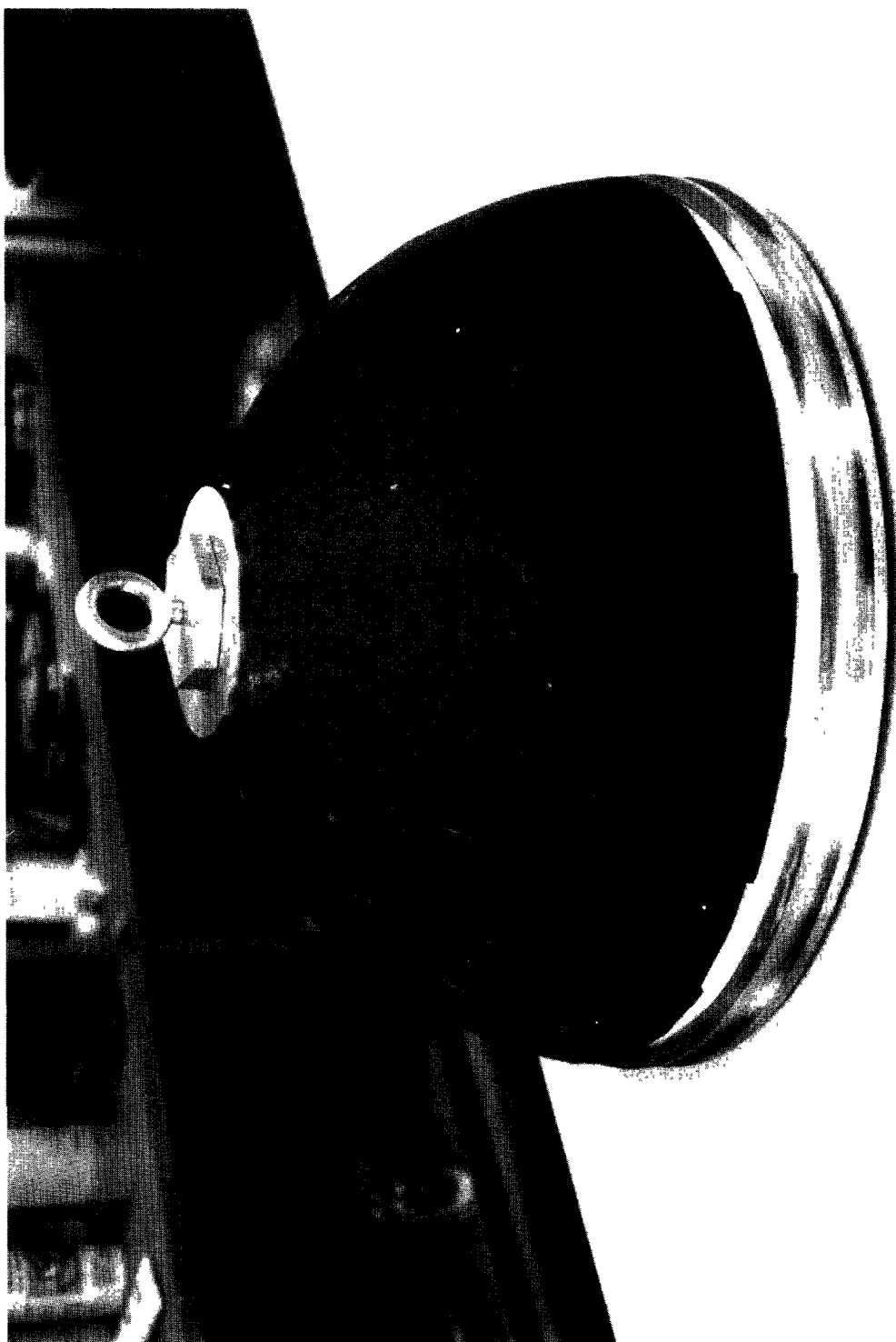
Figure 44   Mod III hemisphere assembly after bonding of neoprene jacket
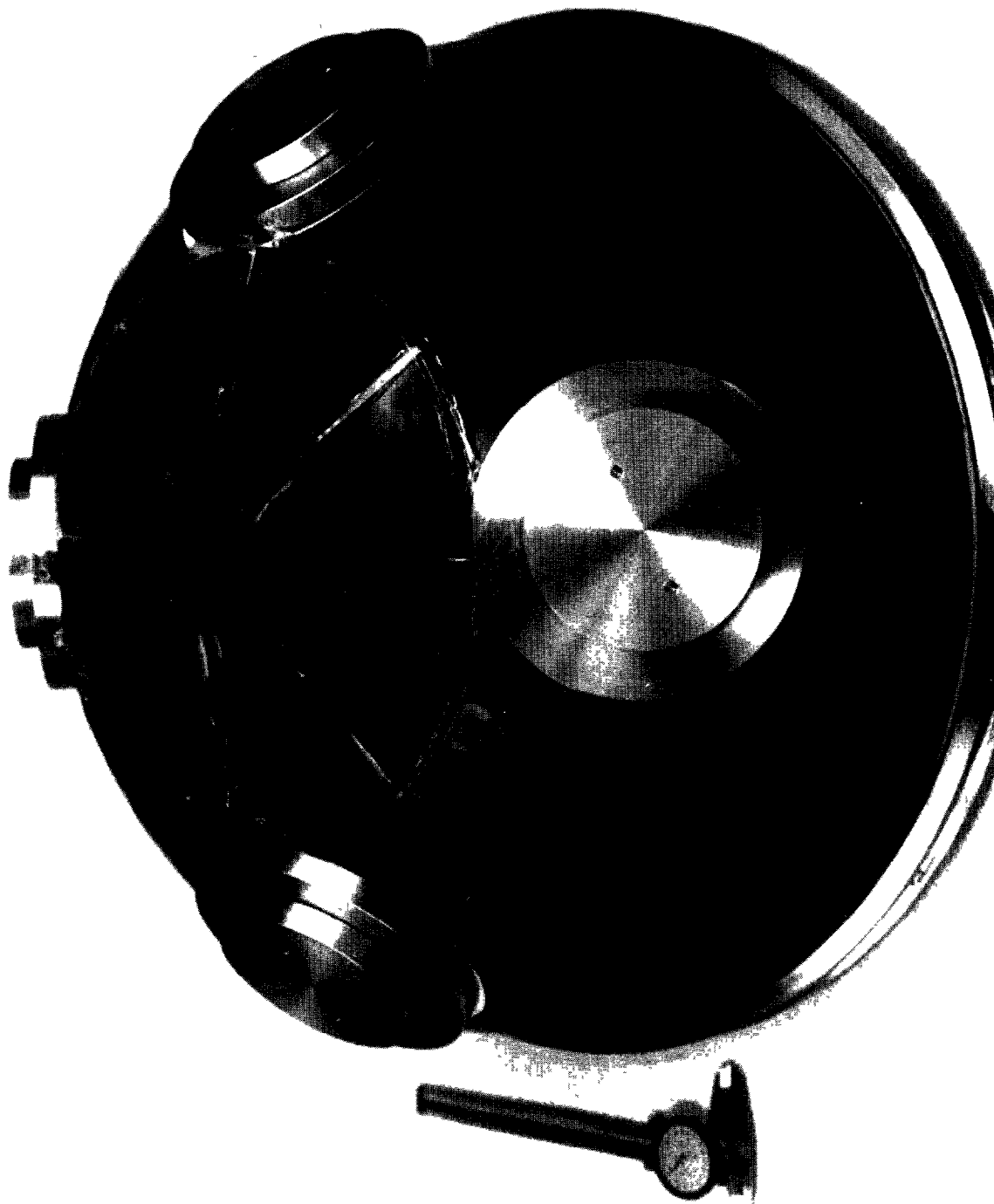
Figure 45   Mod II hemisphere assembly after bonding of neoprene jacket. Note the dummy plugs in penetrations inserts
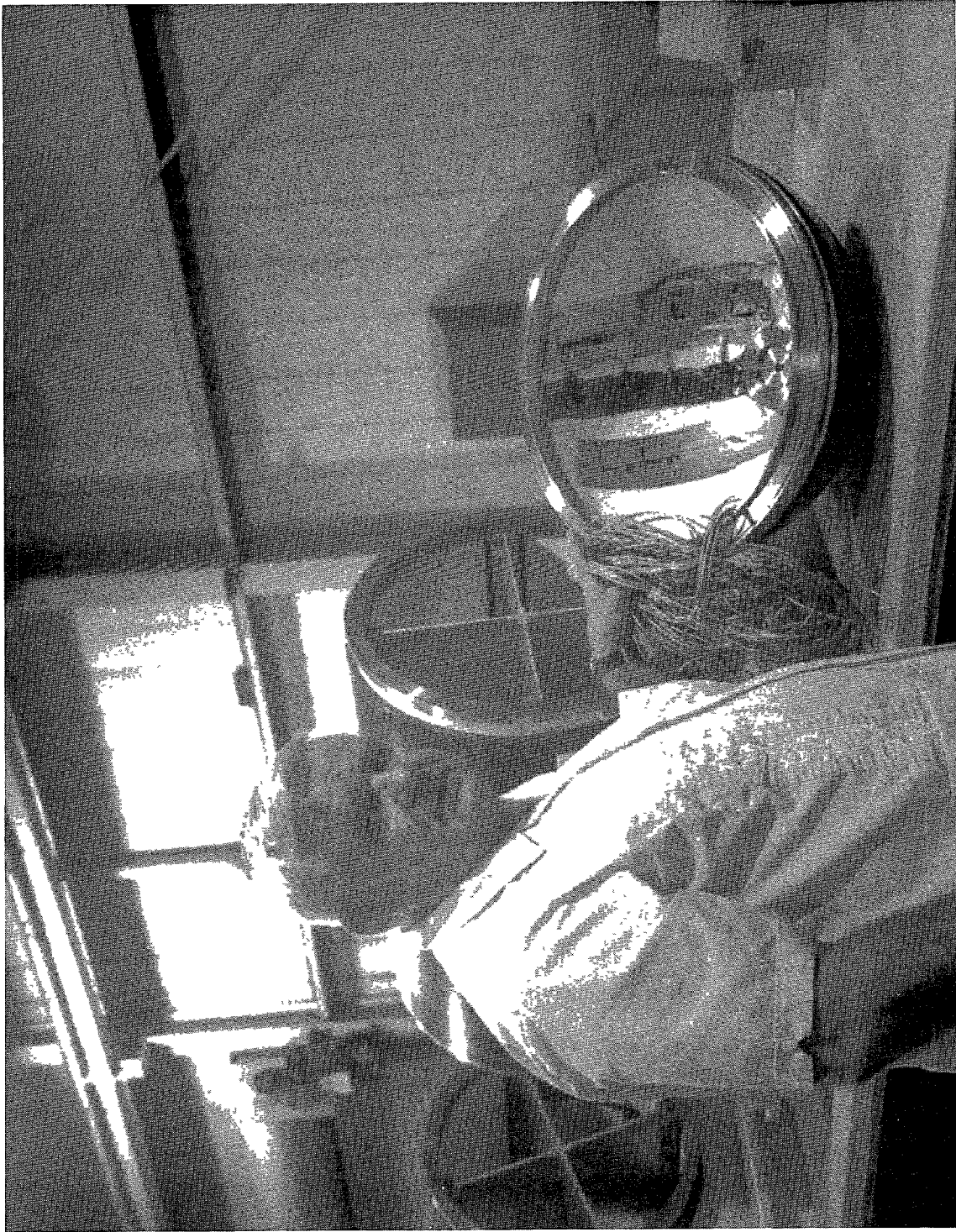
Figure 46. Instrumented Mod III hemisphere prior to mating with the cylindrical section for pressure testing.
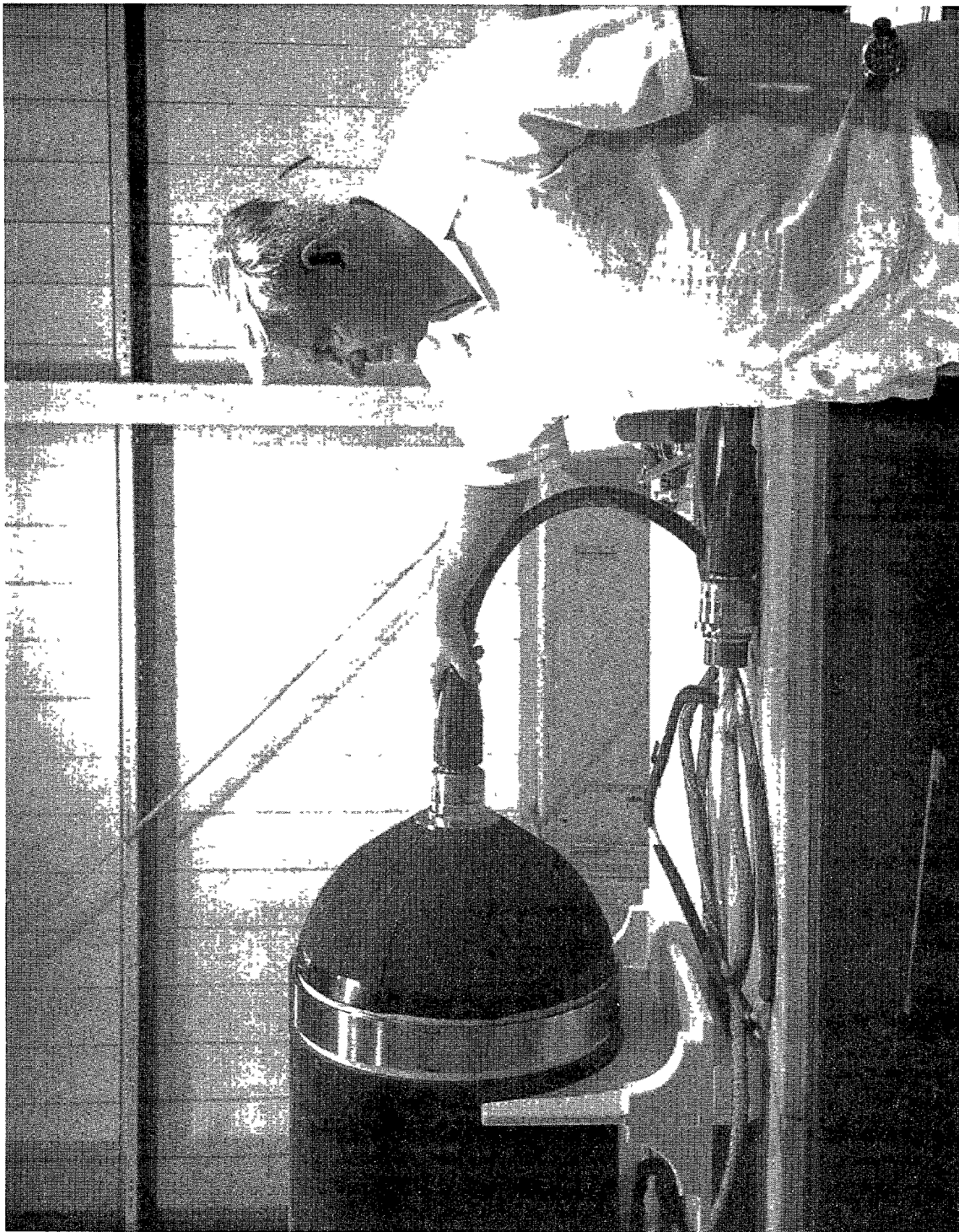
Figure 47. Attachment of instrumentation cable to the assembled housing.

Figure 48. List of components comprising the short (Mod I) housing test assembly made up of one cylinder and two hemispheres.

Figure 49. List of components comprising the long (Mod II) housing test assembly made up of two cylinders, joint stiffener, and two hemispheres.

Figure 50. Assembling the short housing assembly.
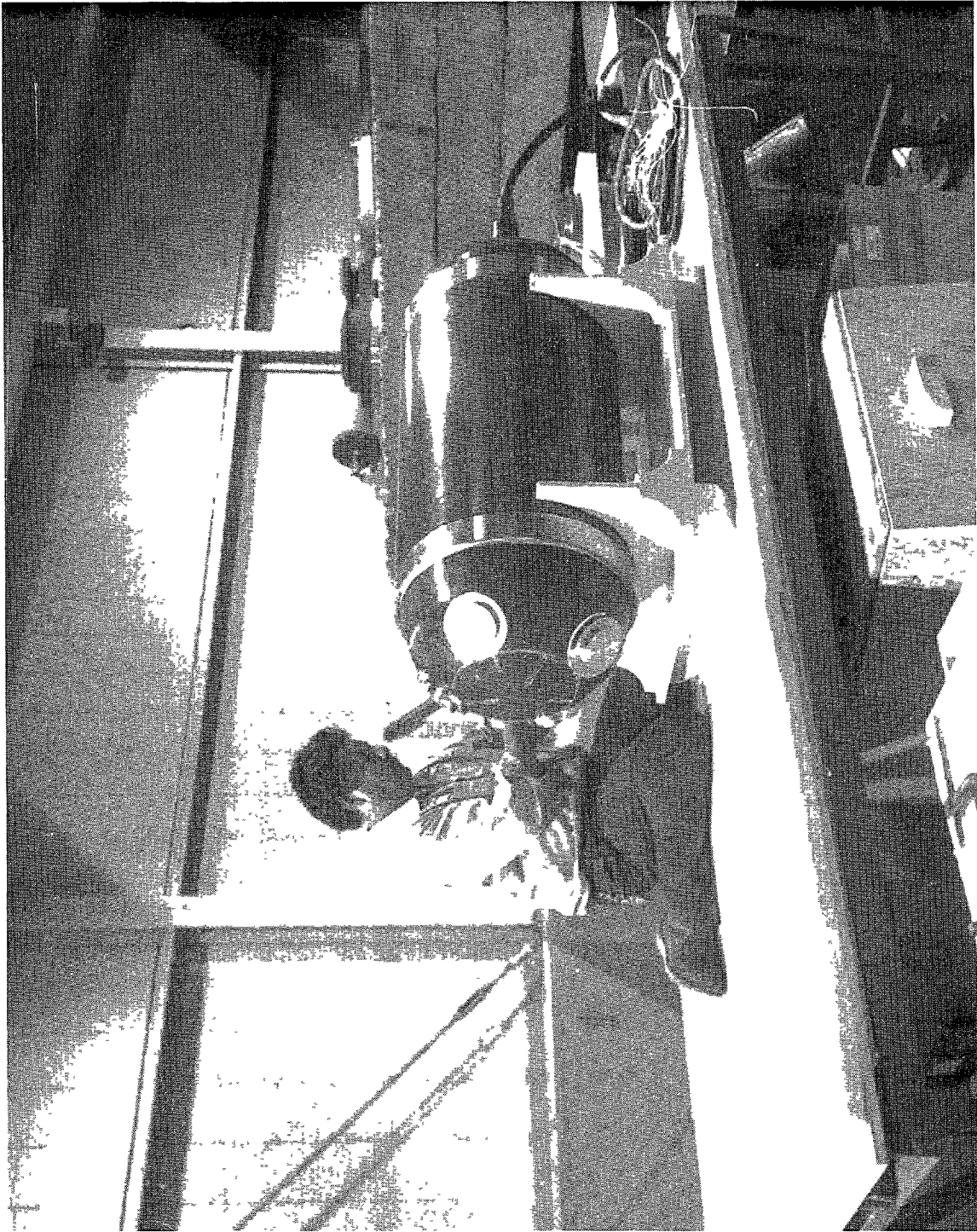
Figure 51. Tightening up the wedge clamps on the assembled short housing.

Figure 52. Lifting the short housing assembly from the cradle

71
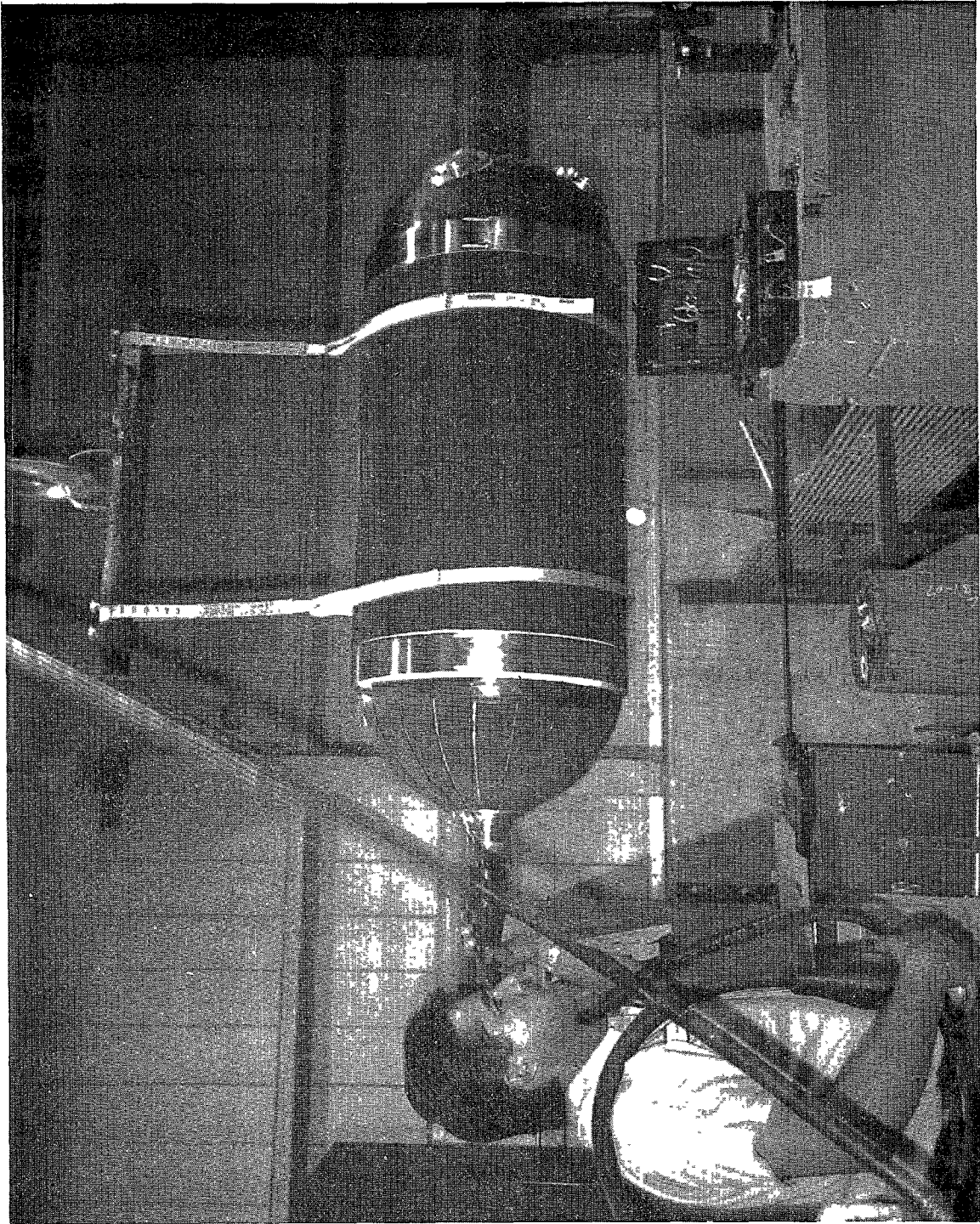
Figure 53. Transporting the short housing assembly to the vicinity of pressure vessel.

Figure 54. Removing the lifting straps from the short housing assembly.
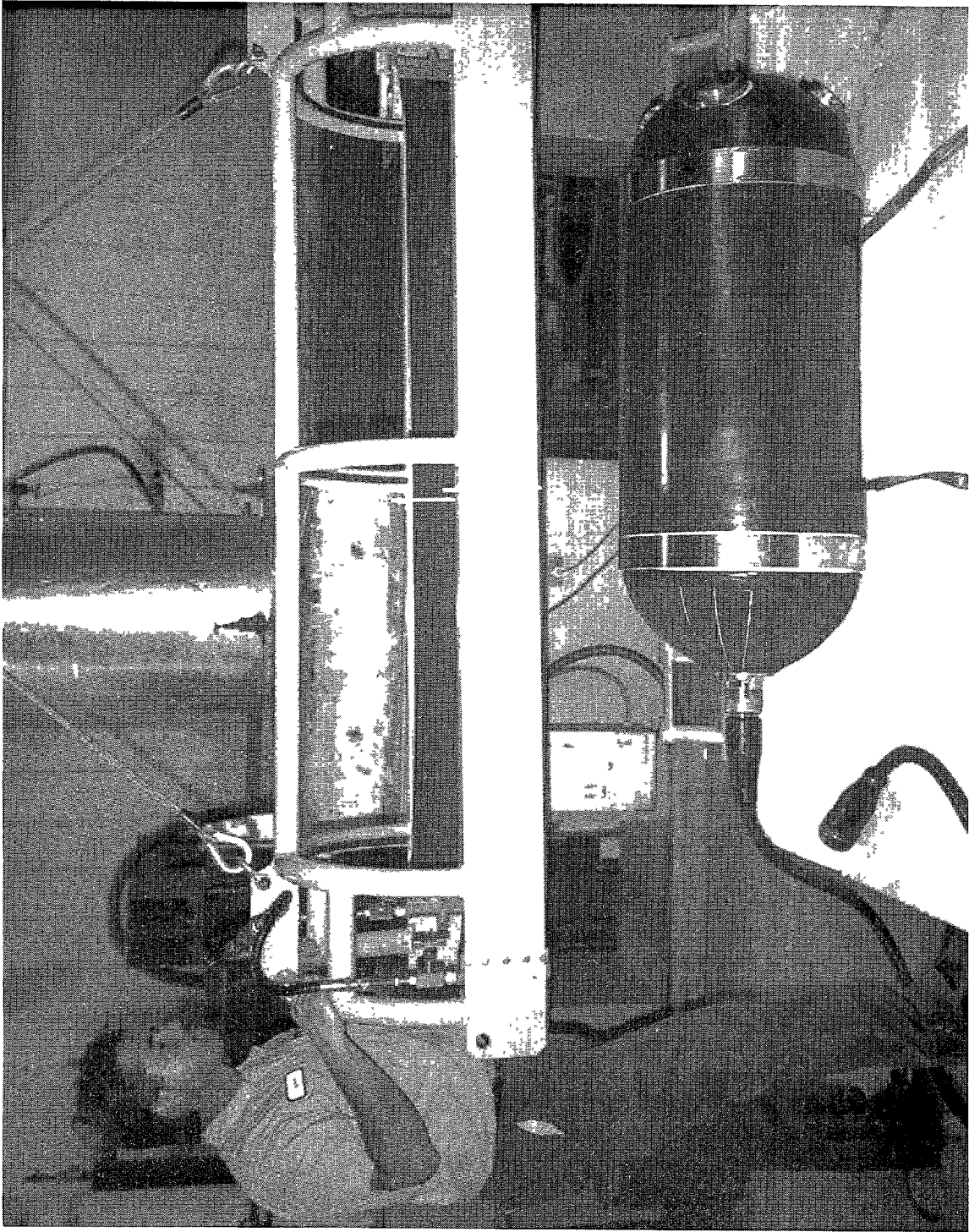
Figure 55. Placing the upper half of lifting cage fixture over the short housing.
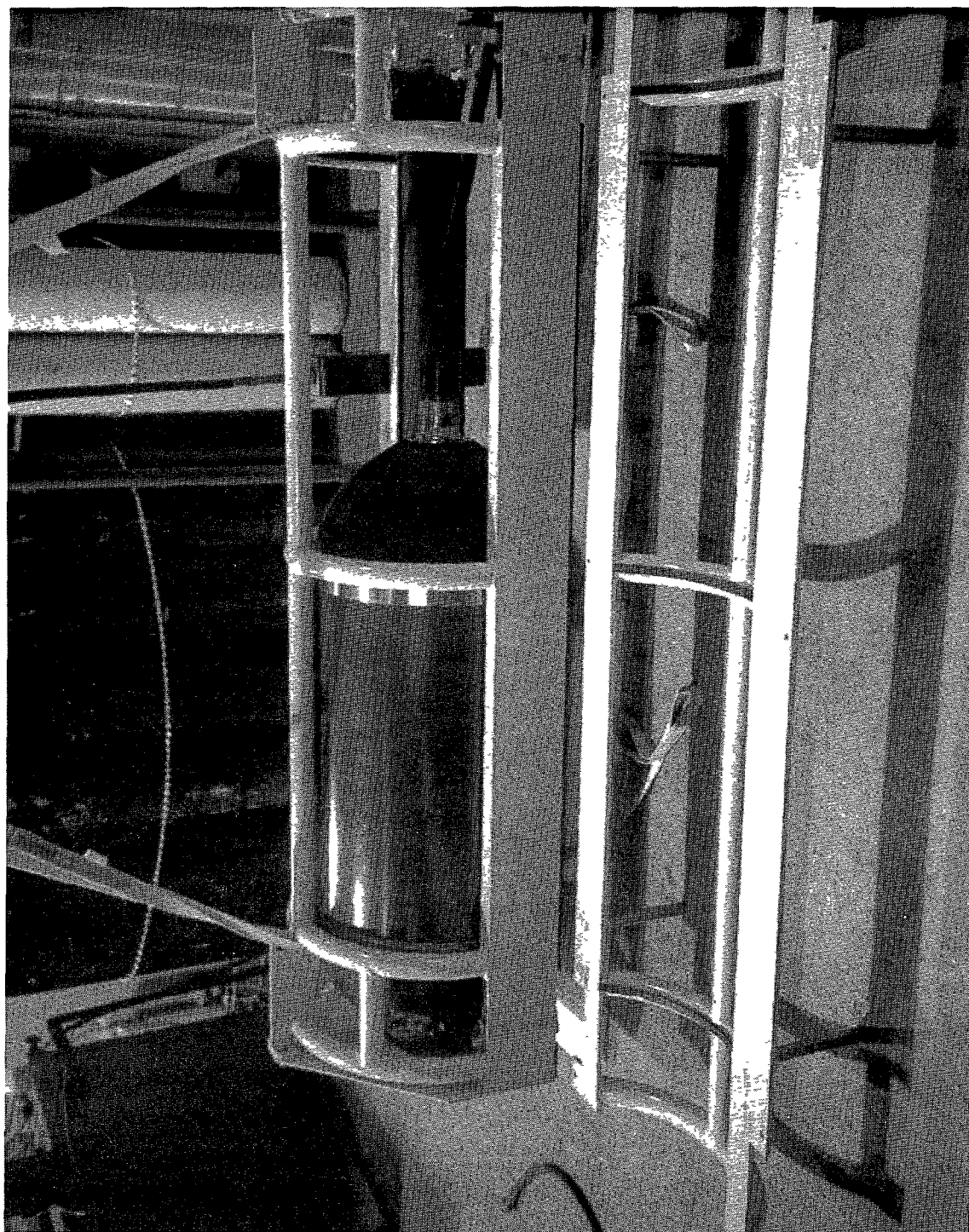
Figure 56. Lifting the short housing with the upper half of cage fixture (after securely gripping the housing with pneumatically inflated elastomeric actuators) and placing it into the lower half of the cage fixture.
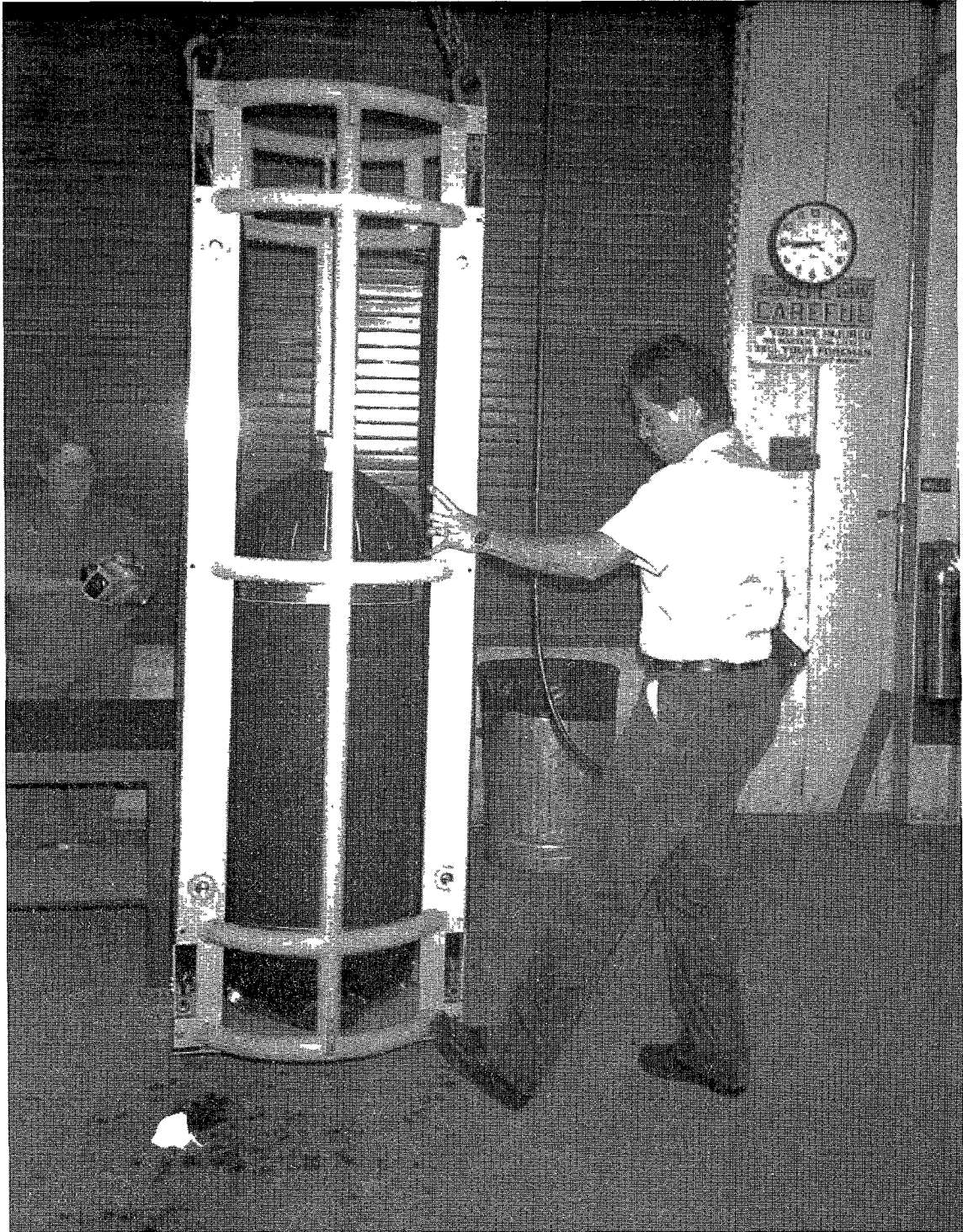
Figure 57. After bolting together the two halves of the cage fixture, the cage is rotated into vertical position and the compressed air line disconnected.
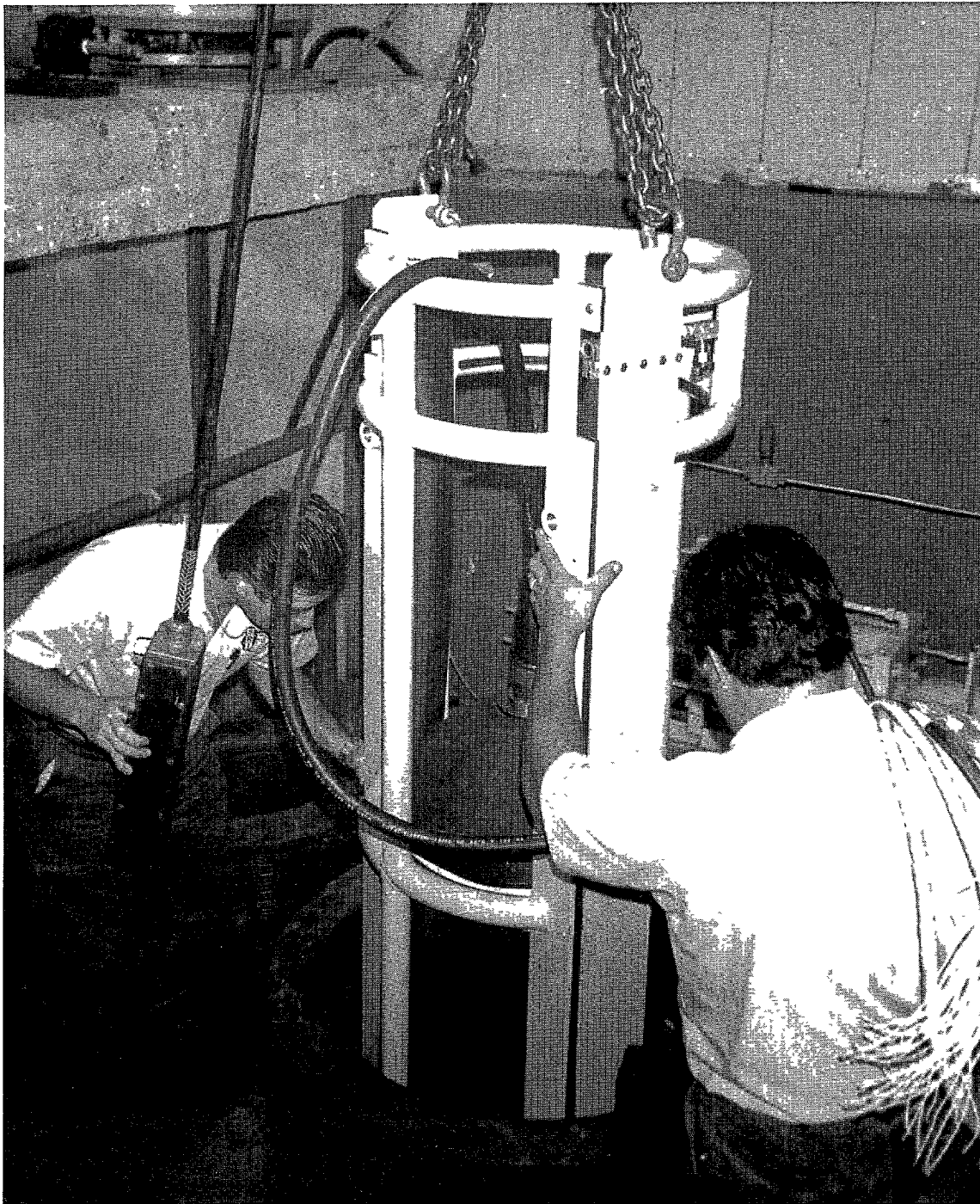
Figure 58. Placing the cage with the short housing assembly into the 30-inch-diameter pressure vessel at Southwest Research Institute.
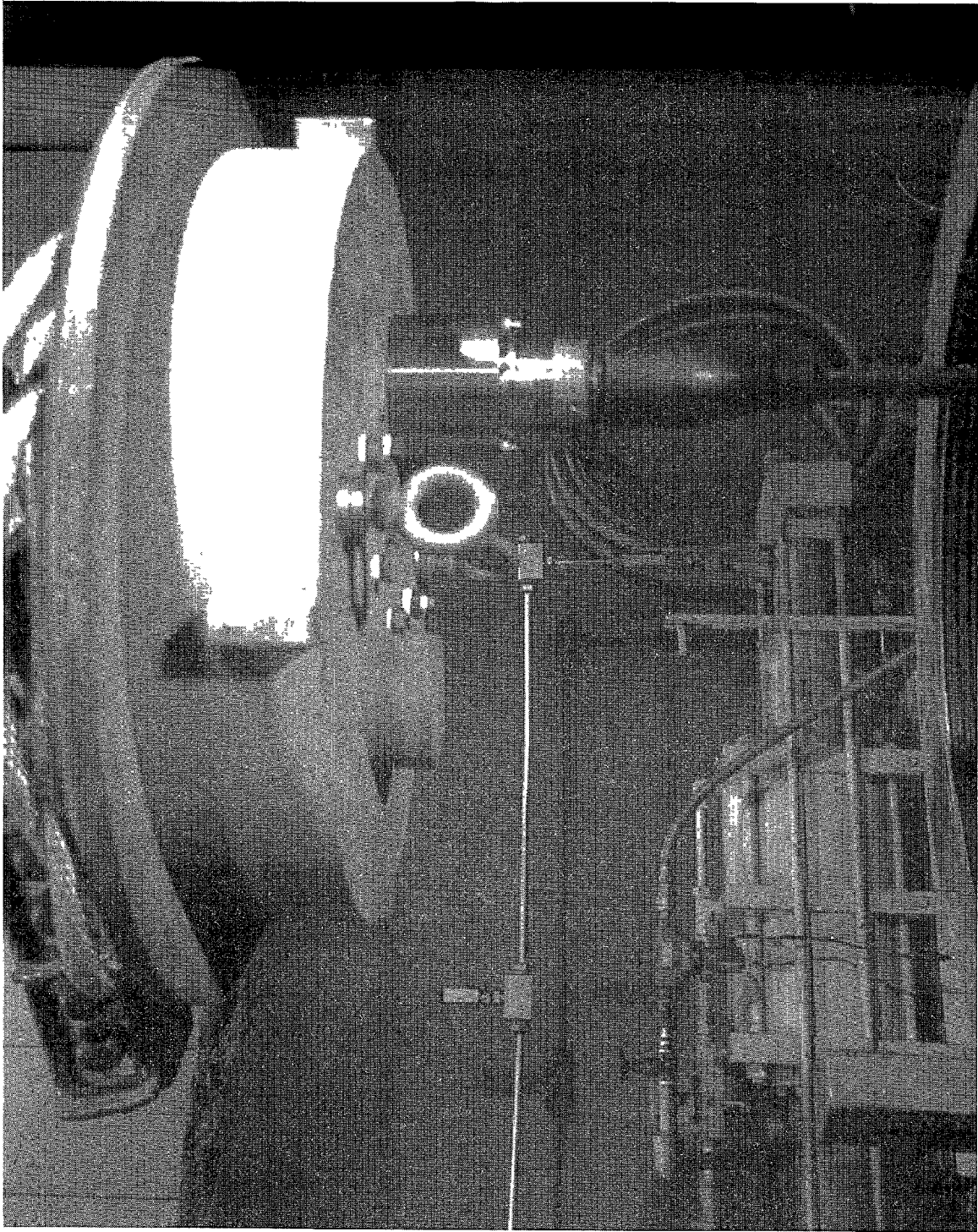
Figure 59. Attaching the instrumentation cable to the pressure vessel end cover completes the preparation of the short housing test assembly for pressure testing.
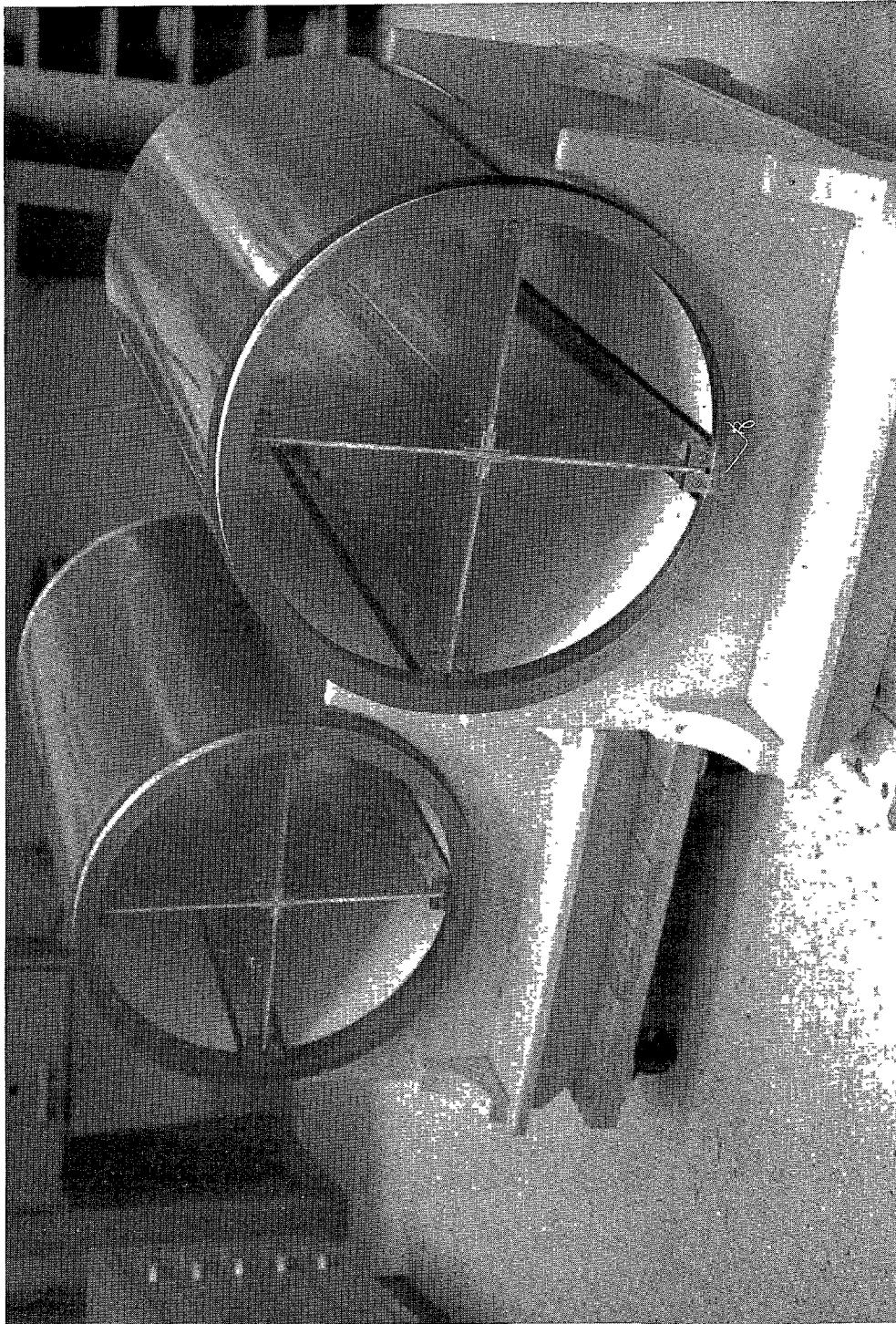
Figure 60. Two cylindrical sections from which the long housing is assembled.
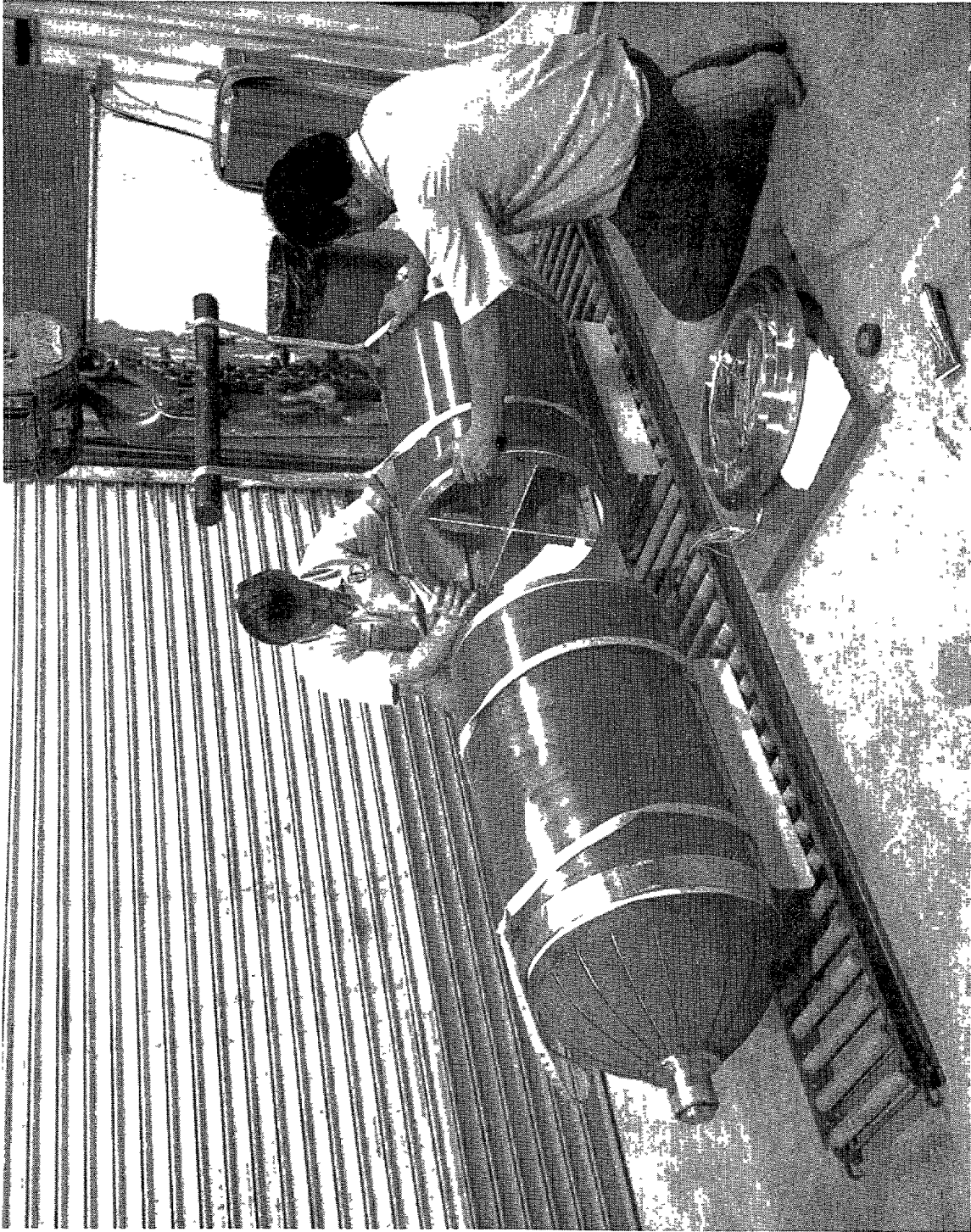
Figure 61. Mating of components for the long housing test assembly. Note the roller conveyer which facilitates the mating of components.

Figure 62. Completed long housing test assembly.

81
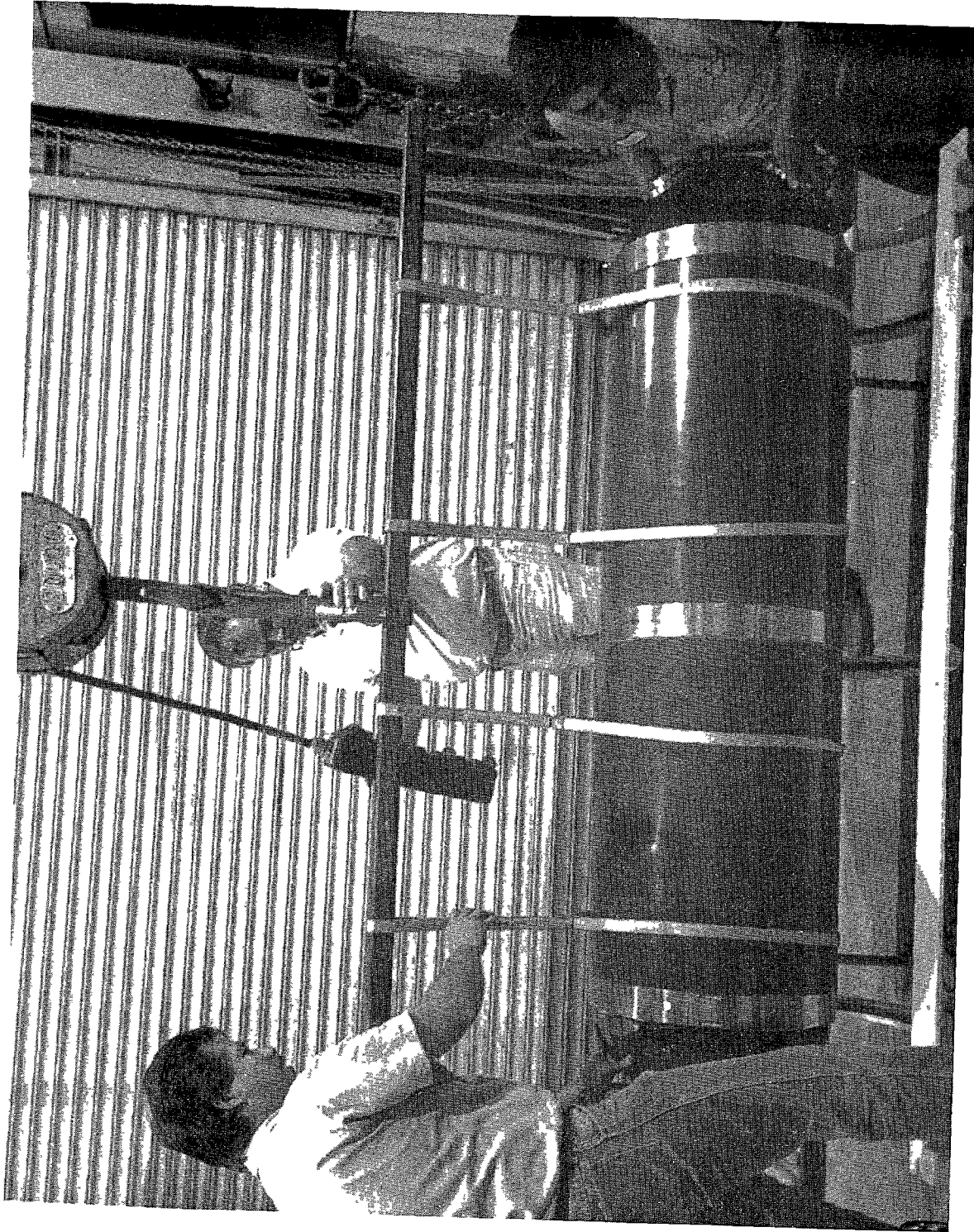
Figure 63: Lifting of the long housing test assembly from the roller conveyer and placing it into the lower half of the cage fixture.
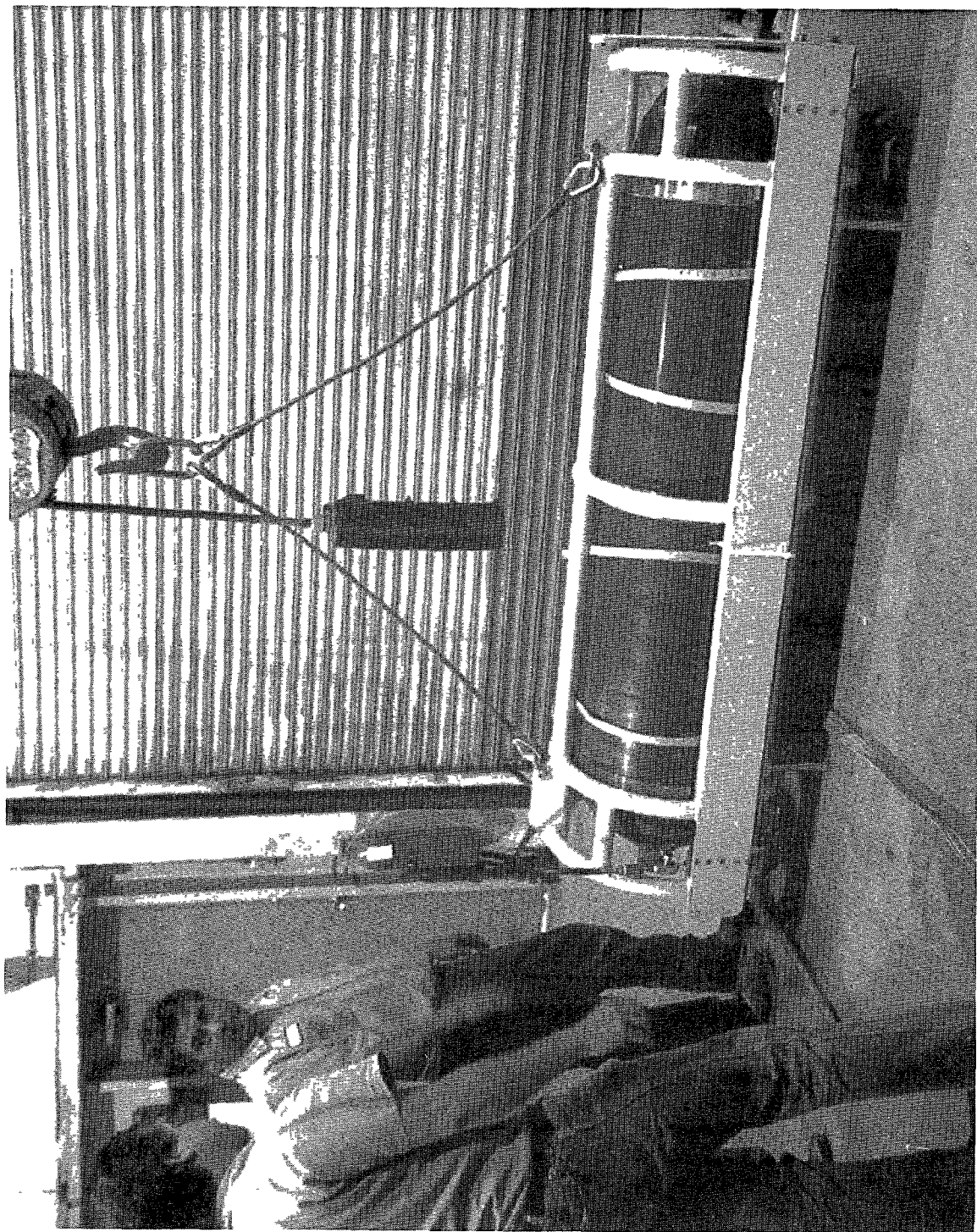
Figure 64. Lifting of the assembled cage with long housing assembly.
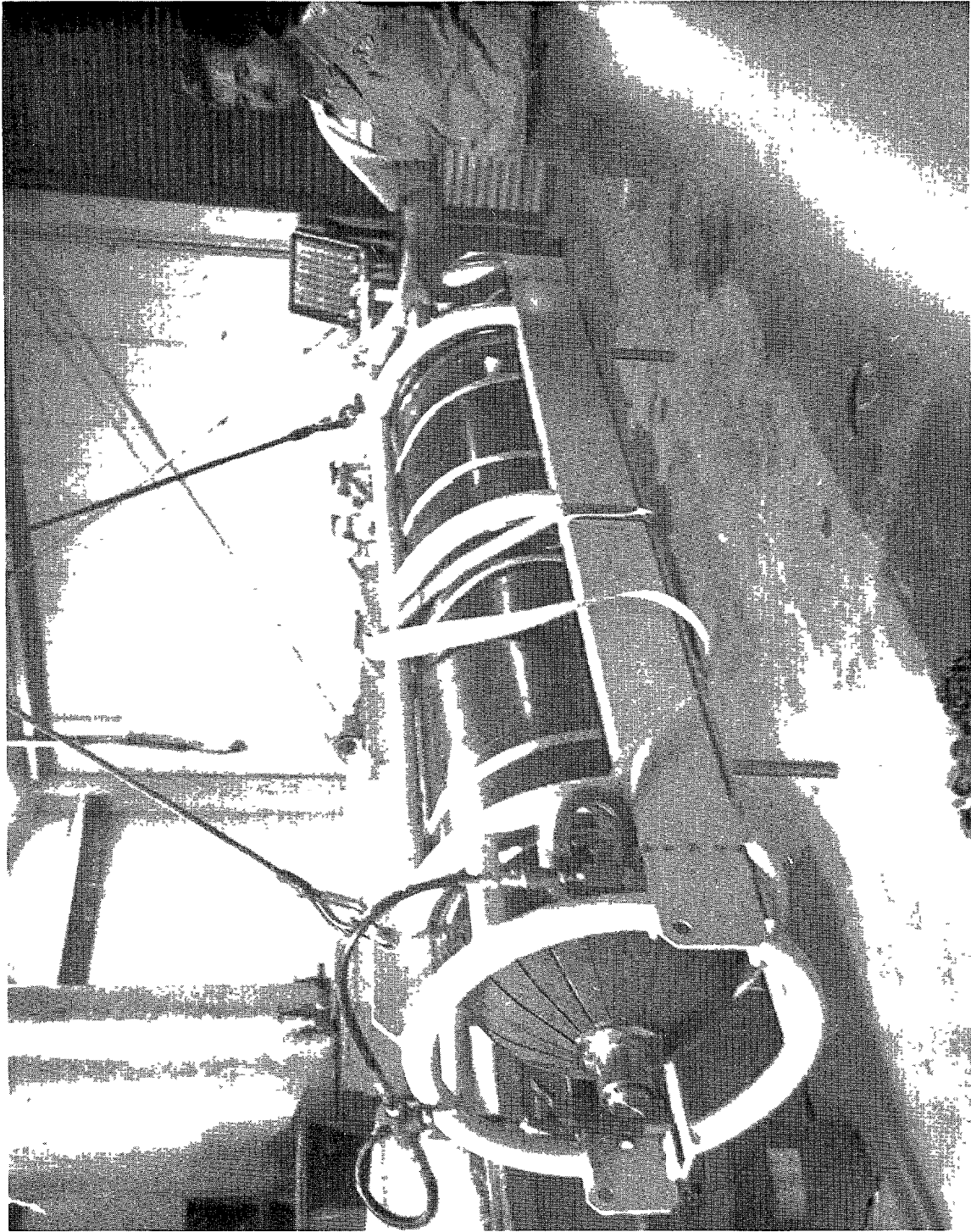
Figure 65. Transporting the cage with the long housing assembly to the pressure vessel. Note that the bottom half of the cage is bolted securely to the upper half of the cage, providing assurance against accidental release of housing in case of air pressure failure.
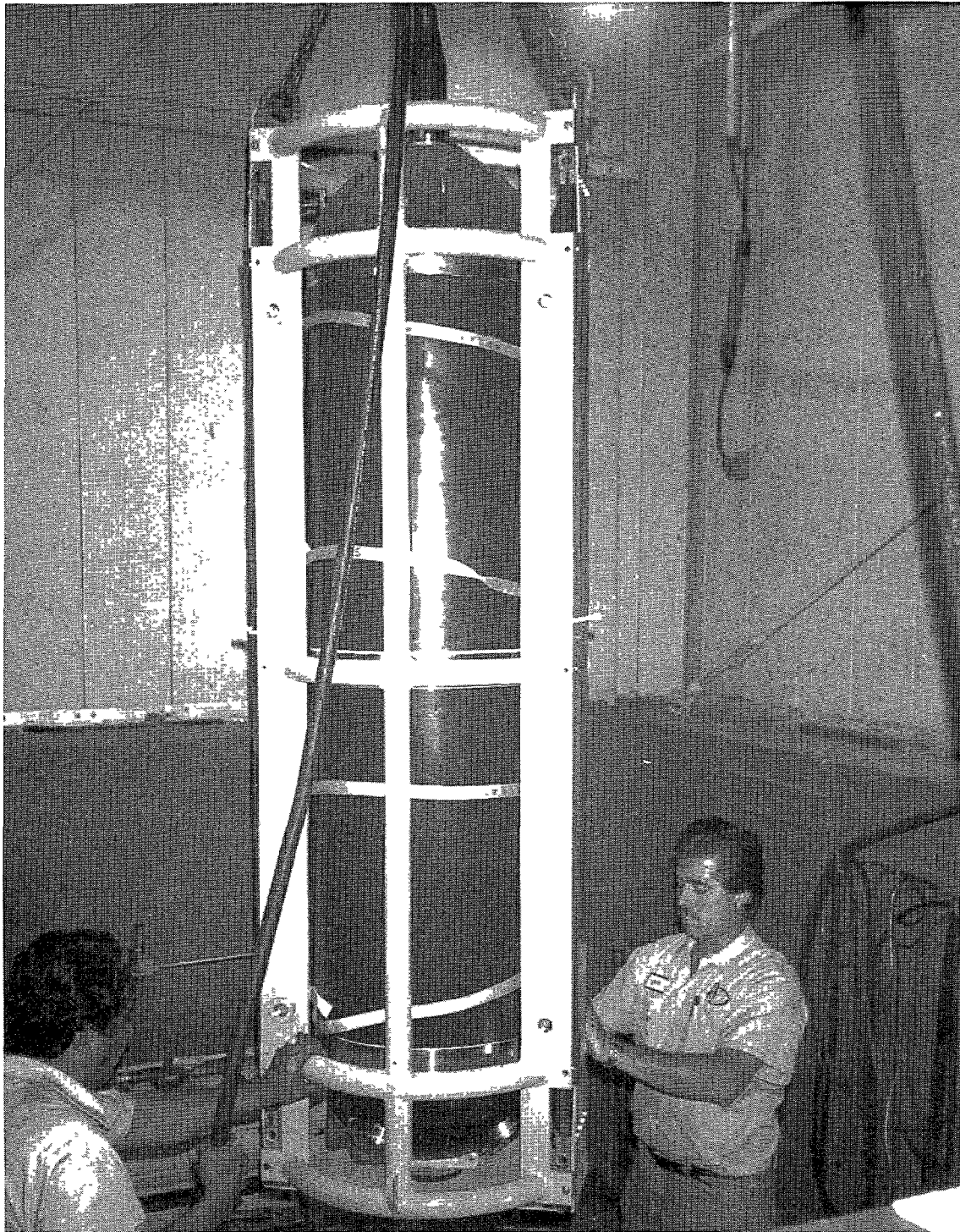
Figure 66. Lowering of the test fixture with long test housing into the 30-inch-diameter pressure vessel at Southwest Research Institute.
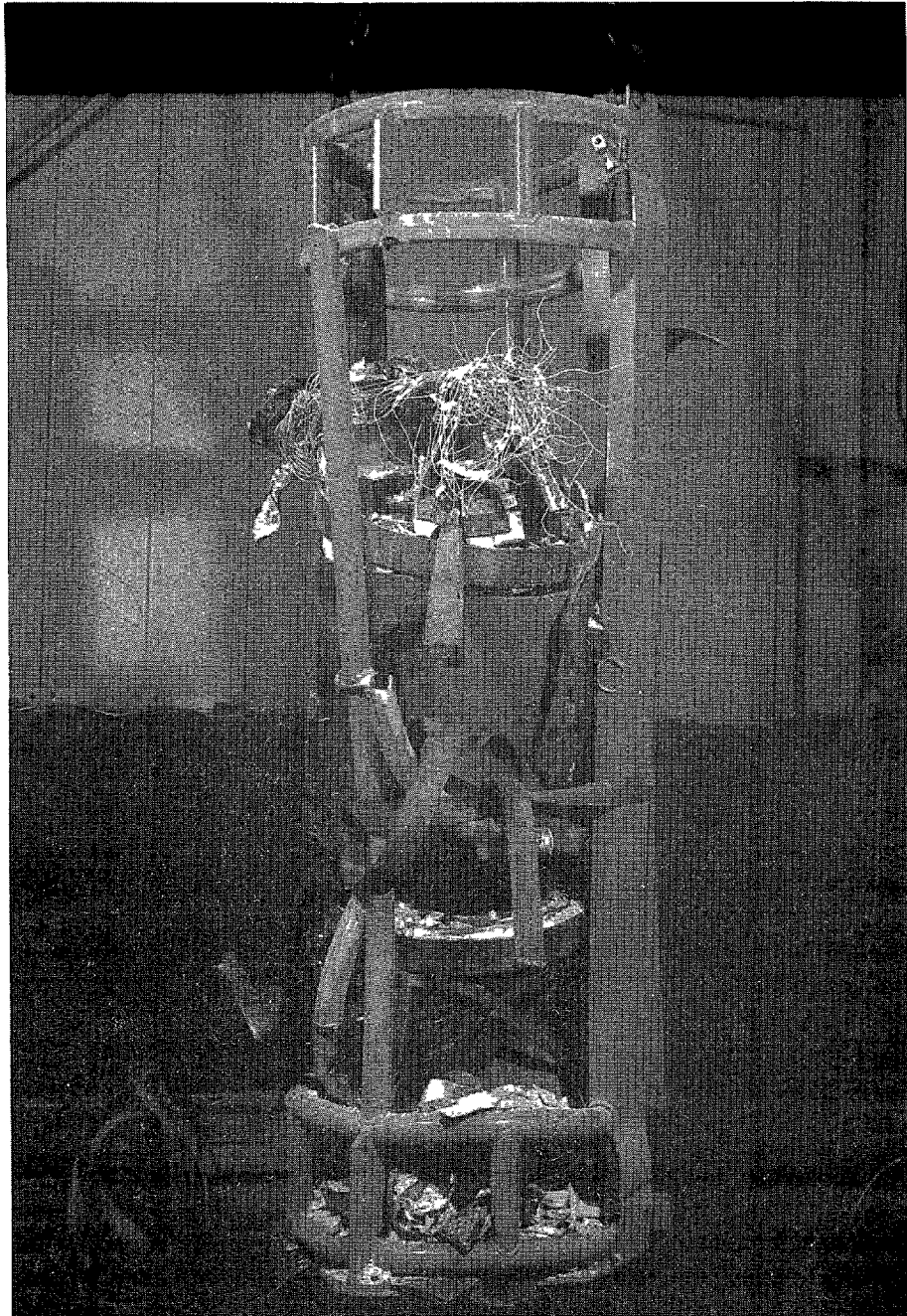
Figure 67. Imploded long housing assembly.

Figure 68. Fragments of the imploded long housing assembly.

Figure 69. Remnants of an imploded cylinder. Locally bent mounting rails indicate that the implosion originated at the edge of joint stiffener and not at the other end mated with the hemisphere.
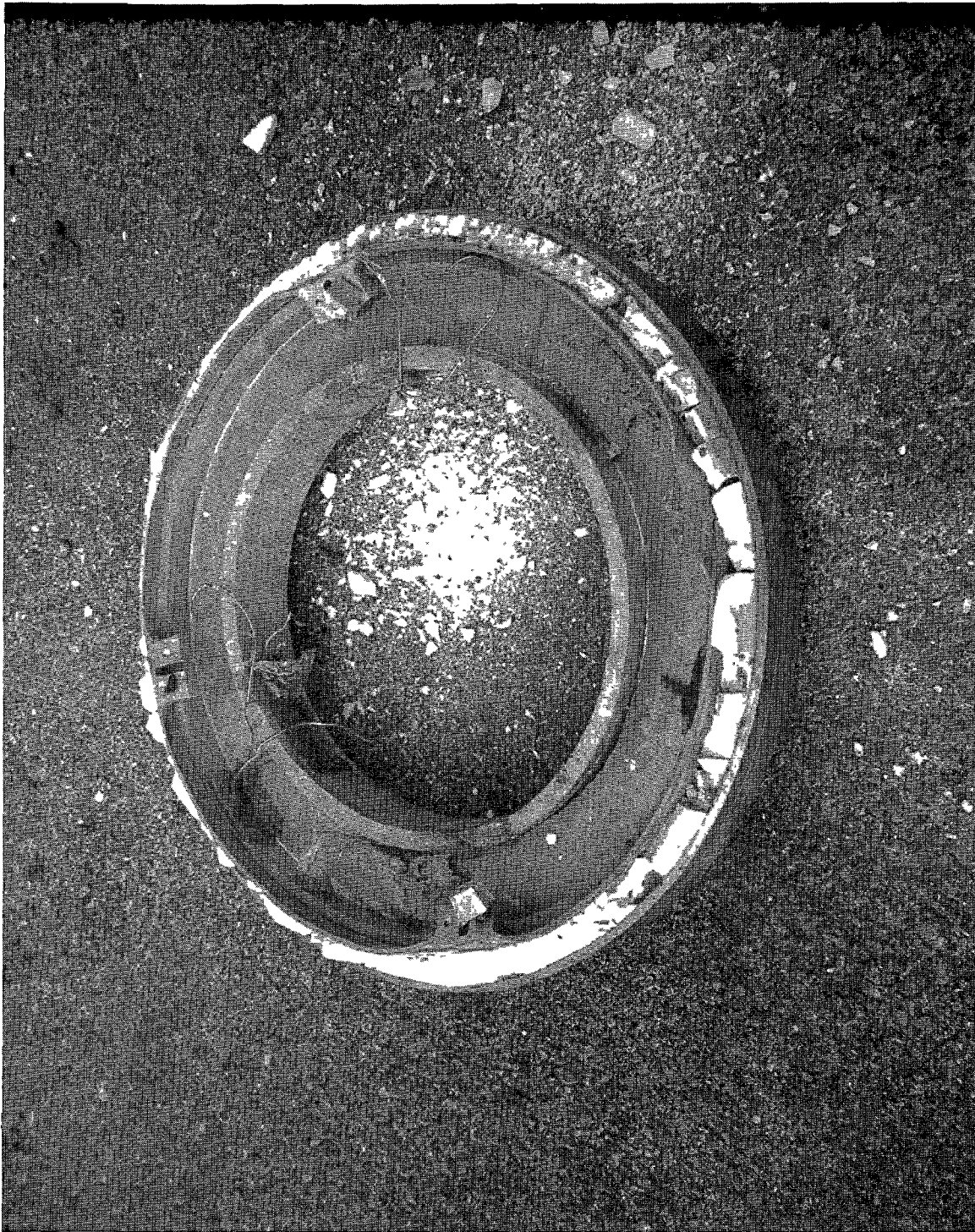
Figure 70. The circularity of the joint stiffener indicates that the implosion was not triggered by elastic instability of the joint stiffener.

Figure 71 The circularity of the wedge clamp band and the hemisphere end cap indicates that the implosion was not triggered by the failure of the hemisphere to which the instrumentation cable was attached

Figure 72. The end cap protector for the other hemisphere. The circularity of the fitting indicates that this hemisphere also did not initiate the implosion.
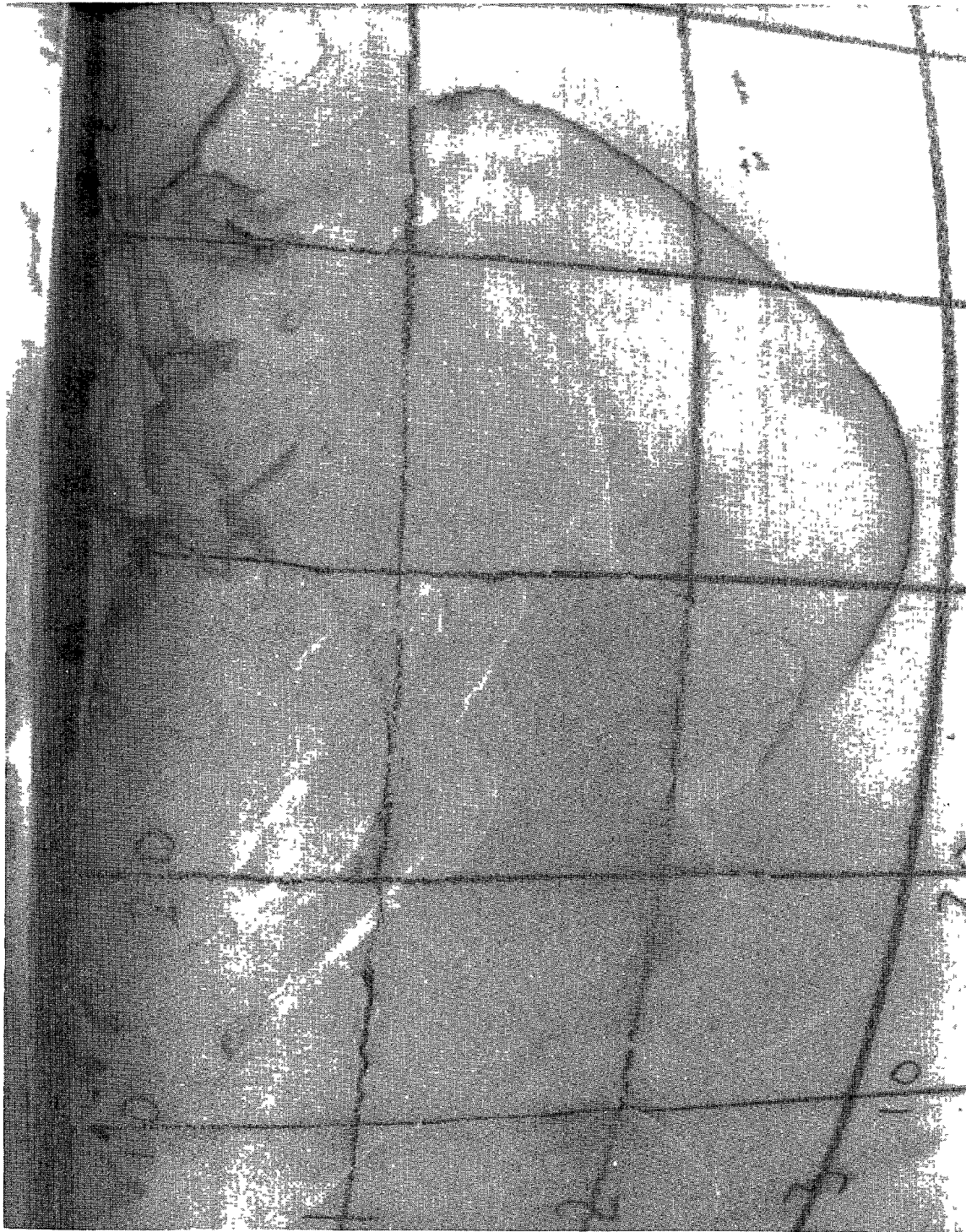
Figure 73. Typical spalling on the outside of ceramic shells observed near the end caps prior to catastrophic failure. The spalls are thickest at the bearing surface where they originate and then thin out with distance from the bearing surface.

STRAINGAGE LOCATIONS ON HEMISPHERES

CERAMIC HEMISPHERE MOD III
INTERIOR SURFACE

SEE DWG 0121705

EQUAL SPACING

CERAMIC HEMISPHERE MOD II
INTERIOR SURFACE

SEE DWG 0121954

45°
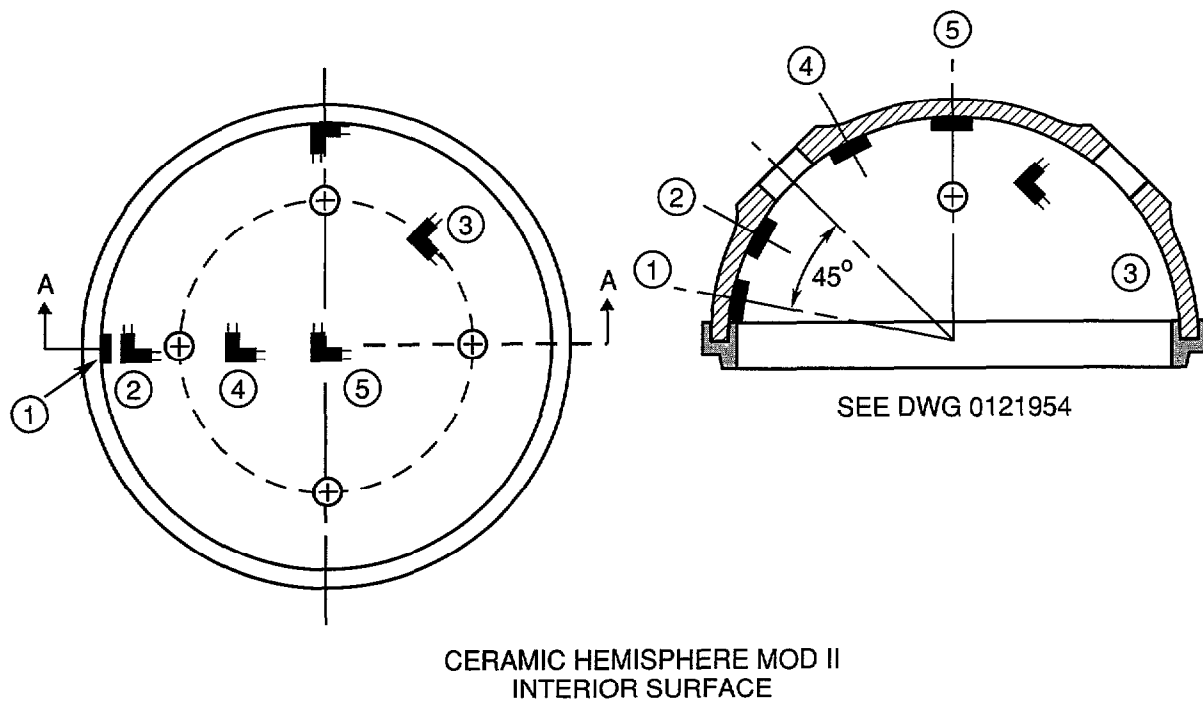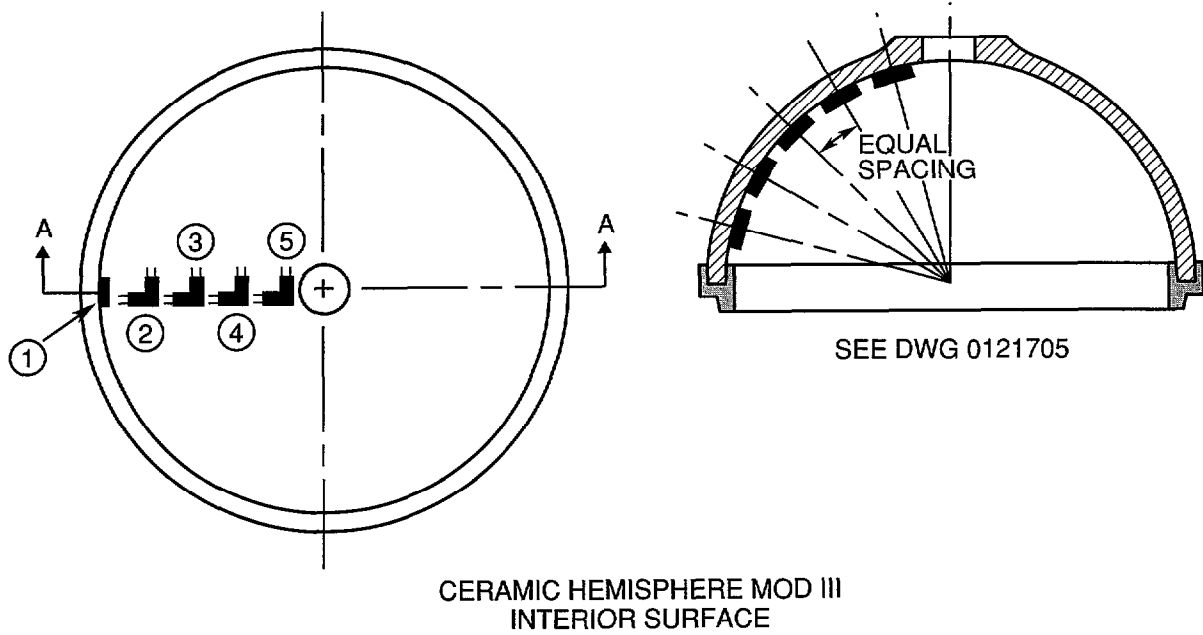
Figure 74. Location of strain gages on the interior surfaces of hemispheres.

GAGES:
TYPE CEA-06-125WT-350
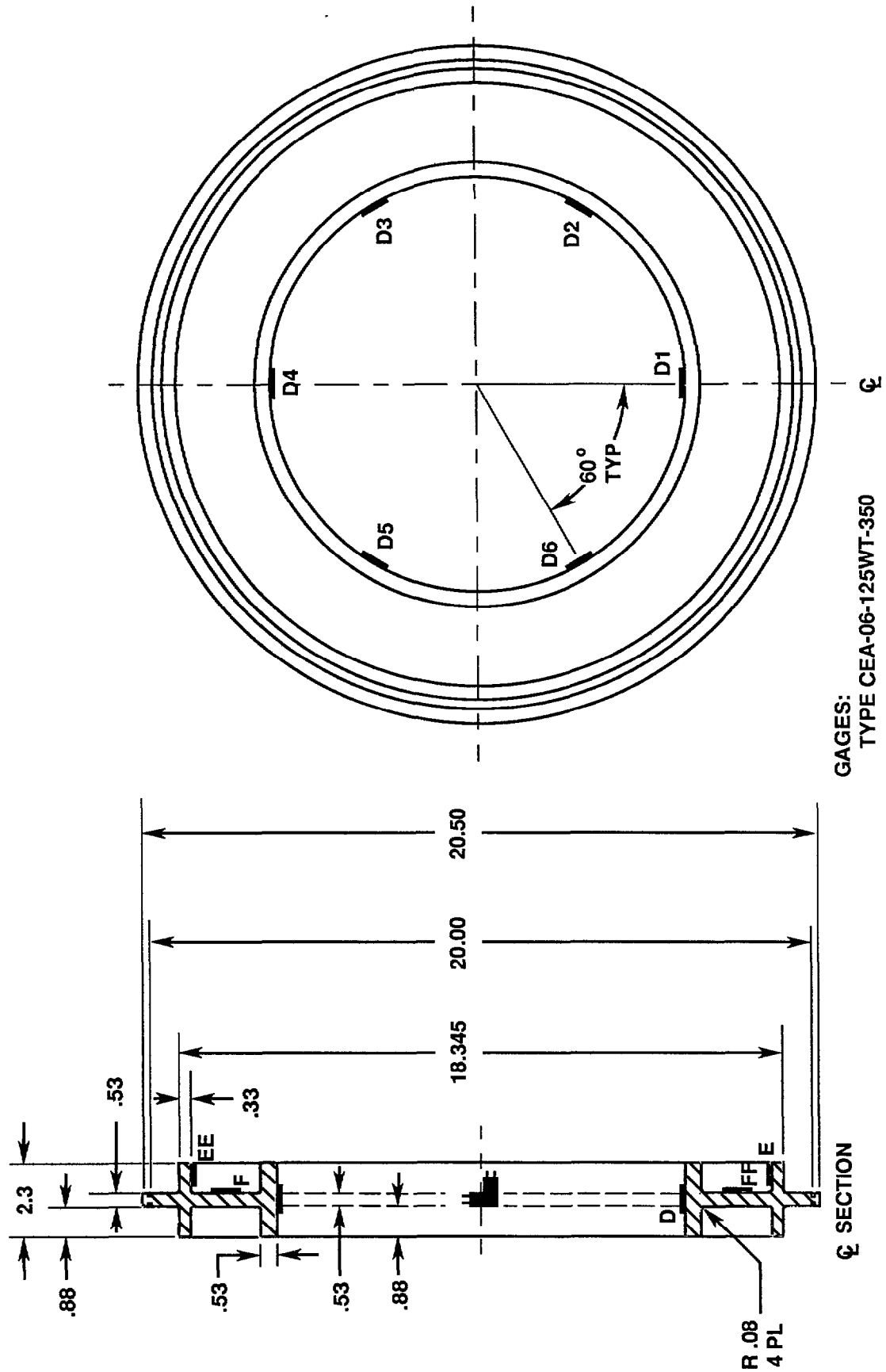
Figure 75. Location of strain gages on the joint stiffener.
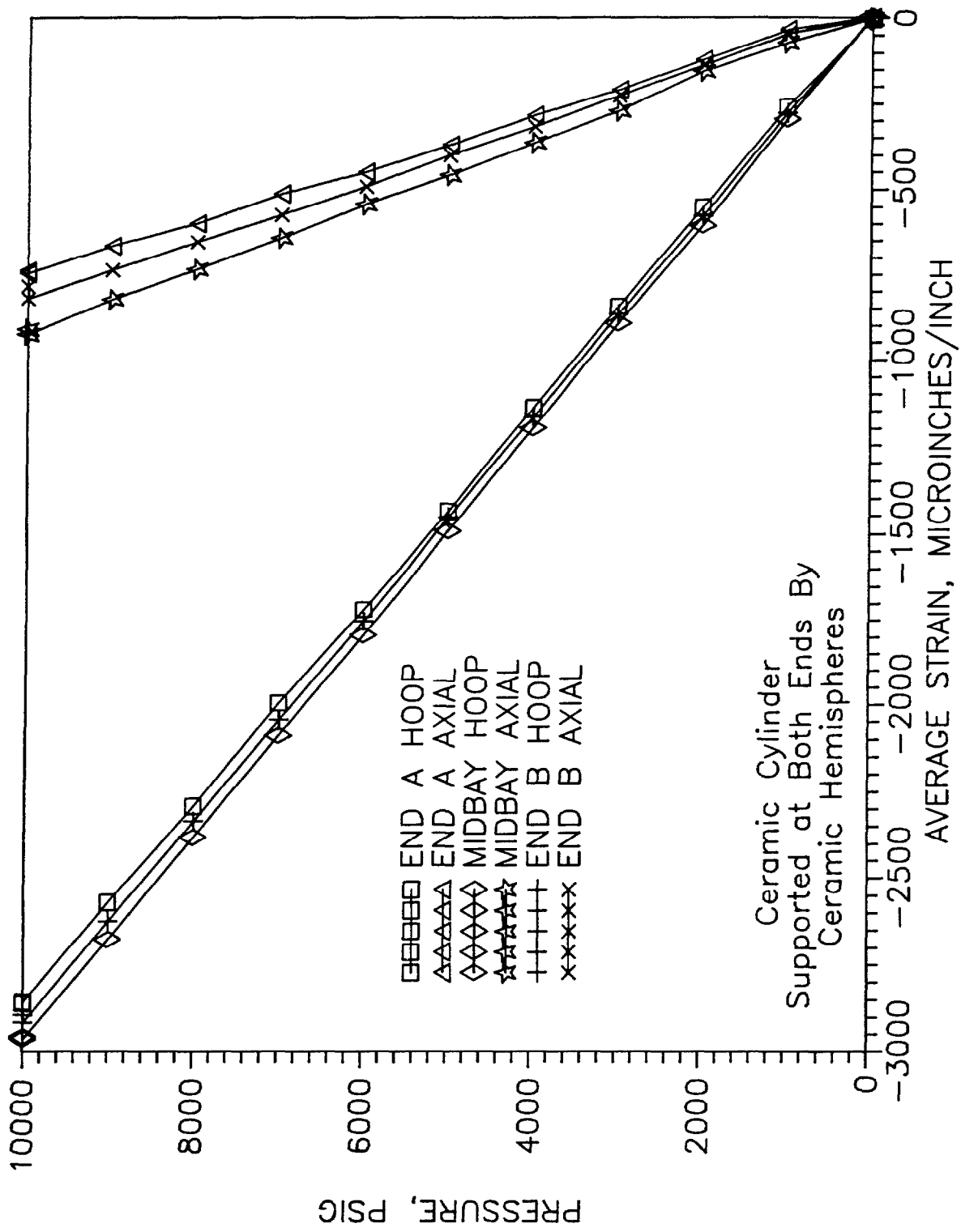
Figure 76. Averaged strains from 10 strain gage rosettes bonded to the interior surface of the ceramic cylinder.
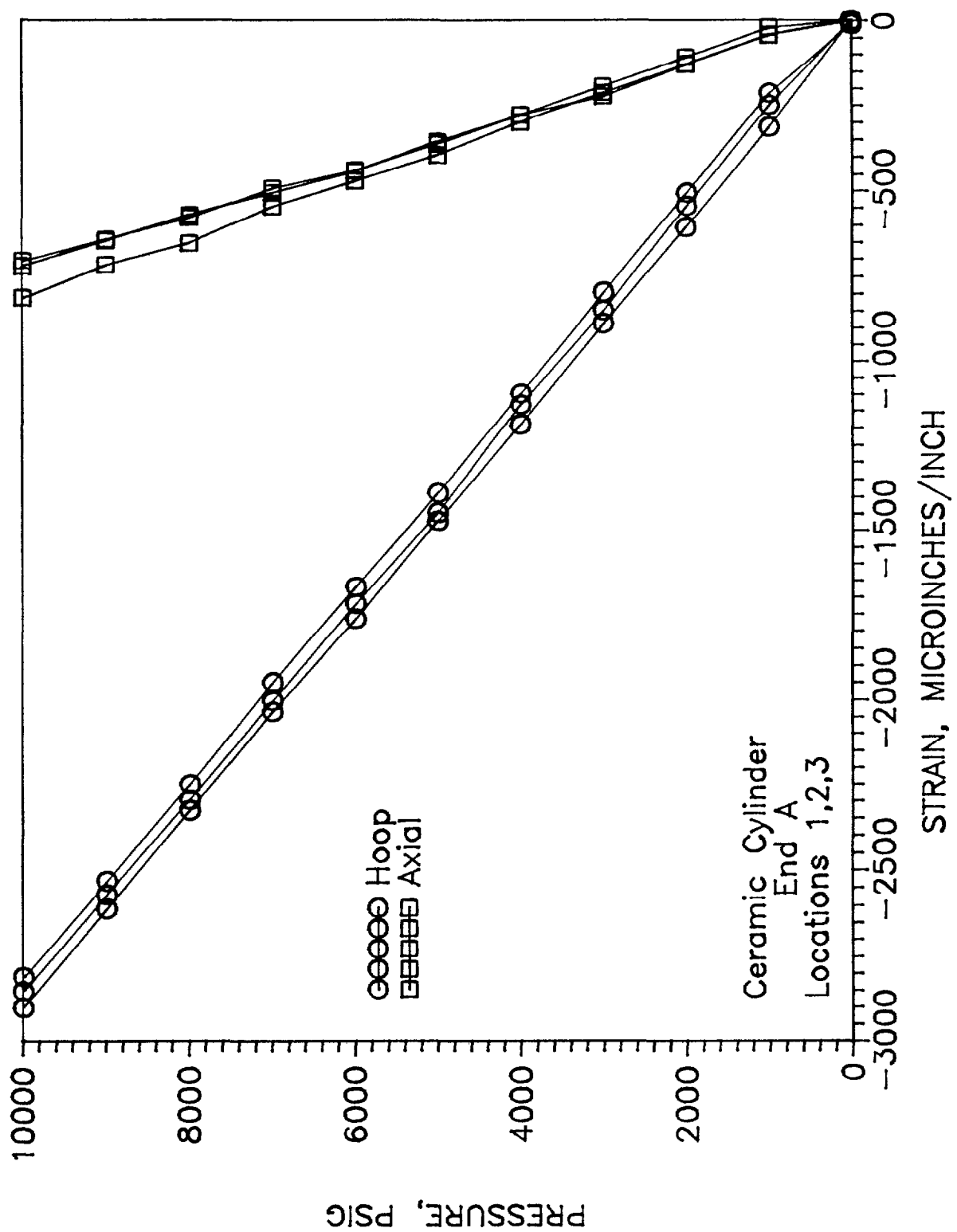
Figure 77. Strains on the interior surface of the cylinder near End A.
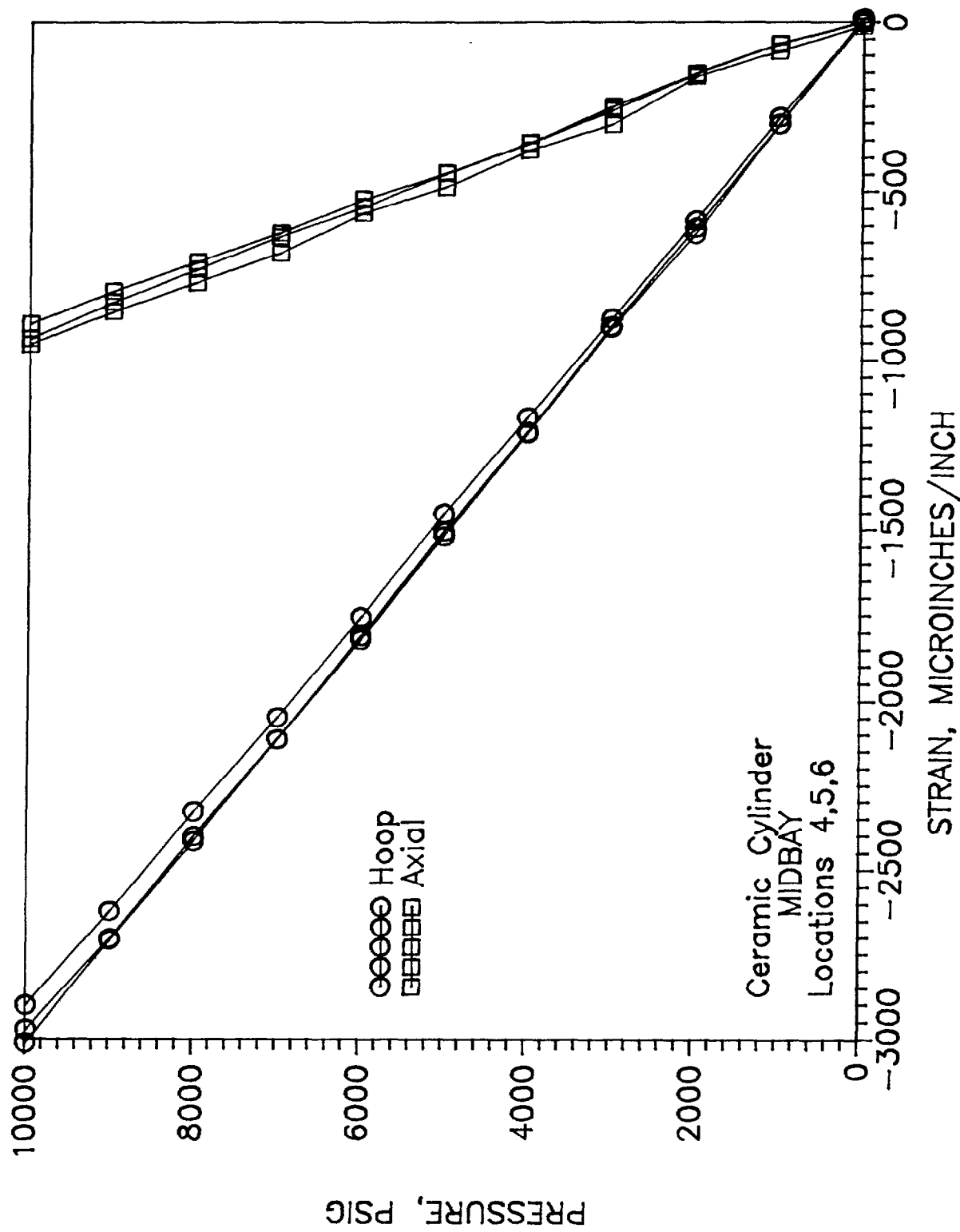
Figure 78. Strains on the interior surface of the cylinder at midbay.

STRAIN, MICROINCHES/INCH

PRESSURE, PSIG

Ceramic Cylinder
MIDBAY
Locations 4,5,6

○○○○○ Hoop
▣▣▣▣▣ Axial

97

STRAIN, MICROINCHES/INCH

PRESSURE, PSIG

Ceramic Cylinder
END B
Locations 7,8,9
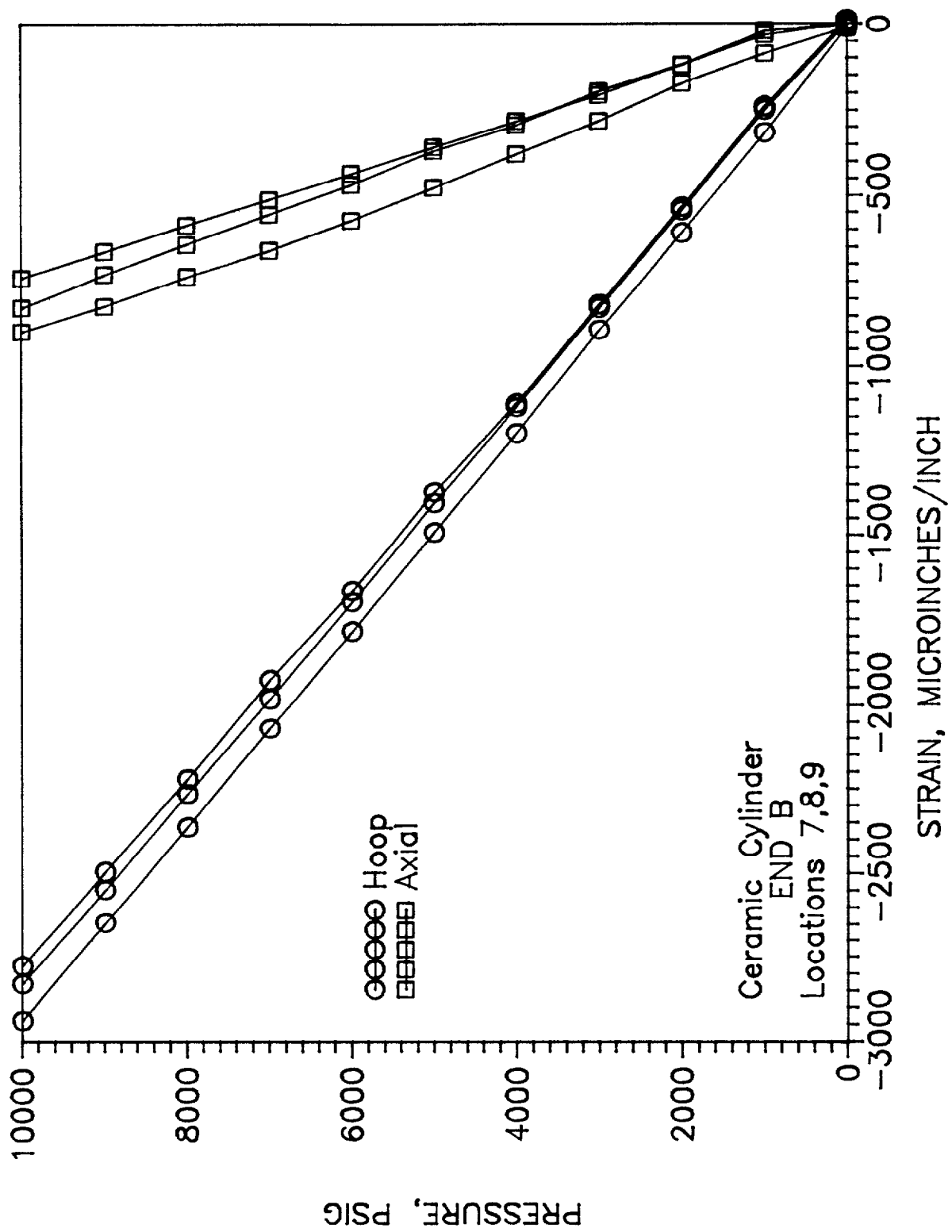
◎◎◎◎◎ Hoop
⊟⊟⊟⊟⊟ Axial

Figure 79. Strains on the interior surface of the cylinder wear End B.
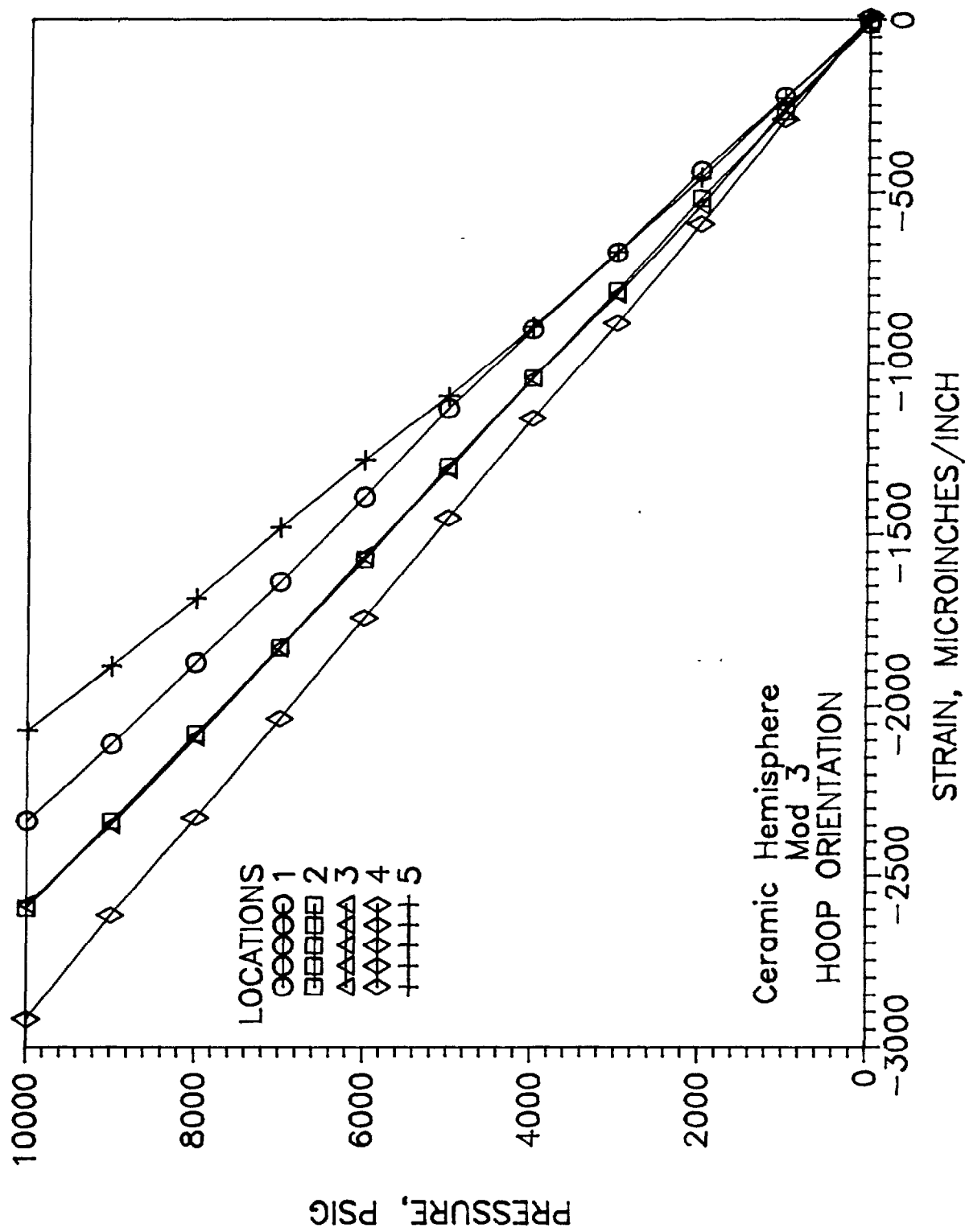
Figure 80. Strains on the interior surface of the hemisphere Mod III; hoop orientation.
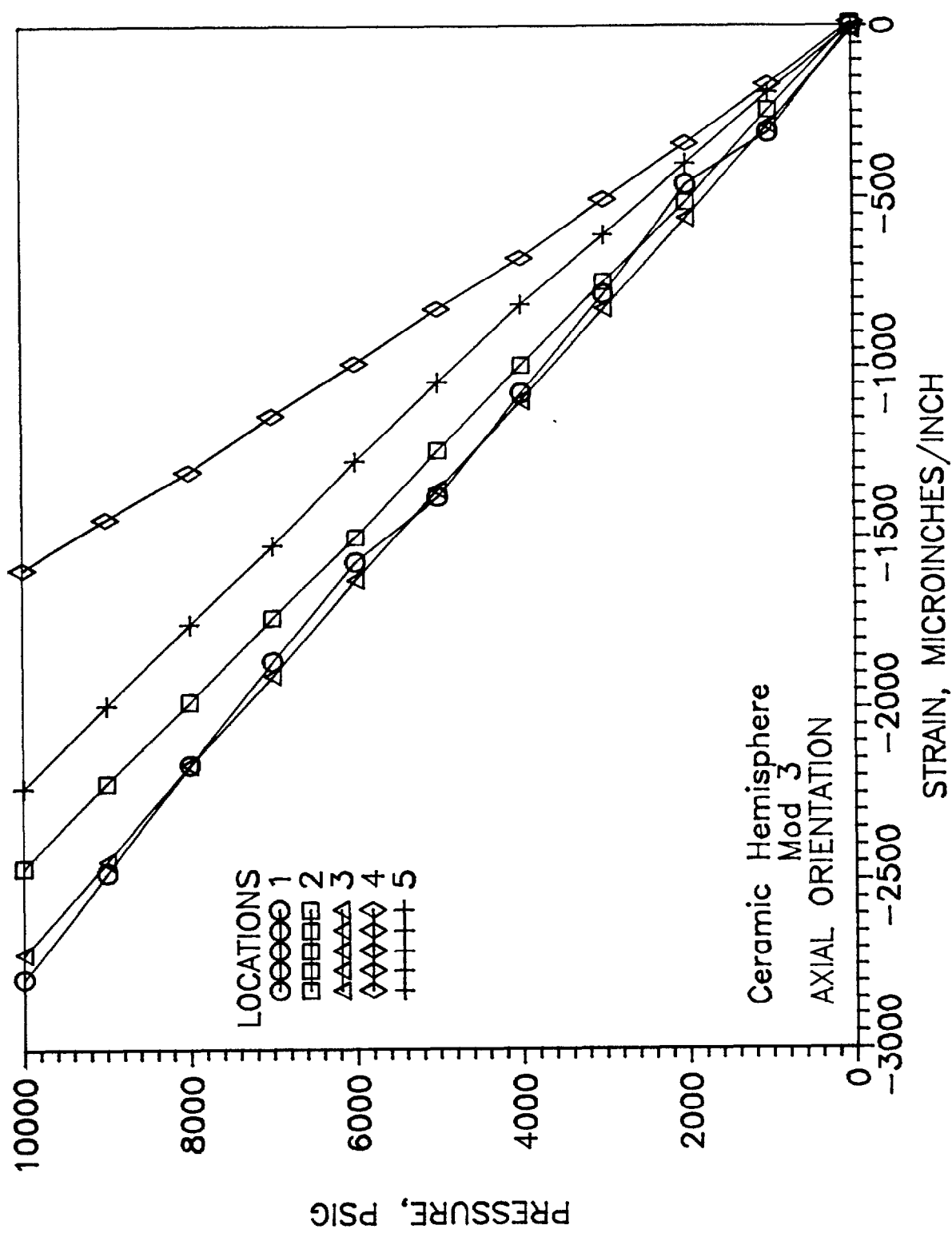
Figure 81. Strains on the interior surface of the hemisphere Mod III, axial orientation.
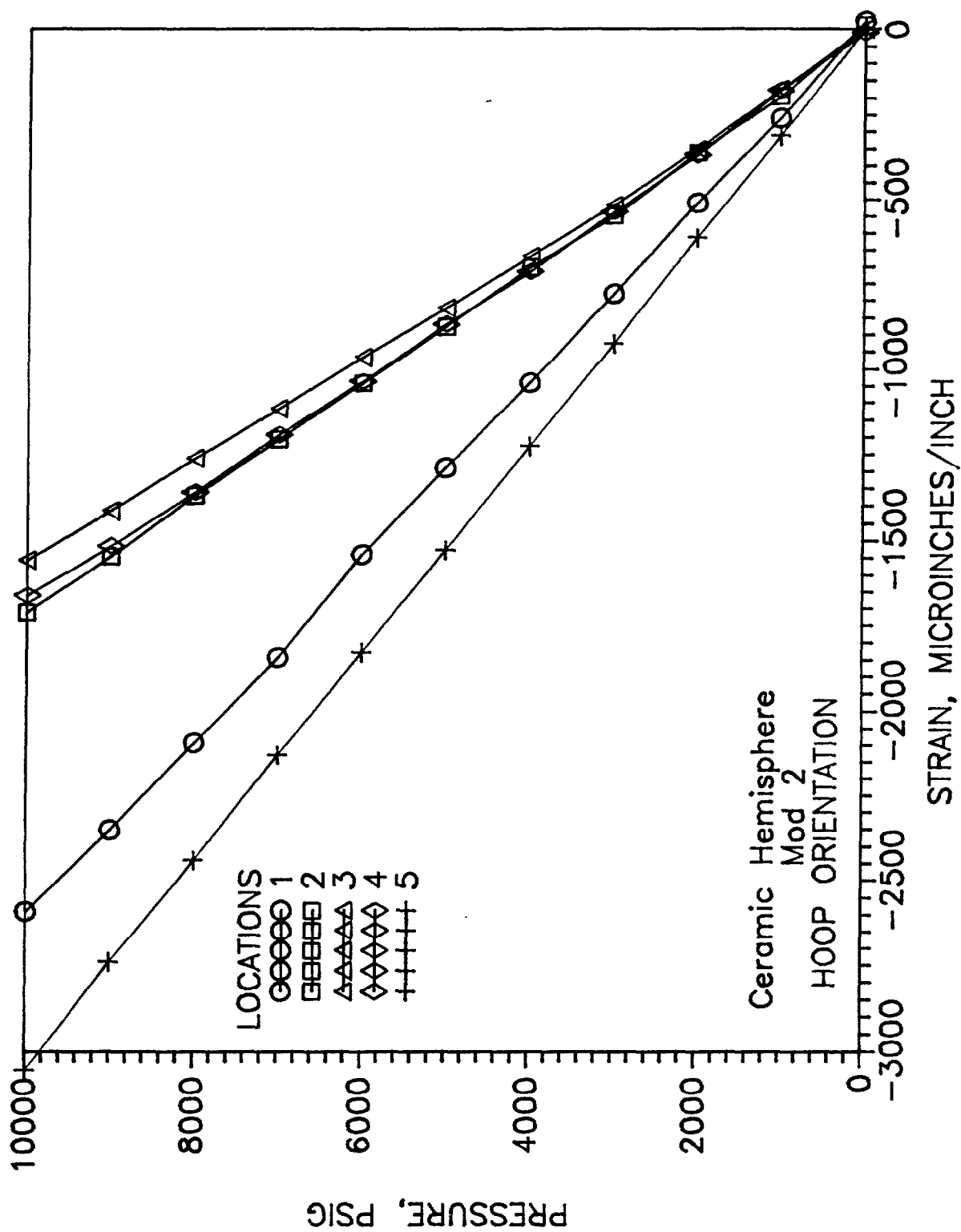
Figure 82. Strains on the interior surface of the hemisphere Mod II; hoop orientation.
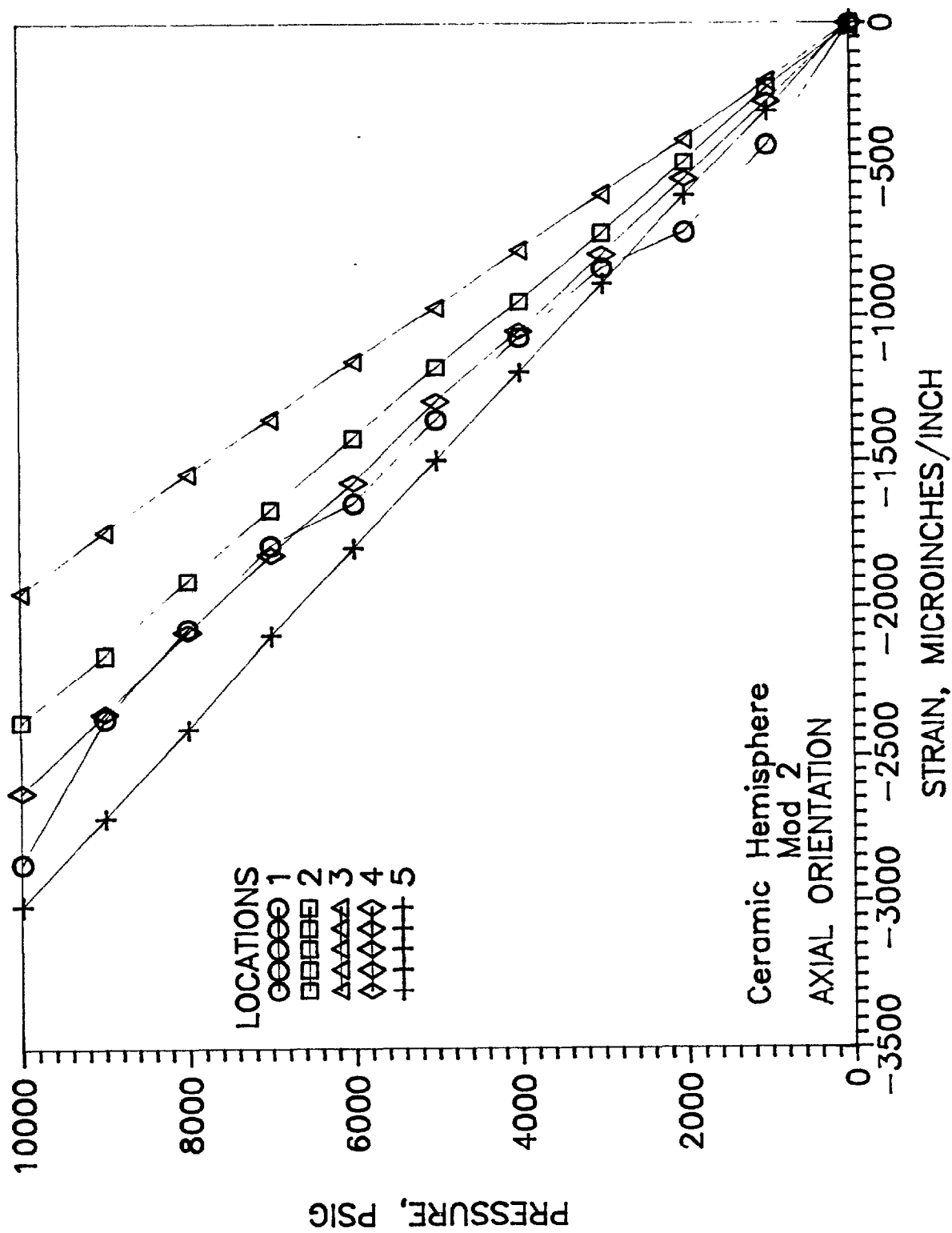
Figure 83. Strains on the interior surface of the hemisphere Mod II, axial orientation.
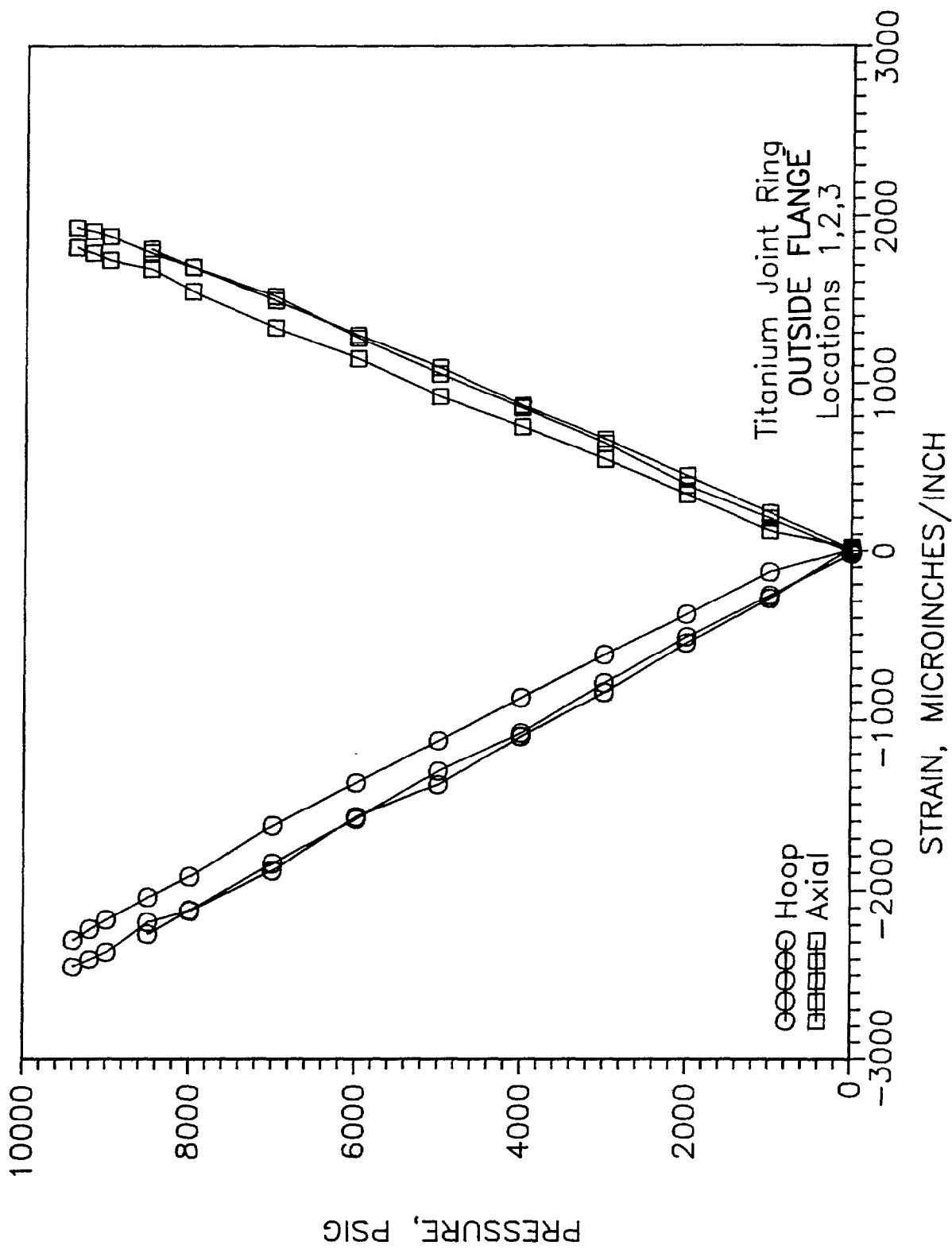
Figure 84. Strains on the lip of the outside flange on titanium joint stiffener.
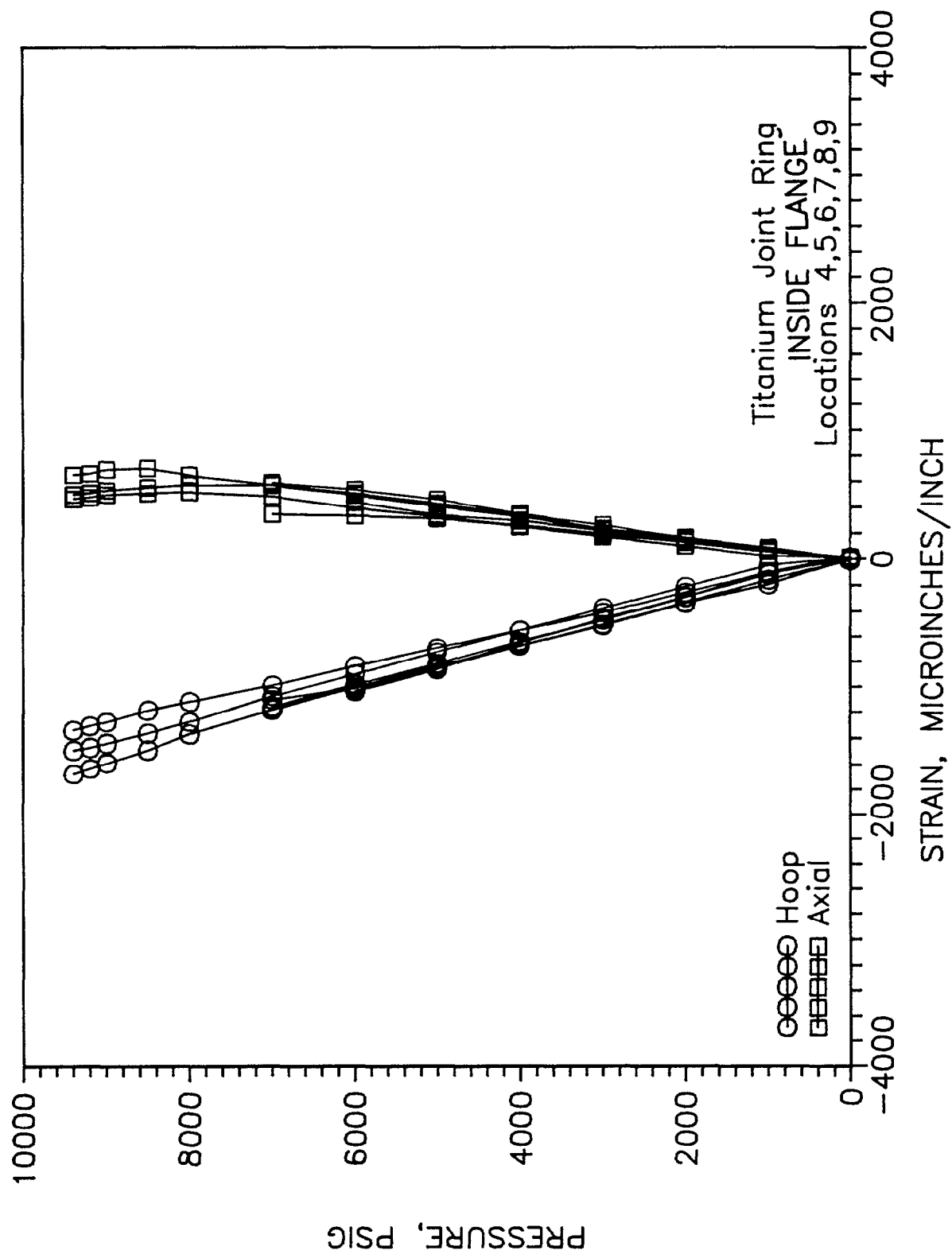
Figure 85. Strains at the center of inside flange on titanium joint stiffener.
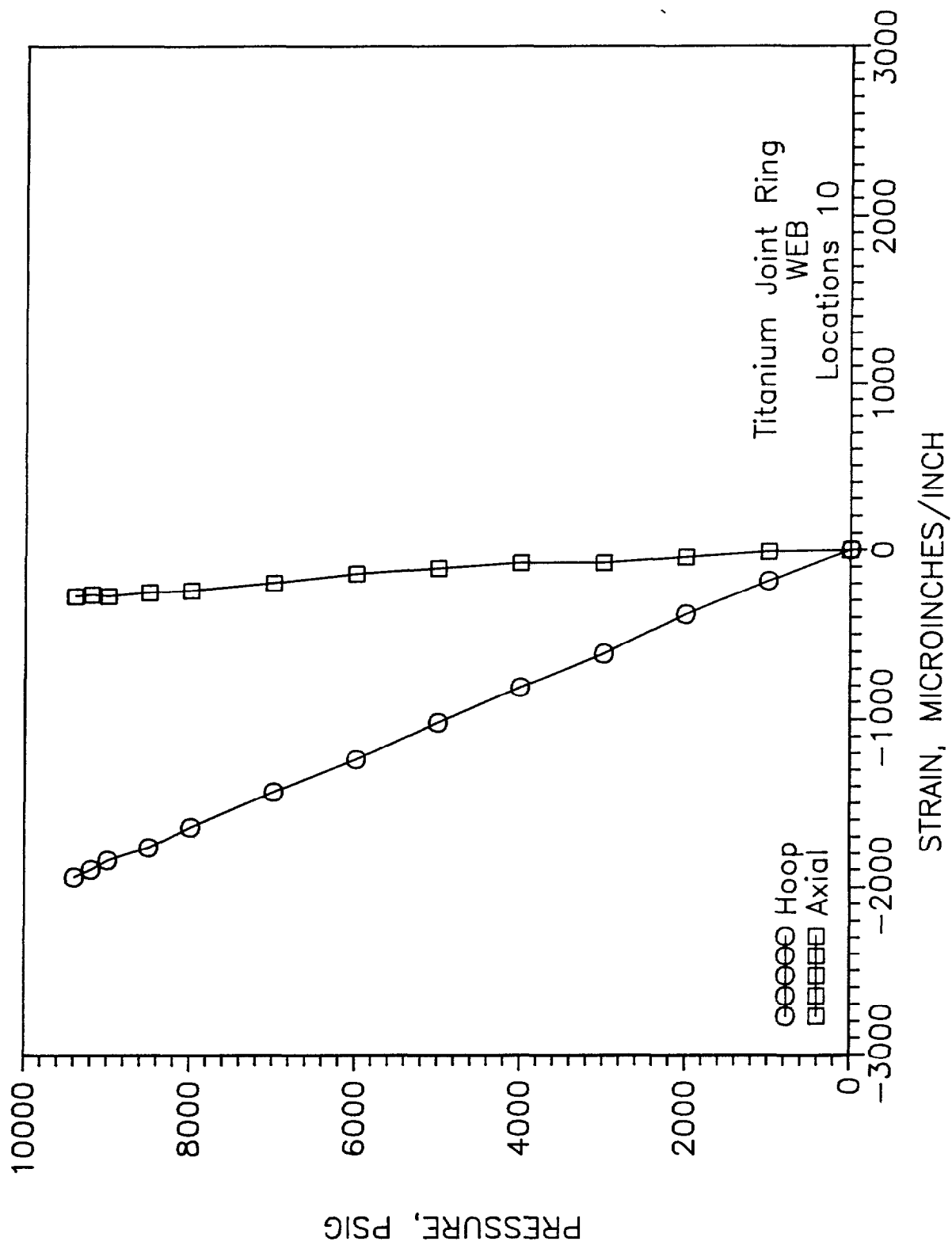
Figure 86. Strains on the web of titanium joint stiffener.
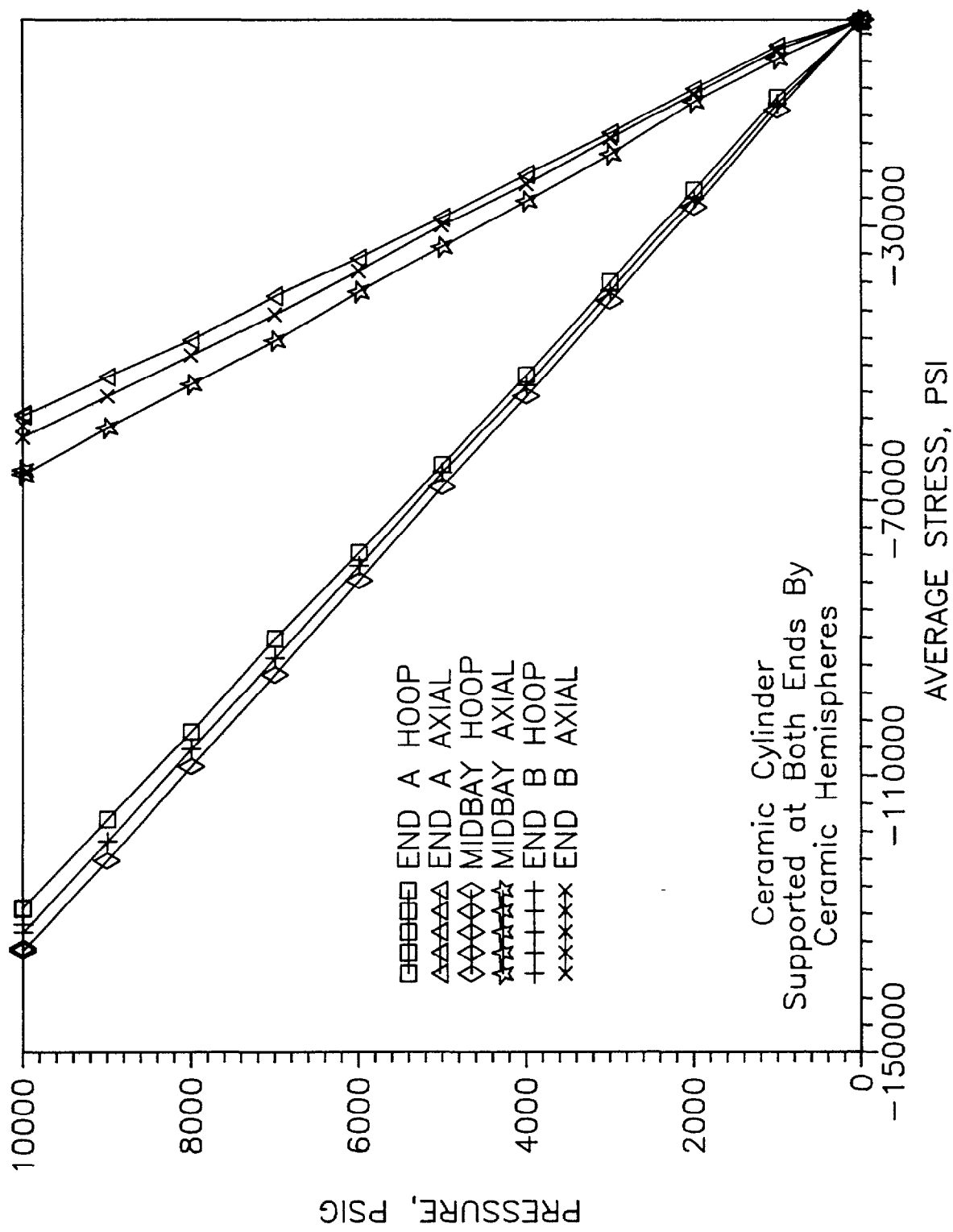
Figure 87. Averaged stresses from 10 strain gage rosettes bonded to the interior surface of the ceramic cylinder.

106
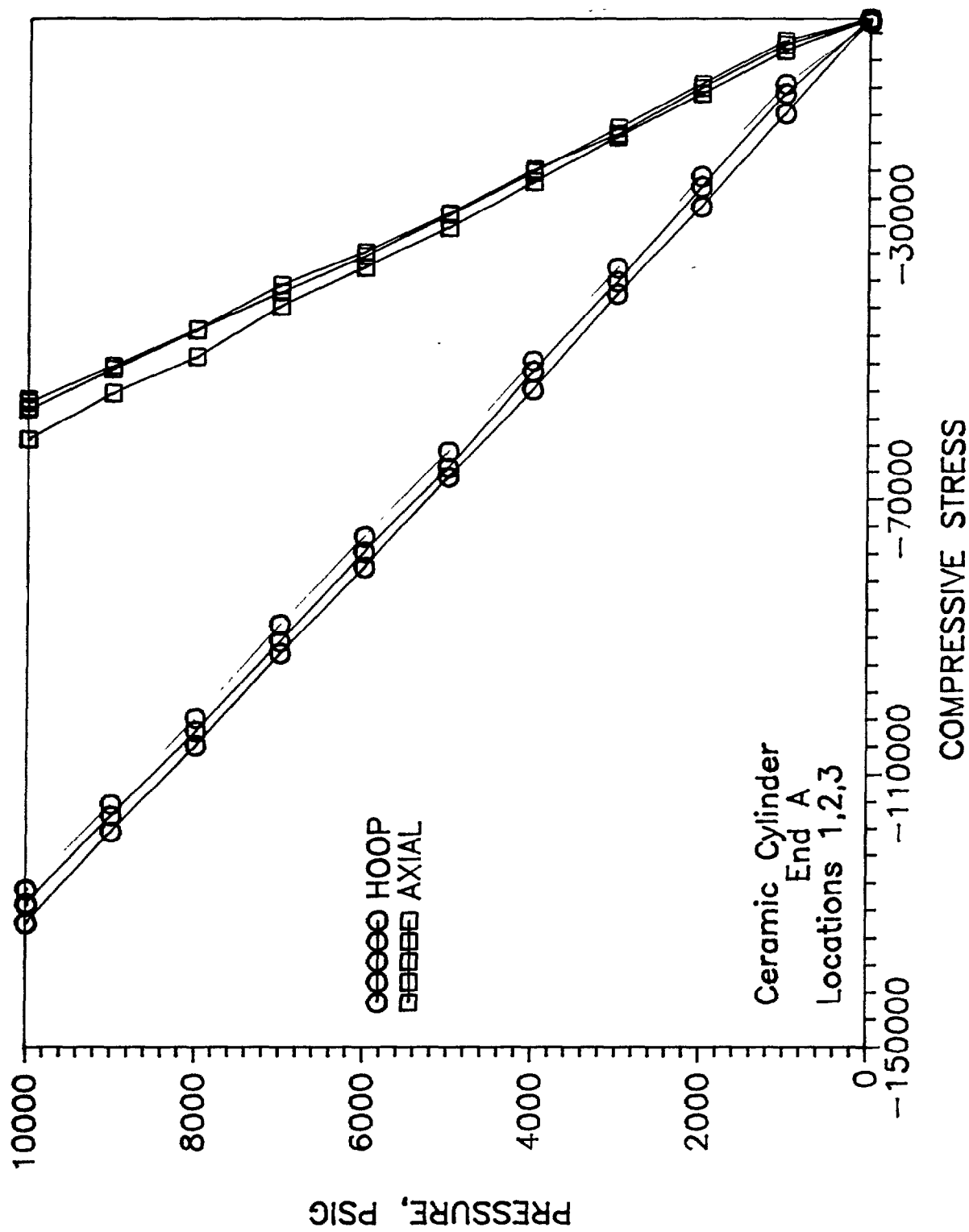
Figure 88. Stresses on the interior surface of the ceramic cylinder near End A.
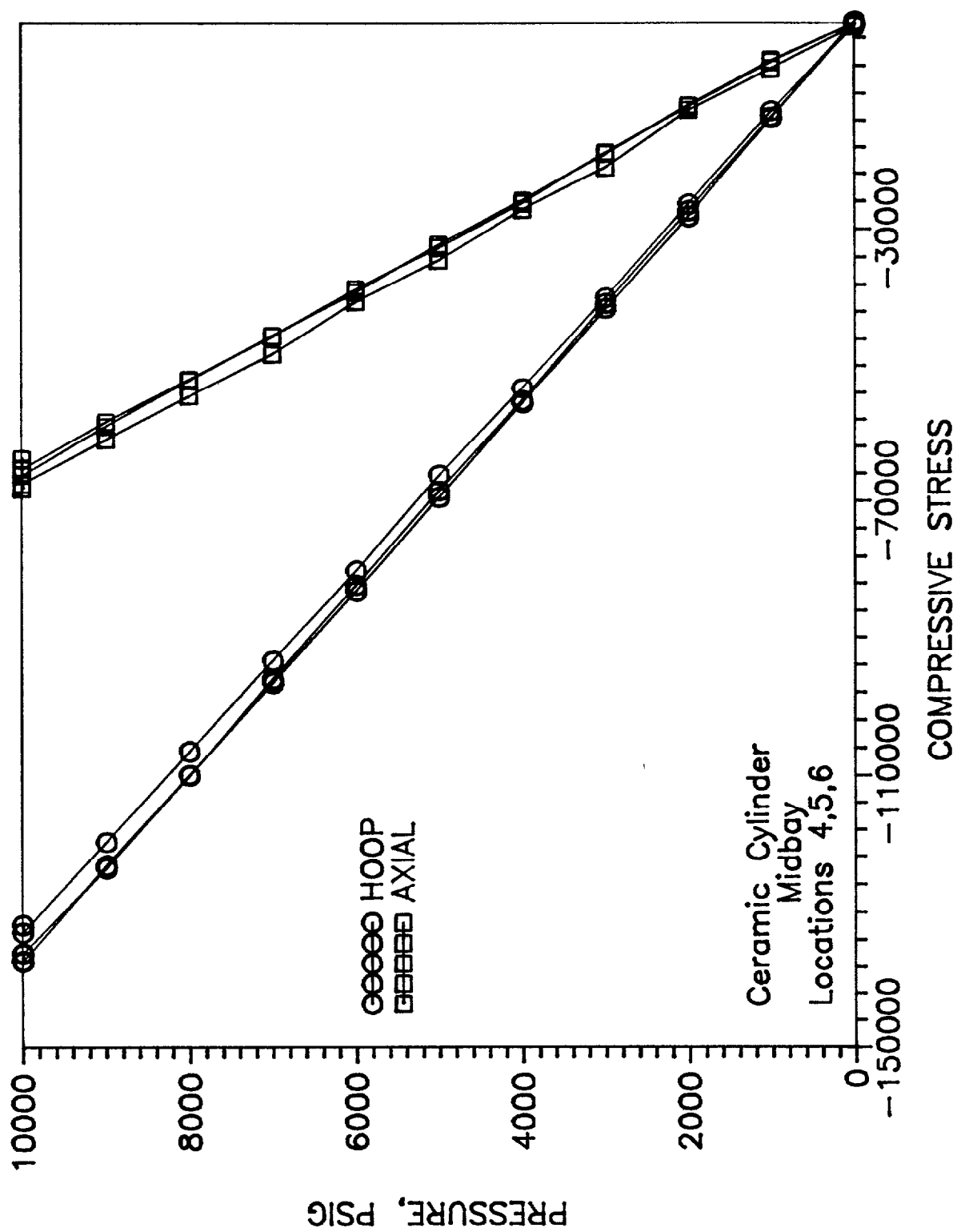
Figure 89. Stresses on the interior surface of the ceramic cylinder at midbay.
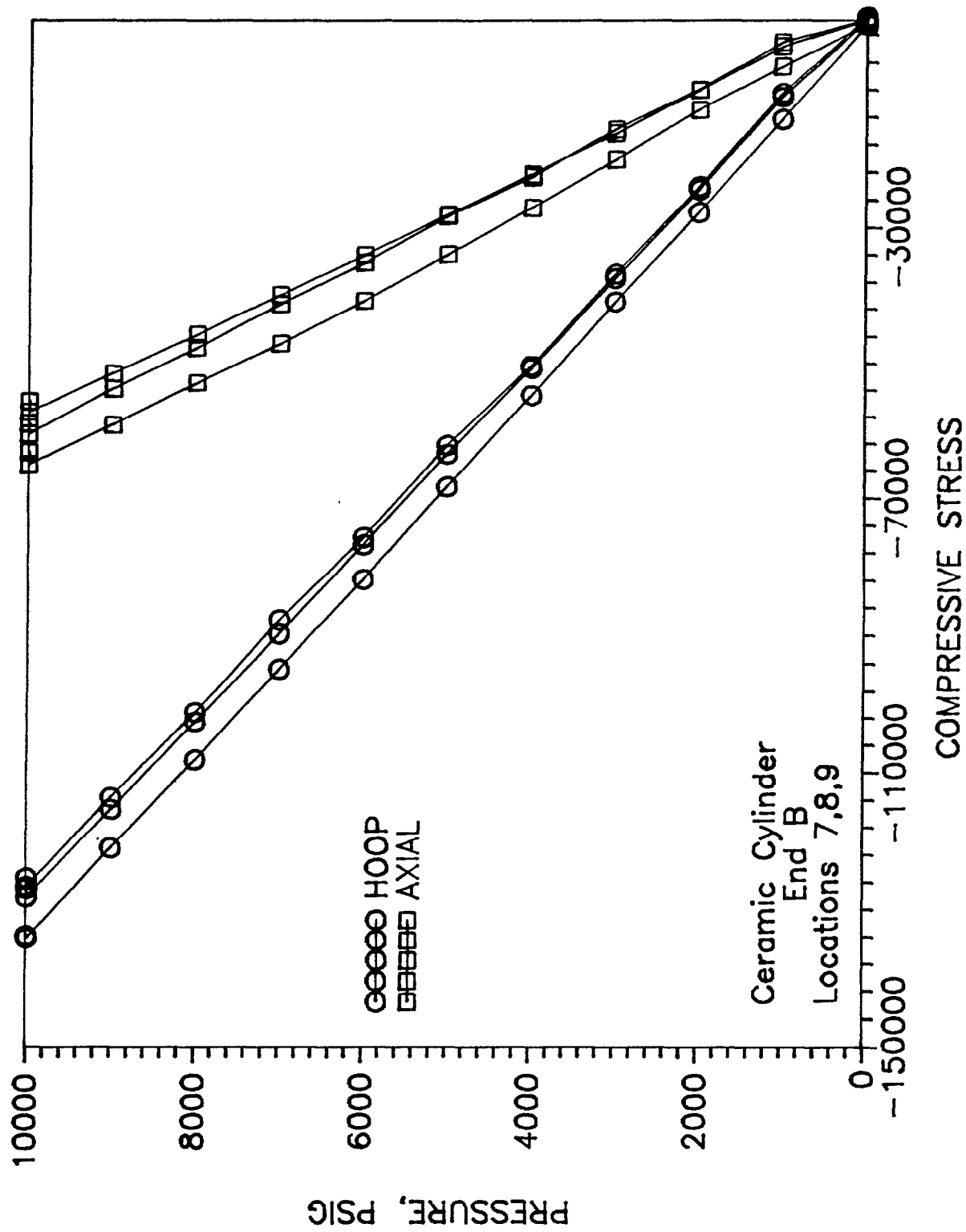
Figure 90. Stresses on the interior surface of the ceramic cylinder at End B.

Ceramic Cylinder
End B
Locations 7,8,9

HOOP
AXIAL

COMPRESSIVE STRESS

PRESSURE, PSIG

109
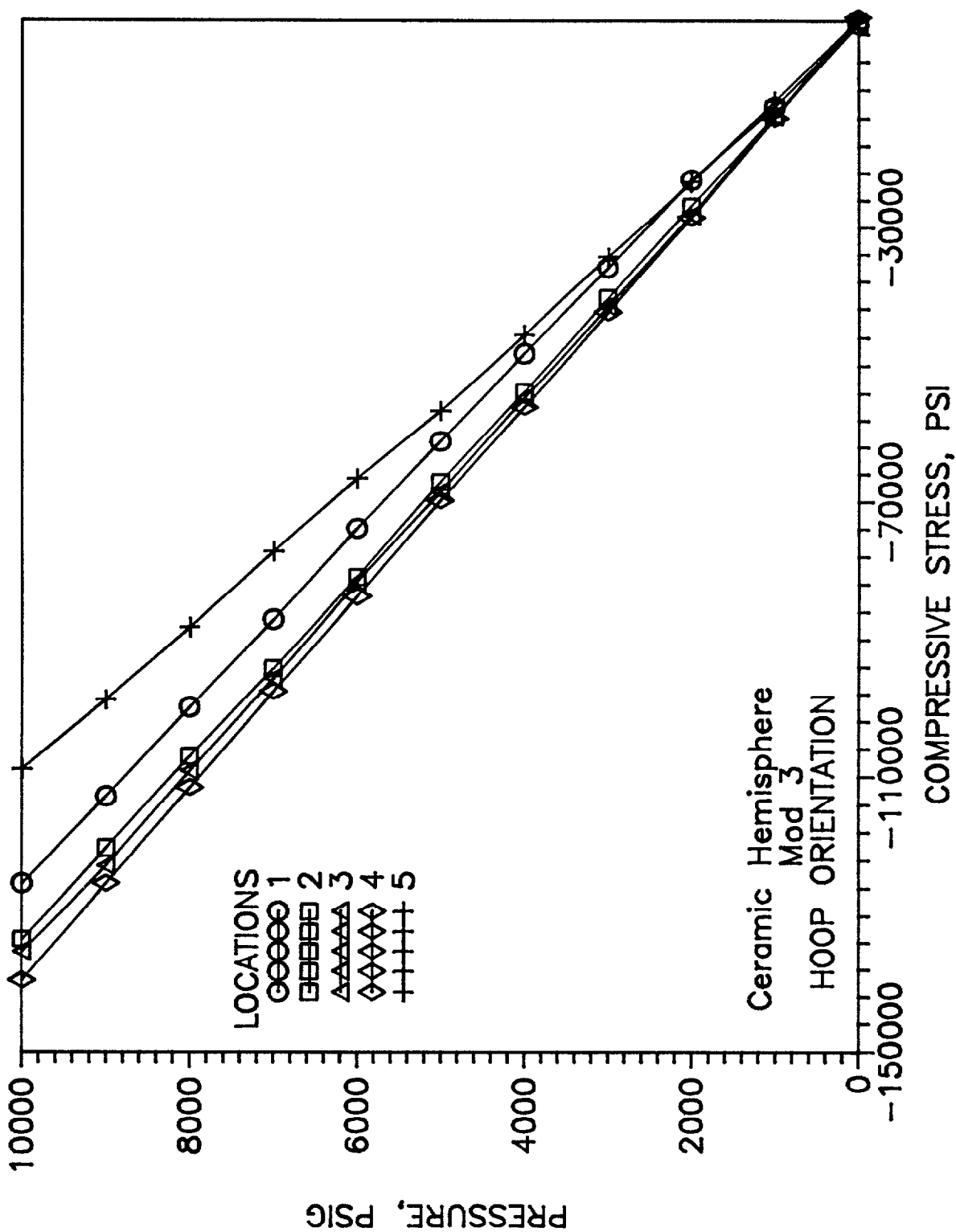
Figure 91. Stresses on the interior surface of Mod III hemisphere; hoop orientation.

110
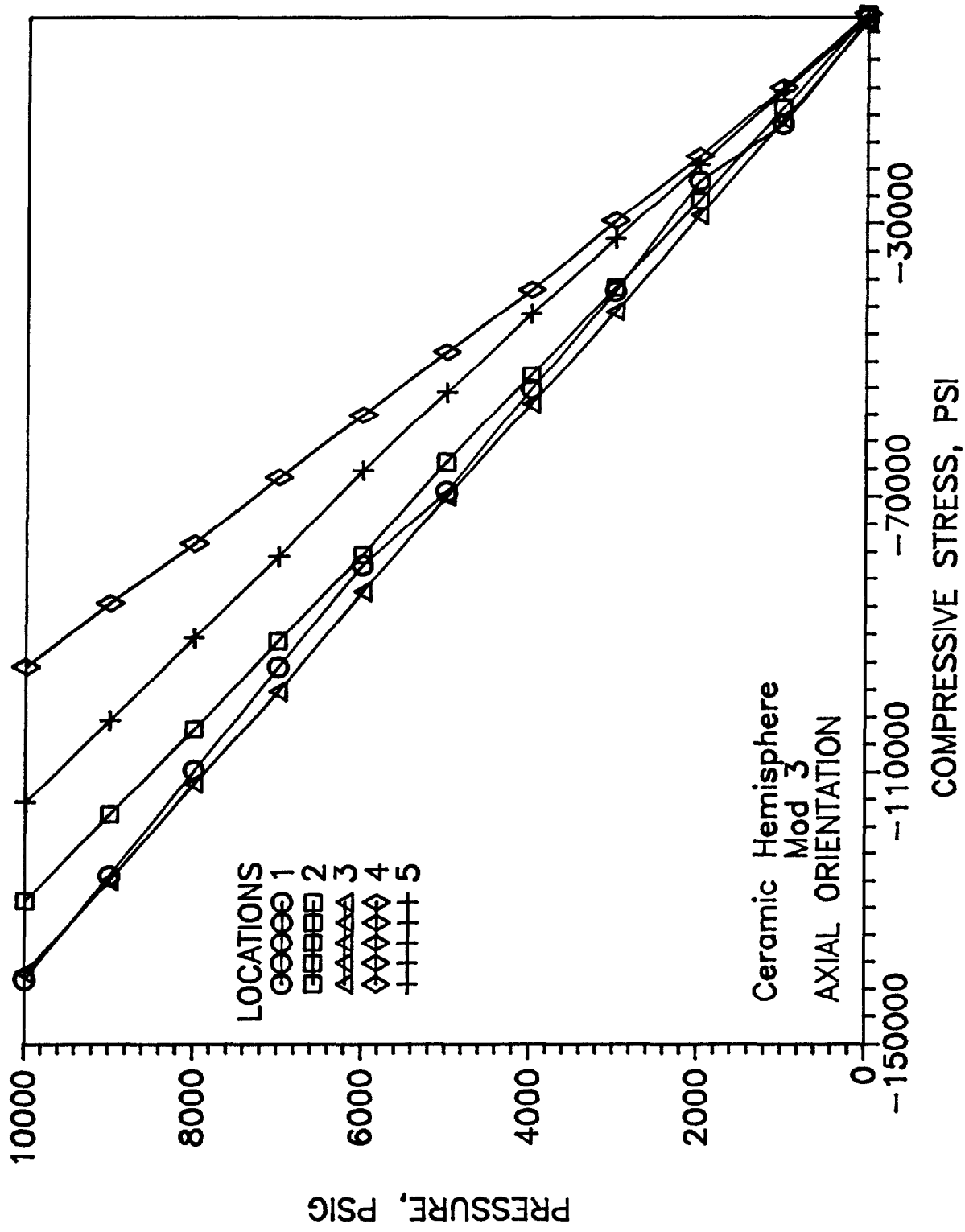
Figure 92. Stresses on the interior surface of Mod III hemisphere; axial orientation.

111
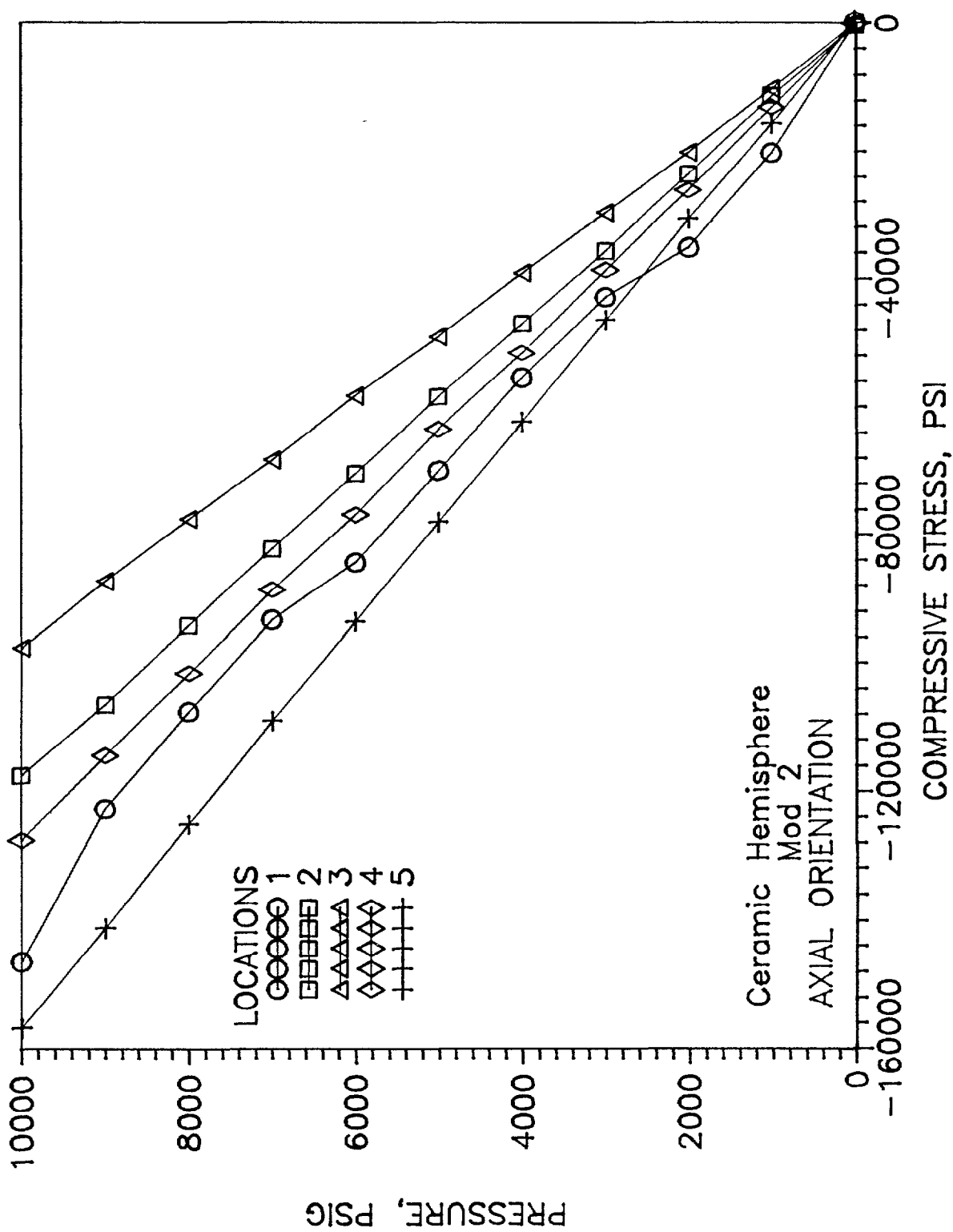
Figure 93. Stresses on the interior surface of Mod II hemisphere; axial orientation.

112
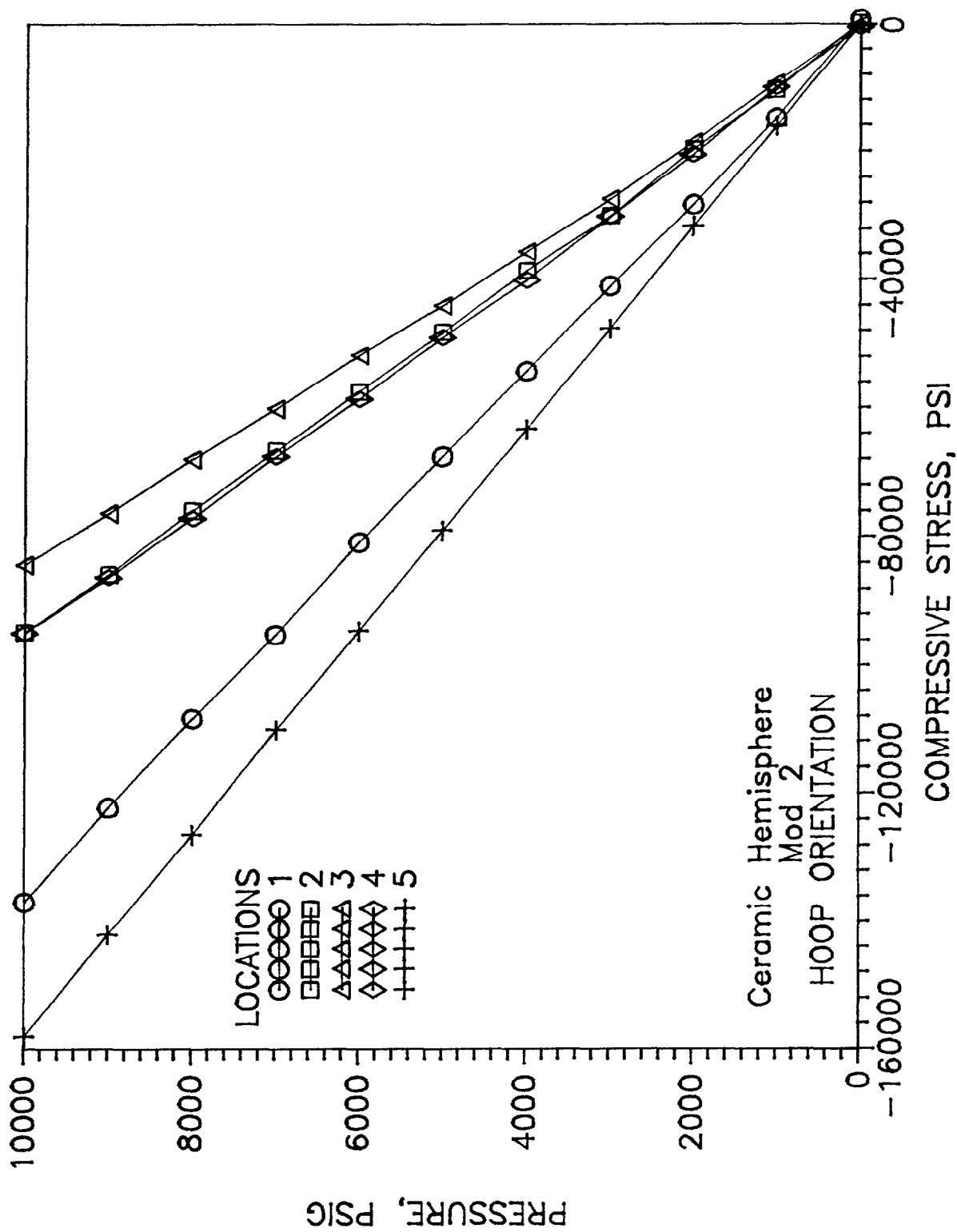
Figure 94. Stresses on the interior surface of Mod II hemisphere; hoop orientation.

113
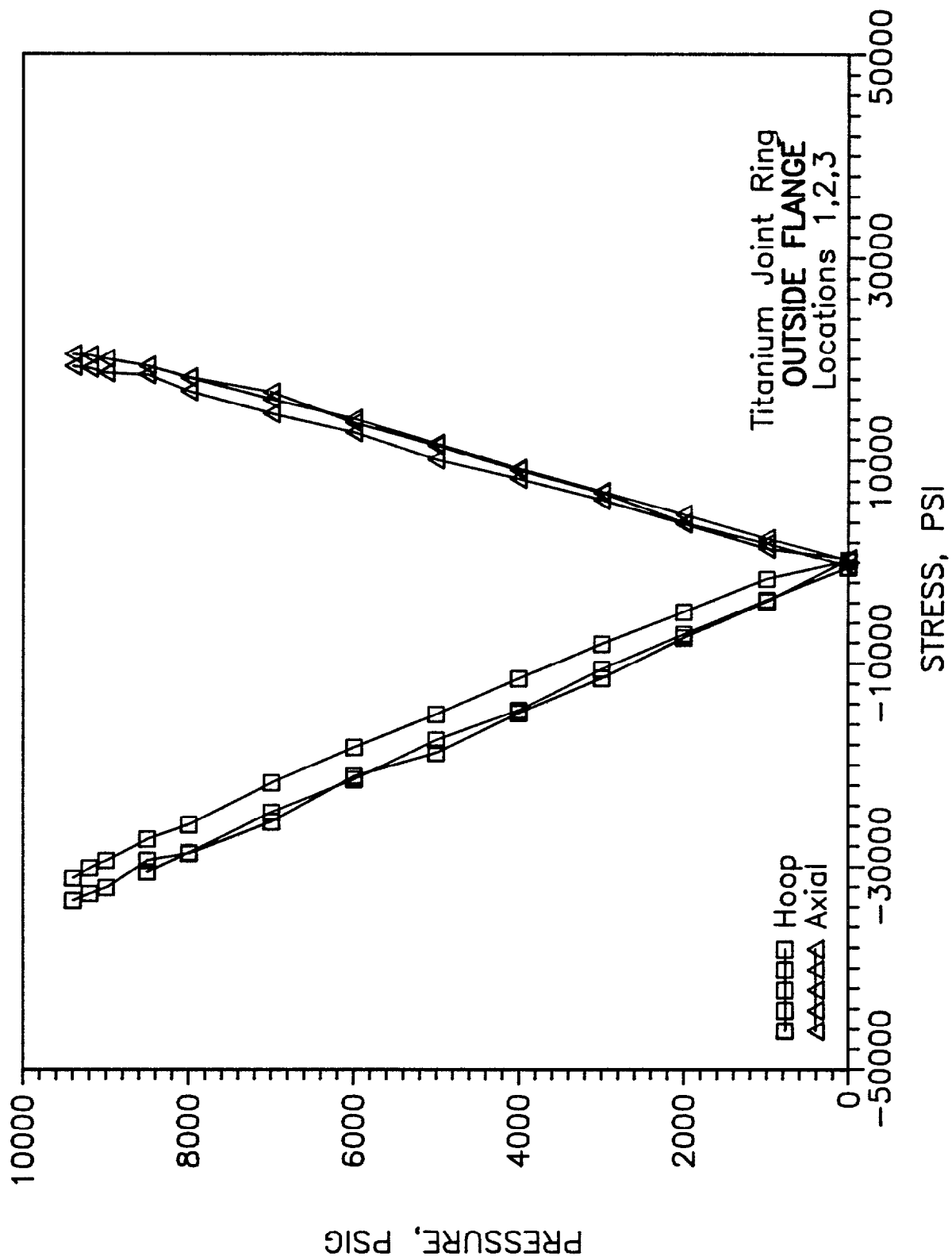
Figure 95. Stresses on the lip of the exterior flange on titanium joint stiffener.
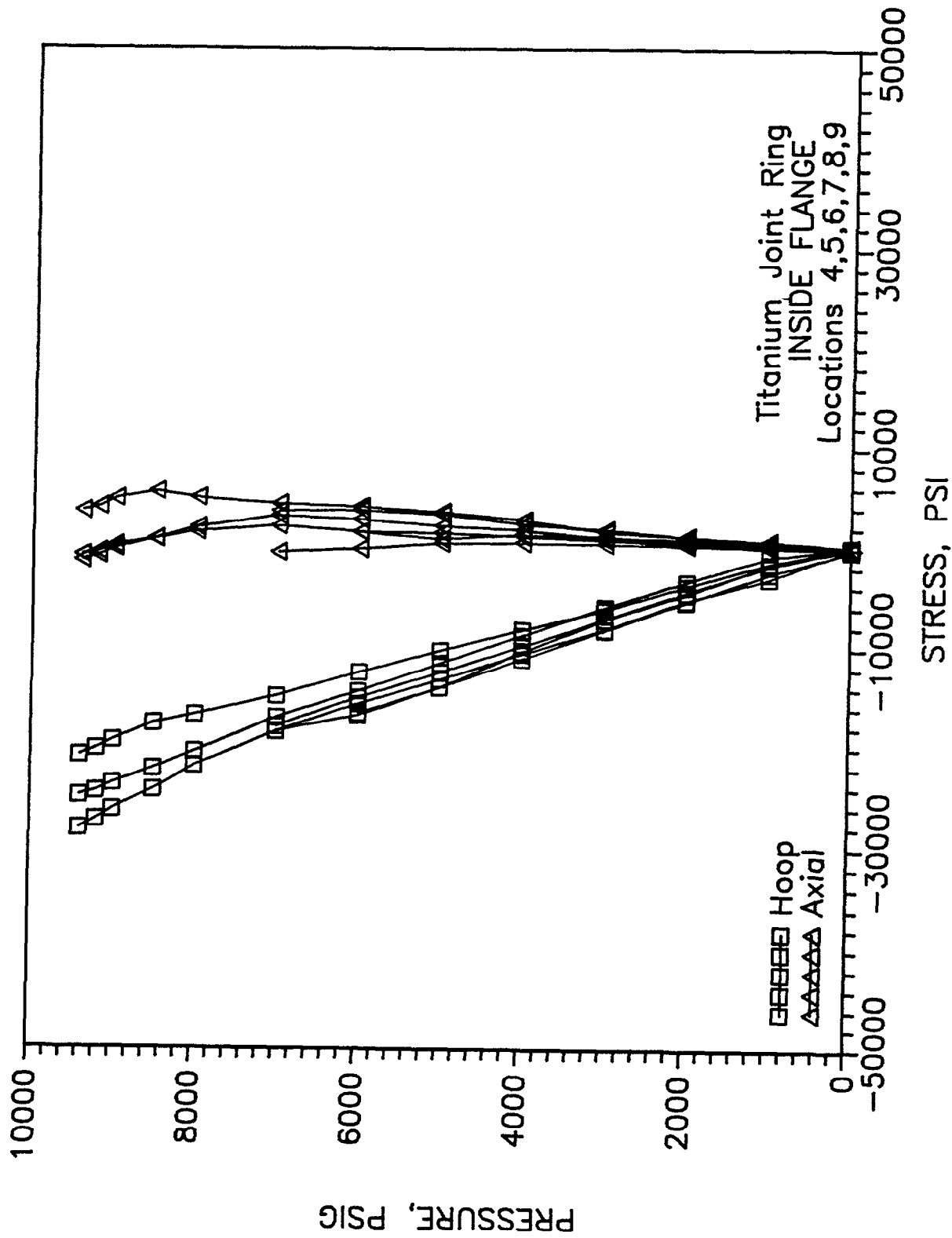
Figure 96. Stresses at the center of the inside flange on titanium joint stiffener.

115
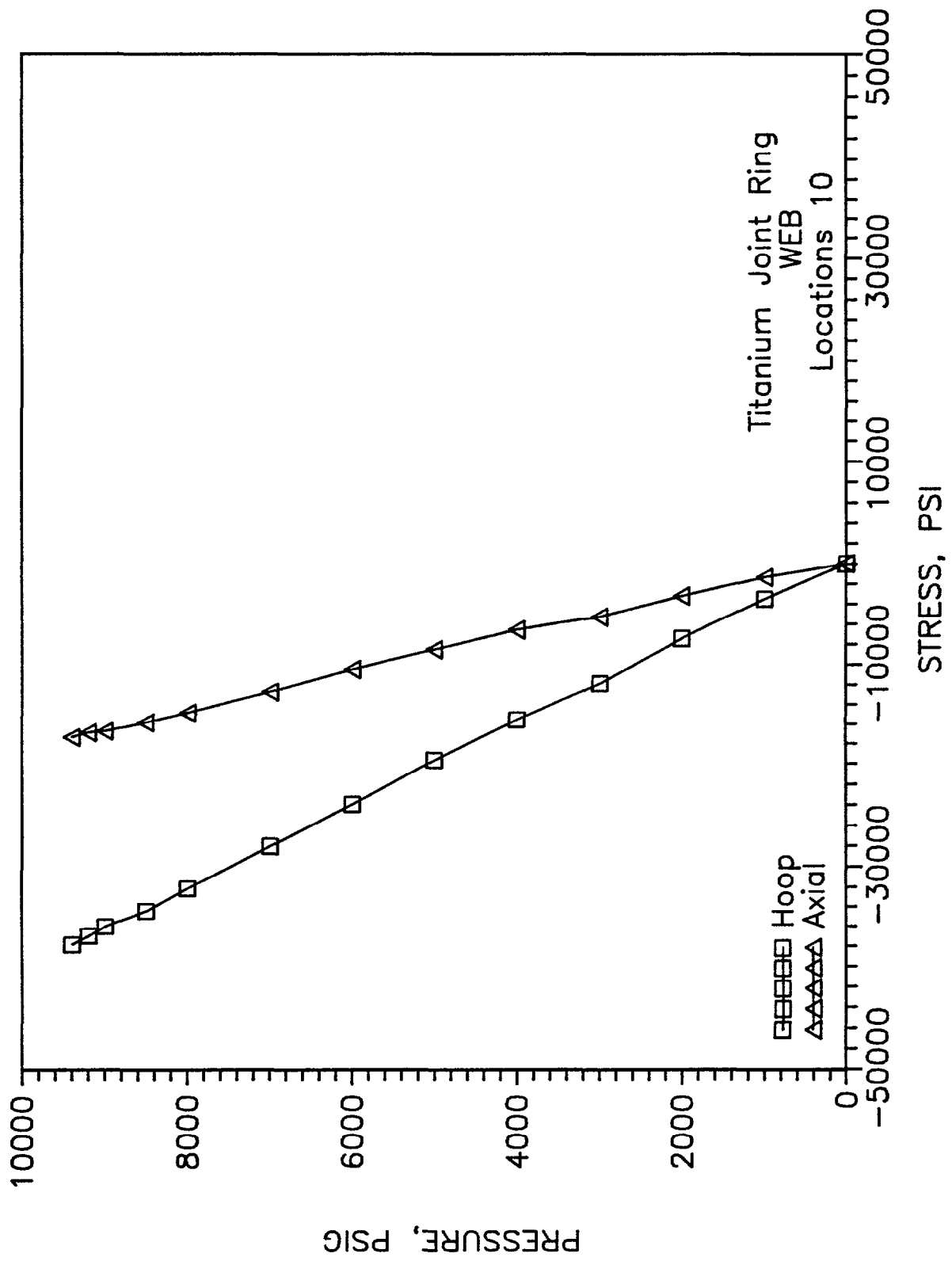
Figure 97. Stresses on the web of the titanium joint stiffener.
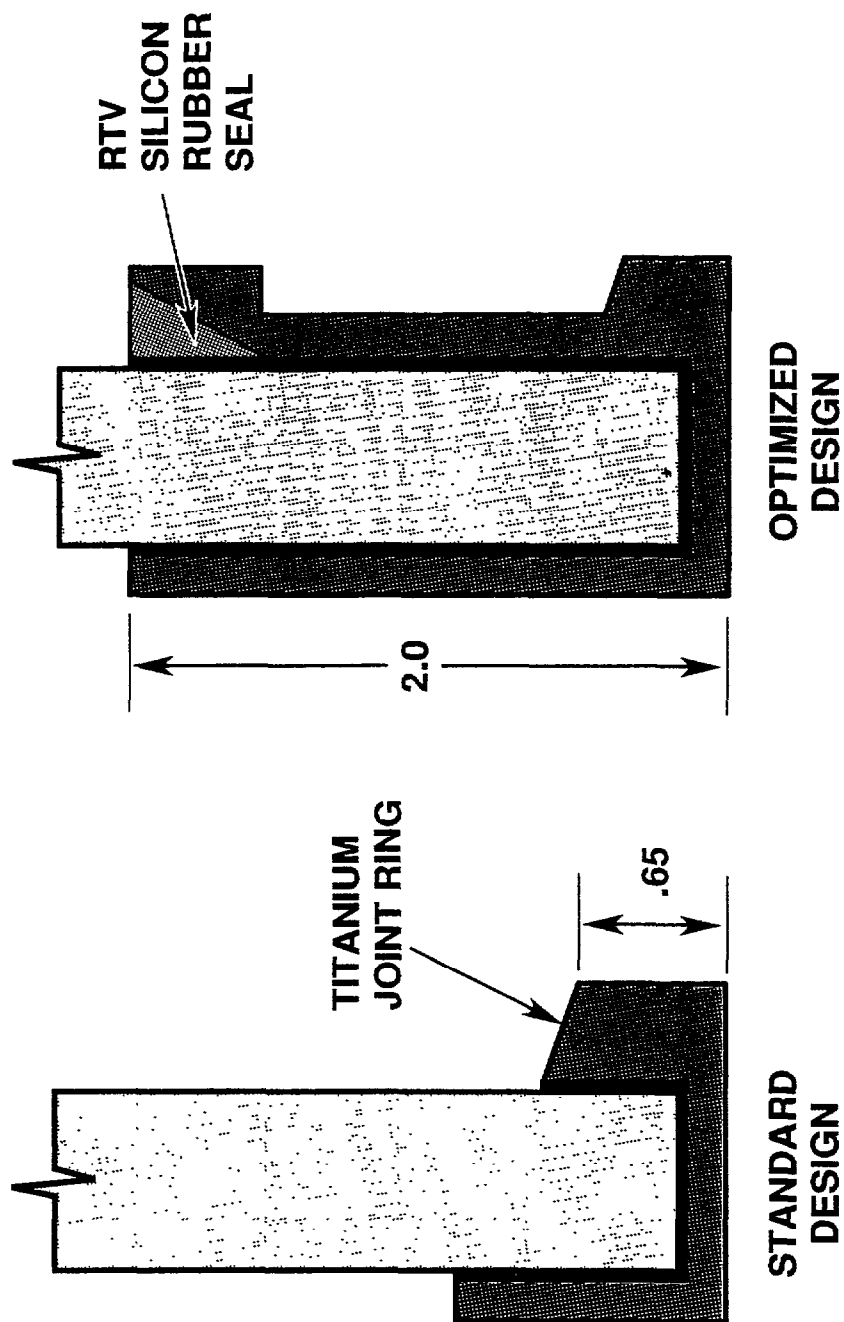
Figure 98. Comparison of end cap sizes for ceramic cylinders; note that the depth of annular cavity in optimized Mod I design is three times deeper that in standard Mod 0 design.
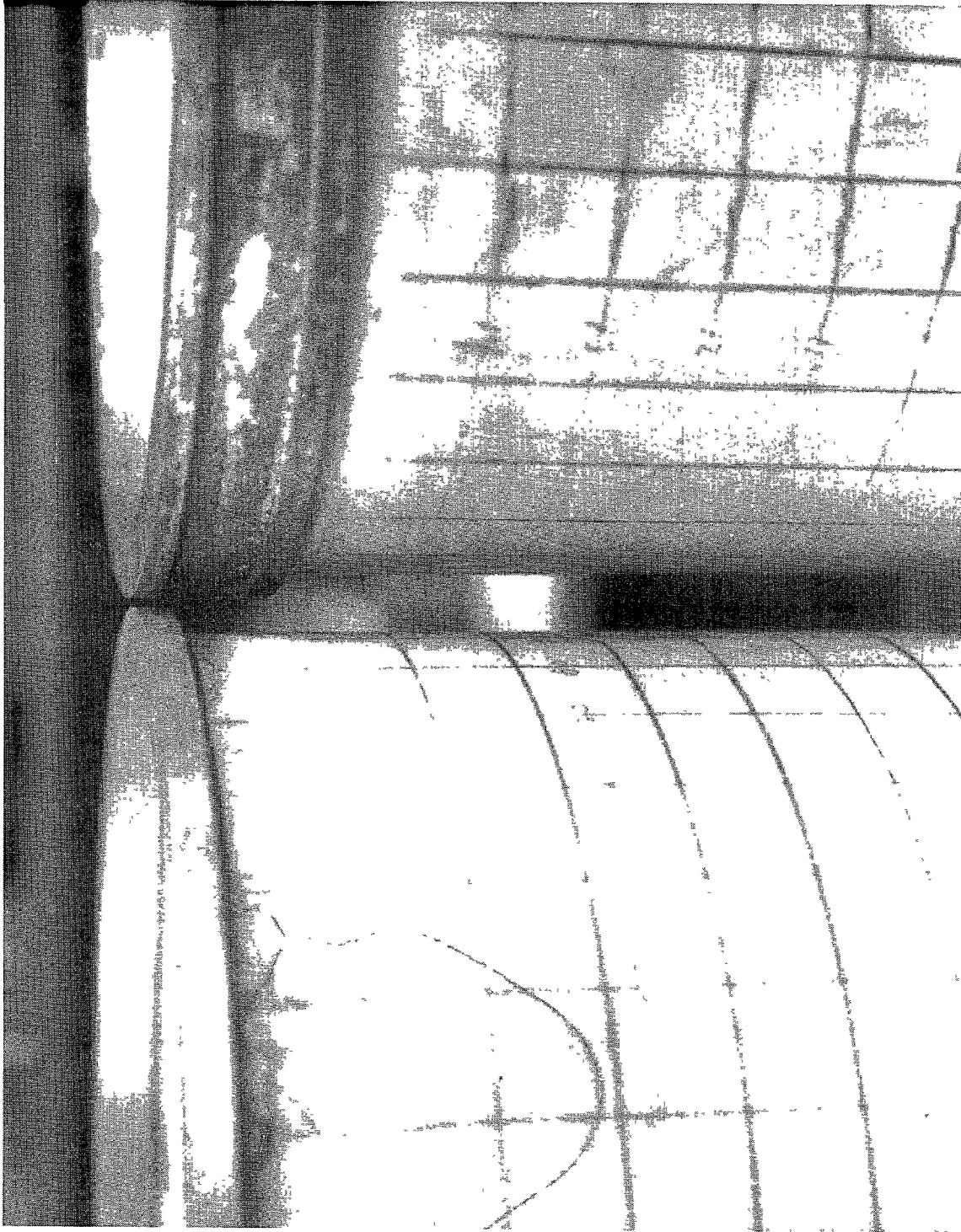
Figure 99. Comparison of Mod 0 and Mod I end cap designs evaluated experimentally on 12-inch-diameter housings. The ceramic cylinder with Mod 0 end caps spalled after only 60 pressure cycles, while Mod I does not exhibit any spalling after 500 pressure cycles to 9000 psi.
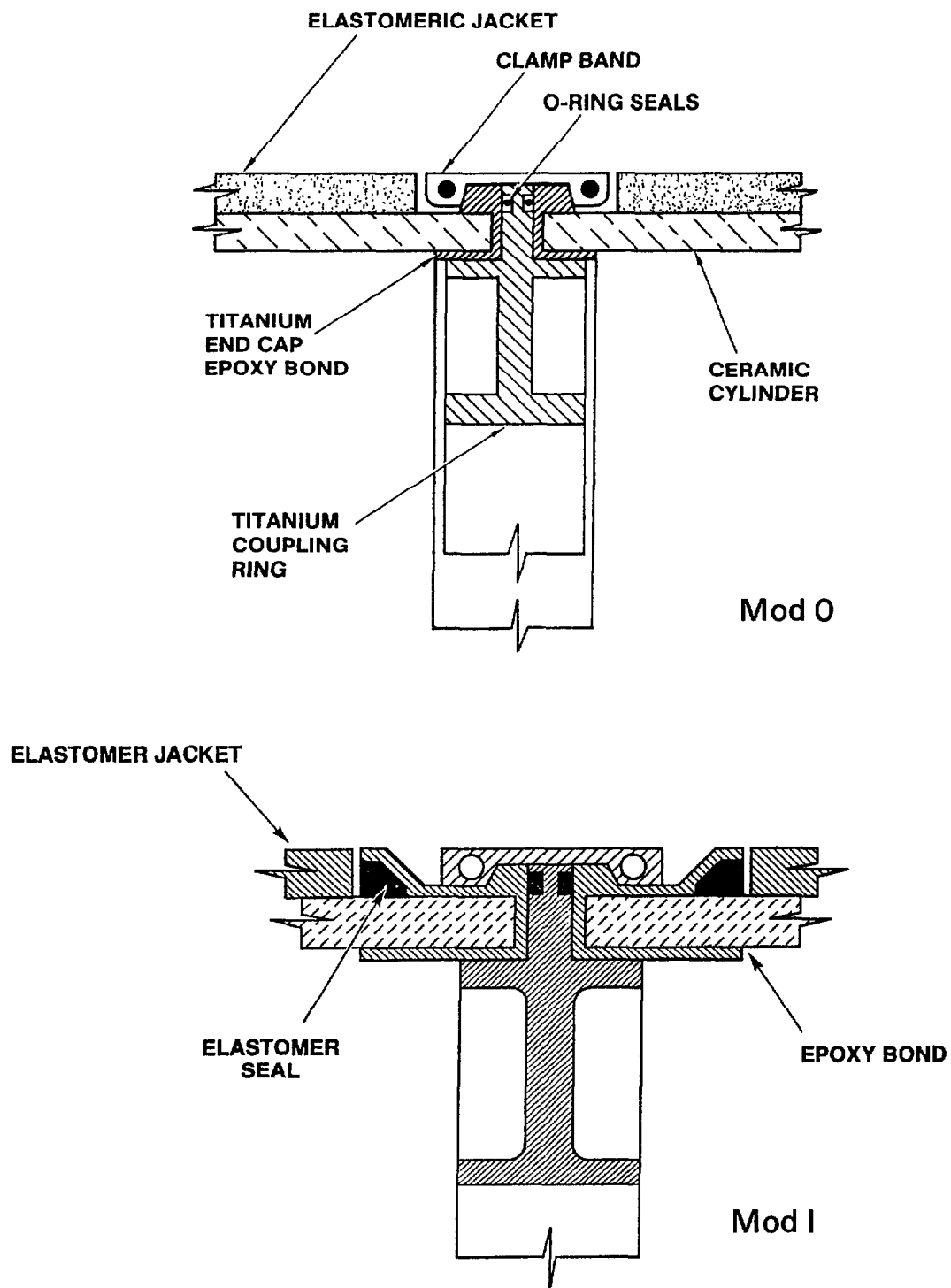
Figure 100. Comparison of Mod 0 and Mod I joint designs for ceramic cylinders. Note the deeper seat cavity and presence of elastomeric seal on Mod I end caps.

119

Figure 101. Fabrication drawing of Mod I end cap design for 20-inch-diameter ceramic cylinder. The use of Mod I end cap requires the use of a redesigned wedge clamp band because its outside diameter is 0.5 inch larger than of Mod 0 end cap.

120
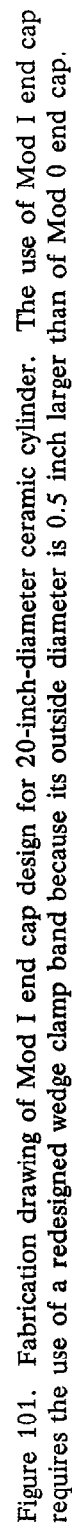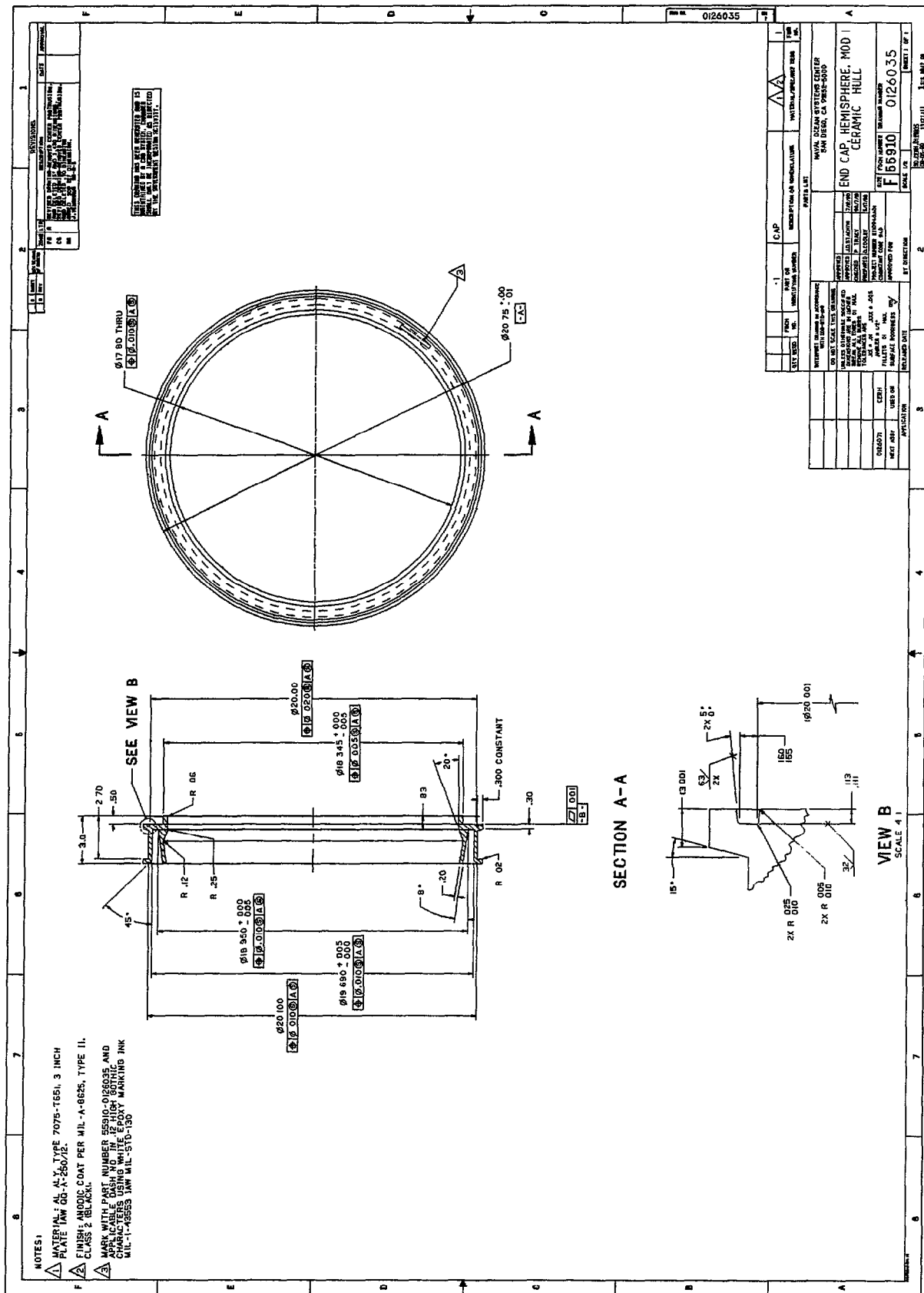
Figure 102. Fabrication drawing of Mod I end cap design for 20-inch-diameter ceramic hemisphere. The use of Mod I end cap requires the use of a redesigned wedge clamp band also.

121
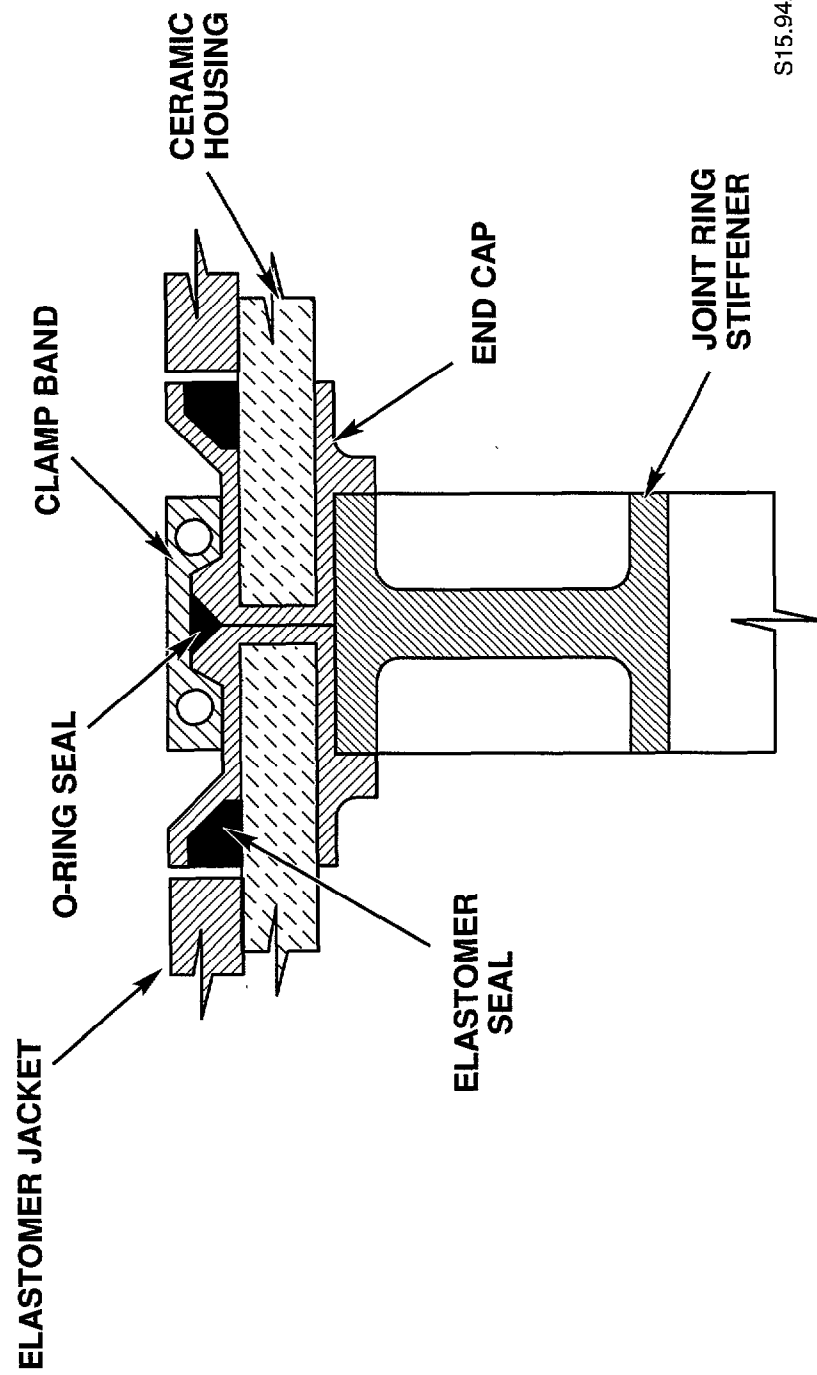
Figure 103. Conceptual design of joint with internal (dry) ring stiffener incorporating the best features of Mod I end caps.

S15.94A

122

Table 1. Premium structural materials for deep submergence.

Material	Weight (lbs/in^3)	Compressive Strength (kpsi)	Strength / Weight	Safety Factor
Steel (HY80)	0.283	80	280	1.25
Steel (HY130)	0.283	130	460	1.25
Aluminum (7075-T6)	0.100	73	730	1.25
Titanium (6AL-4V)	0.160	125	780	1.25
Glass (Pyrex)	0.080	100	1250	2.00
Glass Composite	0.075	100	1330	2.00
Graphite Composite	0.057	100	1750	2.00
Beryllia Ceramic 96%	0.104	225	2160	2.00
Alumina Ceramic 94%	0.130	300	2310	2.00
Glass Ceramic (Pyroceram 9606)	0.093	350	3760	2.00
Boron Carbide Ceramic	0.090	500	5555	2.00

123

Table 2. Properties of alumina ceramics.

PROPERTIES*		UNITS	TEST	ALUMINA AD-85 Nom 85% Al₂O₃	AD-90 Nom 90% Al₂O₃	AD-94 Nom 94% Al₂O₃	AD-96 Nom 96% Al₂O₃	AD-99.5 Nom 99 5% Al₂O₃	AD-99.9% Nom 99 9% Al₂O₃
DENSITY		g/cc (#/cu in)	ASTM C20-83	3 41 (0 12)	3 60 (0 13)	3 70 (0 13)	3 72 (0 13)	3 89 (0 14)	3 96 (0.14)
SURFACE FINISH	AS-FIRED GROUND POLISHED	MICROMETRES (MICROINCHES) CLA	PROFILOMETER (0 75mm cutoff)	1 6 (63) 1 0 (39) 0 2 (8 0)	1 6 (63) 0 5 (20) 0 1 (3.9)	1 6 (63) 1 3 (51) 0 3 (12)	1.6 (63) 1 3 (51) 0 3 (12)	0 9 (35) 0 5 (20) 0 1 (3 9)	0 5 (20) 0.9 (35) <0 03 (<1)
CRYSTAL SIZE	RANGE AVERAGE	MICROMETRES (MICROINCHES)	THIN SECTION	2-12 (79-473) 6 (236)	2-10 (79-394) 4 (158)	2-25 (79-985) 12 (473)	2-20 (79-788) 11 (433)	5-50 (197-1970) 17 (670)	1-6 (39-236) 3 (118)
WATER ABSORPTION		%	ASTM C373-72	0	0	0	0	0	0
GAS PERM.		—	**	0	0	0	0	0	0
COLOR		—	—	WHITE	WHITE	WHITE	WHITE	IVORY	IVORY
FLEXURAL STRENGTH (MOR)	20°C	MPa (psi × 10³)	ASTM F417-78	317 (46)	338 (49)	352 (51)	358 (52)	379 (55)	552 (80)
ELASTIC MODULUS SHEAR MODULUS BULK MODULUS TRANS. SONIC VEL. POISSON'S RATIO	20°C	GPa (psi × 10⁶) GPa (psi × 10⁶) GPa (psi × 10⁶) m/sec (ft/sec) —	ASTM C848-78	221 (32) 96 (14) 138 (20) 8 2 (27) × 10³ 0 22	276 (40) 117 (17) 158 (23) 8 8 (29) × 10³ 0 22	296 (43) 117 (17) 165 (24) 8 9 (29) × 10³ 0 21	303 (44) 124 (18) 172 (25) 9 1 (30) × 10³ 0 21	372 (54) 152 (22) 228 (33) 9 8 (32) × 10³ 0 22	386 (56) 158 (23) 228 (33) 9 9 (32) × 10³ 0 22
STIFFNESS/WEIGHT	20°C	GPa/g/cc	—	65	77	80	81	96	97
COMPRESSIVE STRENGTH	20°C	MPa (kpsi)	ASTM C773-82	1930 (280)	2482 (360)	2103 (305)	2068 (300)	2620 (380)	3792 (550)
HARDNESS		GPa (kg/mm²)	—	9 (960)	10 (1058)	12 (1175)	11 (1088)	14 (1440)	15 (1551)
TENSILE STRENGTH	25° 1000°C	MPa (kpsi)	ACMA TEST #4	155 (22) — (—)	221 (32) 103 (15)	193 (28) 103 (15)	193 (28) 96 (14)	262 (38) — (—)	310 (45) 221 (32)
FRACTURE TOUGHNESS	K₁ᴄ	MPa·m½	NOTCHED BEAM TEST	3-4	3-4	3-4	3-4	3-4	3-4
THERMAL CONDUCTIVITY	20°C	W/m°K (Btu·in/ft²·h·°F)	ASTM C408-82	16 0 (111)	16 7 (116)	22 4 (155)	24 7 (172)	35 6 (247)	38.9 (270)
COEFFICIENT OF THERMAL EXPANSION	25-1000°C	10⁻⁶/°C (10⁻⁶/°F)	ASTM C372-81	7 2 (4 0)	8 1 (4 5)	8 2 (4 6)	8 2 (4 6)	8 0 (4 6)	8 0 (4.5)
SPECIFIC HEAT	100°C	J/kg·°K (cal/g·°C)	ASTM C351-82	920 (0 22)	920 (0 22)	880 (0 21)	880 (0 21)	880 (0 21)	880 (0.21)
THERMAL SHOCK RESISTANCE	ΔTc	°C (°F)	—	300 (570)	300 (570)	300 (570)	250 (480)	200 (392)	200 (392)
MAXIMUM USE TEMPERATURE		°C (°F)	No-load conds	1400 (2552)	1500 (2732)	1700 (3092)	1700 (3092)	1750 (3182)	1900 (3452)
DIELECTRIC STRENGTH	6 35mm 3 18mm 1 27mm SPEC 0 64mm THICK 0 25mm	ac-kv/mm (ac-volts/mil)	ASTM-D116-76	9 4 (240) 13 4 (340) 17 3 (440) 21 6 (550) 28 3 (720)	9 2 (235) 12 6 (320) 17 7 (450) 22 8 (580) 29 9 (760)	8 7 (220) 11 8 (300) 16 7 (425) 21 6 (550) 28 3 (720)	8 3 (210) 10 8 (275) 14 6 (370) 17 7 (450) 22.8 (580)	8 7 (220) 11.4 (290) 16 9 (430) 22 8 (580) 33 1 (840)	9.4 (240) 12 8 (325) 18 1 (460) 23 2 (590) 31.5 (800)
DIELECTRIC CONSTANT	1 kHz 1 MHz 1 GHz	25°C	ASTM D150-81 ASTM D2520-81	8 2 8 2 8 2	8 8 8 8 8 8	9 1 9 1 9 1	9 0 9 0 9.0	9 8 9 7 9 7	9 9 9.8 —
DISSIPATION FACTOR	1 kHz 1 MHz 1 GHz	25°C	ASTM D150-81 ASTM D2520-81	0 0014 0 0009 0 0014	0 0006 0 0004 0 0007	0 0007 0 0004 0 0010	0 0011 0 0001 0 0002	0 0002 0 0003 0.0002	0 0020 0.0002 —
LOSS INDEX	1 kHz 1 MHz 1 GHz	25°C	ASTM D150-81 ASTM D2520-81	0 011 0 007 0 010	0 005 0 004 0 005	0 007 0 004 0.009	0 010 0 001 0.002	0 002 0 003 0 002	0.020 0 002 —
VOLUME RESISTIVITY	25°C 300°C 500°C 700°C 1000°C	ohm-cm²/cm	ASTM D1829-66	>10¹⁴ 4 6 × 10¹⁰ 4 0 × 10⁸ 7 0 × 10⁶ —	>10¹⁴ 1 4 × 10¹¹ 2 8 × 10⁸ 7 0 × 10⁶ 8 6 × 10⁵	>10¹⁴ 1 2 × 10¹¹ 4 8 × 10⁸ 2.1 × 10⁷ 5 0 × 10⁵	>10¹⁴ 3 1 × 10¹¹ 4 0 × 10⁹ 1 0 × 10⁸ 1.0 × 10⁶	>10¹⁴ — — — —	>10¹⁴ >10¹⁴ 3 3 × 10¹² 9 0 × 10⁹ 1 1 × 10⁷
Te VALUE		°C(°F)	TEMP AT WHICH RESISTIVITY IS 1 MEGOHM-CM	850 (1562)	960 (1760)	950 (1742)	1000 (1832)	—	1170 (2138)
CORROSION RESISTANCE	WEIGHT LOSS	mg/cm²/day	95% H₂SO₄ @20°C–NOTE 3 95% H₂SO₄ @100°C–NOTE 3	0.04 1 0	0 03 0 5	— —	— —	0 01 0 1	0.01 0.1
IMPINGEMENT		—	NOTE 4	1 00	0 45	0 52	0 63	0 47	0 14
RUBBING		—	NOTE 4	1 00	0 36	—	0.75	—	0 55

(COORS CERAMICS BULLETIN #980)

Table 3. Weights of components for 20-inch-diameter housing.

NAME	MATERIAL	DWG NO.	WT.	
Cylinder	Alumina	0121758	160	lbs.
Hemisphere Mod III	Alumina	0121705	26	lbs.
Hemisphere Mod II	Alumina	0121954	29	lbs.
End Cap, Cylinder (Set of 2)	Titanium	0121967	9.0	lbs.
End Cap, Hemisphere	Titanium	0121968	9.0	lbs.
Penetrator	Titanium	0121963	1.9	lbs.
Ring Stiffener	Titanium	0124009	29	lbs.
Rail (Set of 8)	Aluminum	0121961	4.5	lbs.
Mounting Plates	Aluminum	0121974	7.5	lbs.
Wedge Clamp	Titanium	0121966	4.5	lbs.
Jacket, Cylinder	Polyrethane	0121965	25	lbs.
Jacket, Hemisphere	Neoprene	———	9	lbs.

NOTES: 1. Weight/Displacement of the components.

    a. Bare Cylinder_____0.46

    b. Bare Cylinder with end caps_____0.48

    c. Bare Cylinder with end caps and internal rails_____0.50

    d. Jacketed Cylinder with end caps & rails_____0.52

    e. Bare Hemisphere Mod III_____0.35

    f. Bare Hemisphere Mod III with end cap_____0.48

    g. Bare Hemisphere Mod III with end cap and penetrator____0.50

    h. Jacketed Hemisphere with end cap and penetrator_____0.56

    i. Test Assembly (two hemispheres, cylinder,_____0.57
        jackets, penetrators, clamps, rails and plates)

Table 4. Strains on ceramic cylinder supported on both ends by ceramic hemispheres.

PRESSURE (PSIG)	GAGE LOCATIONS																	
	1		2		3		4		5		6		7		8		9	
	HOOP	AXIAL	HOOP	AXIAL	HOOP	AXIAL	HOOP	AXIAL	HOOP	AXIAL	HOOP	AXIAL	HOOP	AXIAL	HOOP	AXIAL	HOOP	AXIAL
0	-11	0	0	0	0	0	11	-11	0	0	0	0	0	0	11	0	-11	-11
994	-215	-43	-251	-22	-314	-43	-302	-87	-282	-65	-303	-65	-251	-33	-240	-22	-316	-87
1994	-506	-129	-545	-108	-607	-129	-625	-162	-585	-153	-607	-153	-545	-120	-534	-120	-610	-173
2993	-797	-225	-850	-194	-888	-214	-905	-303	-877	-261	-899	-251	-828	-207	-817	-196	-893	-282
3993	-1099	-279	-1133	-280	-1192	-300	-1217	-379	-1170	-359	-1213	-359	-1122	-283	-1111	-294	-1198	-379
4992	-1390	-364	-1449	-356	-1473	-396	-1519	-487	-1452	-447	-1506	-447	-1405	-359	-1373	-370	-1492	-477
5986	-1670	-439	-1721	-442	-1766	-471	-1821	-563	-1755	-545	-1809	-523	-1699	-436	-1667	-468	-1786	-574
6986	-1950	-493	-2004	-506	-2037	-546	-2112	-682	-2047	-632	-2112	-621	-1983	-512	-1928	-556	-2070	-661
7985	-2252	-579	-2298	-571	-2329	-654	-2402	-769	-2329	-730	-2416	-708	-2266	-588	-2222	-643	-2364	-737
8985	-2532	-643	-2571	-646	-2611	-718	-2704	-856	-2622	-828	-2708	-795	-2549	-664	-2495	-730	-2647	-823
9989	-2812	-707	-2854	-722	-2903	-814	-2973	-953	-2903	-937	-3012	-893	-2832	-741	-2778	-828	-2941	-899
9984	-2812	-696	-2865	-711	-2903	-814	-2995	-964	-2882	-915	-2990	-861	-2810	-708	-2756	-795	-2941	-856
0	22	21	22	11	0	21	22	0	87	87	65	76	76	87	76	87	-22	11

126

Table 5. Strains on ceramic hemisphere Mod 3.

STRAINS ON CERAMIC HEMISPHERE MOD 3

PRESSURE	1		2		3		4		5	
(PSIG)	HOOP	AXIAL	HOOP	AXIAL	HOOP	AXIAL	HOOP	AXIAL	HOOP	AXIAL
0	-11	0	0	11	-11	-11	11	11	0	0
1005	-225	-312	-269	-246	-259	-291	-291	-172	-229	-196
2000	-439	-463	-517	-514	-539	-560	-593	-345	-458	-403
2995	-675	-786	-786	-750	-797	-830	-883	-506	-675	-610
3995	-900	-1077	-1045	-996	-1045	-1099	-1164	-679	-893	-817
5000	-1136	-1379	-1304	-1243	-1314	-1357	-1454	-830	-1100	-1046
5995	-1393	-1573	-1573	-1500	-1562	-1627	-1745	-991	-1285	-1275
6995	-1639	-1864	-1832	-1736	-1832	-1907	-2036	-1142	-1481	-1525
7995	-1875	-2165	-2079	-1982	-2090	-2165	-2327	-1304	-1688	-1754
8995	-2111	-2478	-2338	-2218	-2349	-2446	-2618	-1444	-1885	-1993
9995	-2336	-2790	-2596	-2464	-2586	-2715	-2920	-1594	-2070	-2233
9995	-2336	-2790	-2596	-2475	-2596	-2726	-2920	-1594	-2070	-2233
0	11	0	0	11	0	-11	0	11	11	0

Table 6. Strains on ceramic hemisphere Mod 2.

STRAINS ON CERAMIC HEMISPHERE MOD 2

PRESSURE.					GAGE LOCATIONS					
(PSIG.)	1		2		3		4		5	
0	22	0	11	−11	0	0	−11	0	0	11
1005	−260	−416	−197	−220	−175	−198	−178	−266	−312	−299
2000	−509	−712	−361	−474	−351	−397	−368	−532	−613	−587
2995	−780	−833	−548	−716	−515	−584	−535	−787	−925	−886
3995	−1040	−1074	−701	−947	−668	−771	−713	−1052	−1225	−1196
5000	−1289	−1358	−876	−1179	−822	−969	−869	−1296	−1526	−1496
5995	−1538	−1643	−1041	−1421	−964	−1157	−1036	−1573	−1827	−1795
6995	−1842	−1786	−1205	−1663	−1117	−1355	−1192	−1817	−2128	−2094
7995	−2091	−2070	−1369	−1906	−1260	−1542	−1359	−2083	−2440	−2404
8995	−2351	−2366	−1545	−2159	−1413	−1740	−1515	−2349	−2741	−2714
9995	−2589	−2870	−1709	−2379	−1555	−1950	−1660	−2625	−3053	−3013
9995	−2611	−2837	−1709	−2379	−1566	−1939	−1660	−2603	−3041	−3002
0	0	11	−11	11	0	0	−11	−11	−11	0

Table 7. Strains on titanium stiffener between two ceramic cylinders.

PRESSURE (PSIG)	1		2		3		4		5		6		7		8		9		10	
	HOOP	AXIAL	AXIAL	HOOP	AXIAL	HOOP	AXIAL	HOOP	AXIAL	HOOP	AXIAL	HOOP	AXIAL	HOOP	AXIAL	HOOP	AXIAL	HOOP	AXIAL	HOOP
0	-22	-11	11	11	22	-11	0	-11	0	11	11	0	11	0	11	0	0	0	0	0
994	-269	194	227	-288	119	-131	65	-162	55	-110	22	-54	65	-120	77	-109	88	-197	-11	-186
1999	-517	388	444	-554	336	-381	130	-336	131	-296	99	-218	163	-296	153	-261	164	-340	-44	-383
2993	-786	636	661	-842	542	-621	195	-509	219	-460	175	-381	261	-471	230	-414	230	-515	-77	-613
3998	-1077	851	867	-1097	737	-871	260	-682	296	-657	252	-556	349	-646	340	-556	329	-679	-77	-811
4997	-1304	1056	1094	-1385	921	-1122	314	-856	340	-865	329	-730	458	-822	427	-697	405	-843	-110	-1019
5991	-1584	1271	1289	-1573	1148	-1373	336	-1018	438	-1041	394	-904	534	-986	504	-839	493	-1008	-142	-1238
6991	-1842	1519	1495	-1883	1332	-1623	347	-1105	—	—	482	-1078	588	-1161	570	-991	570	-1183	-197	-1435
7990	-2112	1691	1690	-2116	1549	-1917	—	—	—	—	515	-1275	—	—	646	-1122	570	-1369	-241	-1643
8495	-2252	1799	1777	-2182	1679	-2037	—	—	—	—	504	-1362	—	—	701	-1187	548	-1490	-252	-1764
8990	—	—	1874	-2360	1733	-2168	—	—	—	—	493	-1438	—	—	690	-1275	526	-1588	-274	-1840
9192	—	—	1907	-2404	1777	-2222	—	—	—	—	471	-1471	—	—	657	-1307	504	-1632	-263	-1895
9394	—	—	1928	-2448	1809	-2288	—	—	—	—	460	-1492	—	—	646	-1340	493	-1676	-274	-1939
0	-11	11	0	0	32	0	-11	11	44	88	55	54	54	44	22	54	-11	0	-33	0

GAGE LOCATIONS

Table 8. Principal stresses on ceramic cylinder supported by ceramic hemispheres.

GAGE LOCATIONS

PRESSURE (PSIG)	1 HOOP	1 AXIAL	2 HOOP	2 AXIAL	3 HOOP	3 AXIAL	4 HOOP	4 AXIAL	5 HOOP	5 AXIAL	6 HOOP	6 AXIAL	7 HOOP	7 AXIAL	8 HOOP	8 AXIAL	9 HOOP	9 AXIAL
0	-472	-99	0	0	0	0	373	-373	0	0	0	0	0	0	472	99	-571	-571
994	-9609	-3781	-10964	-3204	-13855	-4673	-13737	-6452	-12681	-5328	-13582	-5517	-11063	-3676	-10492	-3105	-14337	-6578
1994	-22865	-10091	-24349	-9541	-27197	-11000	-28266	-12578	-26470	-11832	-27413	-12030	-24457	-10056	-23985	-9957	-27722	-12915
2993	-36211	-16829	-38205	-15977	-40015	-17177	-41546	-21148	-39967	-19094	-40820	-18863	-37379	-16337	-36808	-15766	-40842	-20139
3993	-49651	-21866	-51118	-22215	-53829	-23604	-55613	-27218	-53417	-25936	-55261	-26324	-50673	-22244	-50301	-22617	-54798	-27047
4992	-62898	-28133	-65356	-28321	-66746	-30253	-69539	-34570	-66305	-32251	-68621	-32737	-63496	-28053	-62223	-28237	-68291	-33898
5986	-75583	-33871	-77797	-34459	-79989	-36109	-83177	-40550	-80184	-39184	-82302	-38726	-76800	-34004	-75716	-35088	-81774	-40707
6986	-88079	-38710	-90512	-39754	-92288	-41766	-96730	-48275	-93491	-45545	-96180	-45659	-89666	-39822	-87703	-41214	-94739	-46996
7985	-101807	-45118	-103708	-45190	-105785	-49029	-109952	-54619	-106470	-52289	-110003	-52129	-102488	-45631	-101097	-47593	-1E+05	-52904
8985	-114393	-50386	-116093	-50865	-118457	-54314	-123689	-61071	-119920	-59131	-123311	-58490	-115311	-51439	-113590	-53784	-1E+05	-59142
9989	-126979	-55653	-128916	-56674	-131846	-61062	-136100	-67654	-132954	-66337	-137233	-65432	-128143	-57291	-126611	-60536	-1E+05	-65050
9984	-126880	-55181	-129288	-56302	-131846	-61062	-137143	-68324	-131855	-65205	-136001	-63861	-126902	-55677	-125370	-58923	-1E+05	-63205
0	1068	1064	986	629	185	879	883	186	4304	4319	3321	3636	3877	4230	3877	4230	-800	257

Table 9. Principal stresses on ceramic hemisphere Mod 3.

GAGE LOCATIONS

PRESSURE (PSIG)	1 HOOP	AXIAL	2 HOOP	AXIAL	3 HOOP	AXIAL	4 HOOP	AXIAL	5 HOOP	AXIAL
0	-472	-99	99	472	-571	-571	571	571	0	0
1005	-12461	-15409	-13754	-12974	-13730	-14814	-14031	-9998	-11588	-10469
2000	-23000	-23813	-26805	-26703	-28163	-28874	-28542	-20139	-23274	-21411
2995	-36031	-39793	-40468	-39248	-41661	-42779	-42431	-29656	-34446	-32244
3995	-48303	-54301	-53793	-52132	-54721	-56550	-56042	-39608	-45661	-43086
5000	-61146	-69380	-67127	-65060	-68582	-70039	-69840	-48696	-56602	-54772
5995	-73916	-80015	-80979	-78506	-81651	-83854	-83772	-58223	-66600	-66261
6995	-87089	-94713	-94214	-90961	-95754	-98295	-97613	-67321	-77258	-78749
7995	-99922	-109749	-107024	-103737	-109144	-111685	-111554	-76890	-88200	-90436
8995	-112864	-125299	-120258	-116192	-122784	-126071	-125296	-85516	-98802	-102461
9995	-125325	-140708	-133540	-129067	-135372	-139743	-139601	-94670	-108899	-114422
9995	-125325	-140708	-133639	-129539	-135900	-140305	-139601	-94670	-108899	-114422
0	472	99	99	472	-99	-472	99	472	472	99

Table 10. Principal stresses on ceramic hemisphere Mod 2.

PRESSURE	GAGE LOCATIONS									
	1		2		3		4		5	
(PSIG)	HOOP	AXIAL	HOOP	AXIAL	HOOP	AXIAL	HOOP	AXIAL	HOOP	AXIAL
0	944	198	373	-373	0	0	-472	-99	99	472
1005	-14899	-20185	-10431	-11211	-9289	-10069	-10031	-13012	-16075	-15635
2000	-28245	-35123	-19753	-23582	-18631	-20189	-20576	-26133	-31580	-30699
2995	-40958	-42754	-29954	-35646	-27349	-29687	-30036	-38574	-47655	-46334
3995	-54281	-55433	-38597	-46932	-35596	-39086	-40057	-51544	-63315	-62332
5000	-67519	-69857	-48192	-58459	-43985	-48966	-48946	-63415	-78927	-77911
5995	-80766	-84324	-57449	-70325	-51769	-58308	-58604	-76800	-94531	-93446
6995	-95093	-93196	-66663	-82182	-60115	-68179	-67493	-88670	-110134	-108982
7995	-108331	-107620	-75886	-94082	-67932	-77488	-77052	-101584	-126309	-125089
8995	-122149	-122657	-85714	-106519	-76278	-87358	-86139	-114398	-142011	-141096
9995	-136897	-146418	-94730	-117432	-84260	-97645	-94844	-127542	-158087	-156731
9995	-137543	-145201	-94730	-117432	-84633	-97272	-94646	-126599	-157473	-156151
0	99	472	-373	373	0	0	-571	-571	-472	-99

Table 11. Principal stresses on titanium stiffener between two ceramic cylinders.

GAGE LOCATIONS

PRESSURE (PSIG)	1		2		3		4		5		6		7		8		9		10	
	HOOP	AXIAL	HOOP	AXIAL	HOOP	AXIAL	HOOP	AXIAL	HOOP	AXIAL	HOOP	AXIAL	HOOP	AXIAL	HOOP	AXIAL	HOOP	AXIAL	HOOP	AXIAL
0	-480	-345	275	275	140	410	-205	-70	205	70	70	205	70	205	70	205	0	0	0	0
994	-3788	1913	-3933	2408	-1689	1389	-2610	185	-1703	328	-868	68	-1826	451	-1545	745	-3117	392	-3540	-1385
1999	-7184	3959	-7519	4769	-4977	3852	-5444	294	-4691	566	-3439	464	-4488	1163	-3899	1199	-5303	903	-7425	-3250
2993	-10630	6880	-11516	6991	-8148	6173	-8259	409	-7193	1168	-5998	848	-7132	1882	-6265	1665	-8149	1024	-11925	-5325
3998	-14695	9045	-14967	9217	-11575	8225	-11075	525	-10380	1355	-8775	1175	-9838	2413	-8216	2816	-10581	1831	-15619	-6581
4997	-17630	11430	-18900	11625	-15091	10066	-13978	428	-13981	856	-11532	1507	-12431	3331	-10295	3545	-13159	2209	-19709	-8516
5991	-21490	13665	-21171	14071	-18334	12709	-16861	-189	-16643	1568	-14366	1616	-15008	3708	-12456	4081	-15679	2804	-23998	-10502
6991	-24730	16655	-25647	15947	-21831	14556	-18415	-535	-	-	-17054	2154	-17931	3606	-14873	4348	-18455	3130	-28022	-12778
7990	-28676	18151	-28757	18107	-25939	16739	-	-	-	-	-20521	1521	-	-	-16835	4935	-21925	1950	-32182	-14918
8495	-30603	19278	-29437	19312	-27353	18403	-	-	-	-	-22213	763	-	-	-17699	5549	-24322	772	-34509	-15891
8990	-	-	-32143	19993	-29455	18580	-	-	-	-	-23701	76	-	-	-19410	4785	-26290	-260	-36066	-16784
9192	-	-	-32754	20329	-30183	19058	-	-	-	-	-24456	-544	-	-	-20217	3967	-27251	-949	-37023	-16927
9394	-	-	-33442	20442	-31212	19237	-	-	-	-	-24918	-882	-	-	-20902	3552	-28141	-1434	-37913	-17412
0	-135	135	205	70	203	597	135	-135	1921	1379	1356	1369	1163	1287	1147	753	-70	-205	-209	-616

133

APPENDIX A

HANDLING FIXTURES FOR CERAMIC HOUSING COMPONENTS

INTRODUCTION

Because of the brittle nature of alumina ceramic and the weight of ceramic components that exceed the ability of technicians to manhandle them during assembly and shop operations, a set of fixtures had to be developed that would facilitate handling the ceramic housing components by overhead hoists. Two fixtures were developed for this purpose: one for handling individual ceramic cylinders during bonding of the end caps, and another for handling during pressure testing of complete housings assembled from one or more cylinders and hemispherical end closures.

TEST FIXTURE DESIGN

Lifting Tongs

The function of the lifting tongs (figures A-1 and A-2) was to (1) grasp securely the ceramic cylinder reclining inside a shipping box in a horizontal position, (2) raise it aboveground with an overhead hoist, (3) rotate the cylinder into a vertical position, and (4) lower it vertically into a metallic end cap filled beforehand with epoxy resin. After curing of the epoxy adhesive, the elastomeric jacket would be slipped over the cylinder and the jacketed cylinder would be grasped again with the tongs, hoisted from the ground, rotated end for end, and lowered again into an end cap filled with epoxy resin. After curing of the resin in the second end cap, the cylinder assembly would be grasped again by the tongs, hoisted above ground, rotated into horizontal position, and deposited into a wooden cradle prepared for this purpose.

Lifting Cage

The function of the lifting cage (figures A-3 through A-7) was to (1) grasp securely a housing assembly lying in a horizontal position on a cradle or a pad on the floor, (2) lift it with an overhead crane to the pressure vessel site, and (3) lower it into the pressure vessel after changing the cage's orientation from horizontal to vertical. After pressure testing, the procedure was reversed to raise the housing assembly from the pressure vessel and to transport it with the overhead crane to the shop area where the housing was disassembled.

The grasping of the ceramic cylinder was accomplished with two pneumatic actuators shaped like hoses woven from neoprene impregnated fabric. These hose-like actuators were placed inside the channels on both sides of the upper cage half along its full length. These hoses expanded upon application of internal pressure, causing them to exert uniform pressure against the cylindrical sections of the housing just below their central axis. This later pressure against the lower half of the cylindrical housing generated an upward force, which pushed the housing upward until it securely rested against the roof of the cage.

The pneumatic actuators (Merriman Windjammer Part No. 424-280) are rated for 100-psi internal pressure, but in the lifting cage application the maximum operational pressure was kept below 20 psi to prevent permanent deformation of the cage. To prevent accidental release of the housing assembly due to loss of air pressure during lifting of the upper cradle half, a manual shutoff valve was incorporated into the air supply line. By closing off the air supply line after the actuators have been pressurized, the pressure inside the actuators could be retained, even in case of accidental rupture of pressurized air supply hose.

As an additional safety measure, the ceramic housing test assembly was prevented from accidental release by mechanically fastening the lower cage half to the upper half; now the housing assembly was enclosed on all side by the cage framework that kept it from being released inside the pressure vessel after the hydrostatic pressure inside the vessel collapsed the pneumatic actuators during pressure testing.

Figure A-1. Fabrication drawing of lifting fixture for ceramic cylinders; assembly.

LIFT,
CERAMIC CYLINDER

NAVAL OCEAN SYSTEMS CENTER
SAN DIEGO, CA 92152-5000
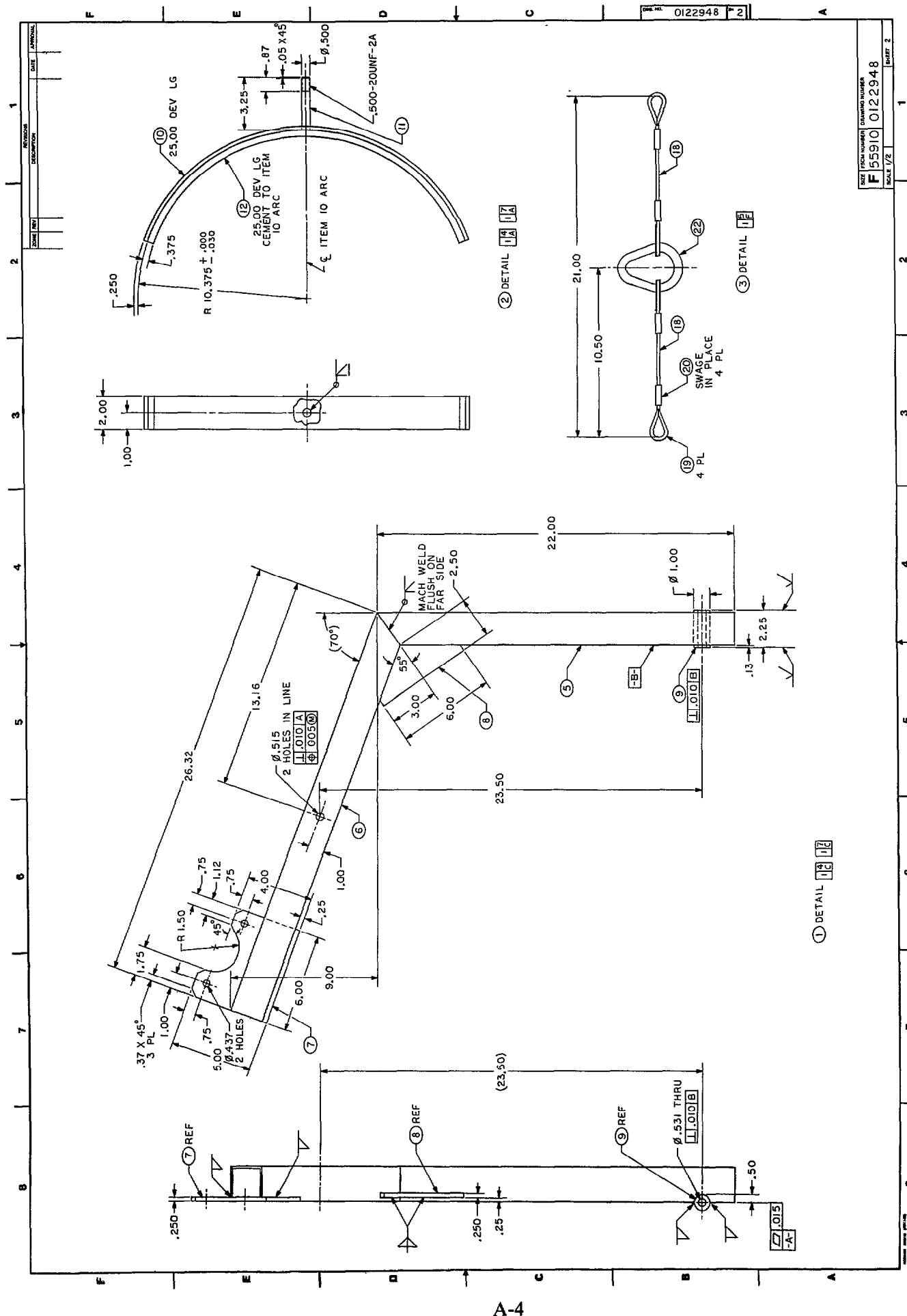
F | 55910 | 0122948

SCALE 1/2 | SHEET 1 OF 2

0122948

Figure A-2. Fabrication drawing of lifting fixture for ceramic cylinders; details.

A-4

Figure A-3. Fabrication drawing of lifting cage; assembly.

A-5
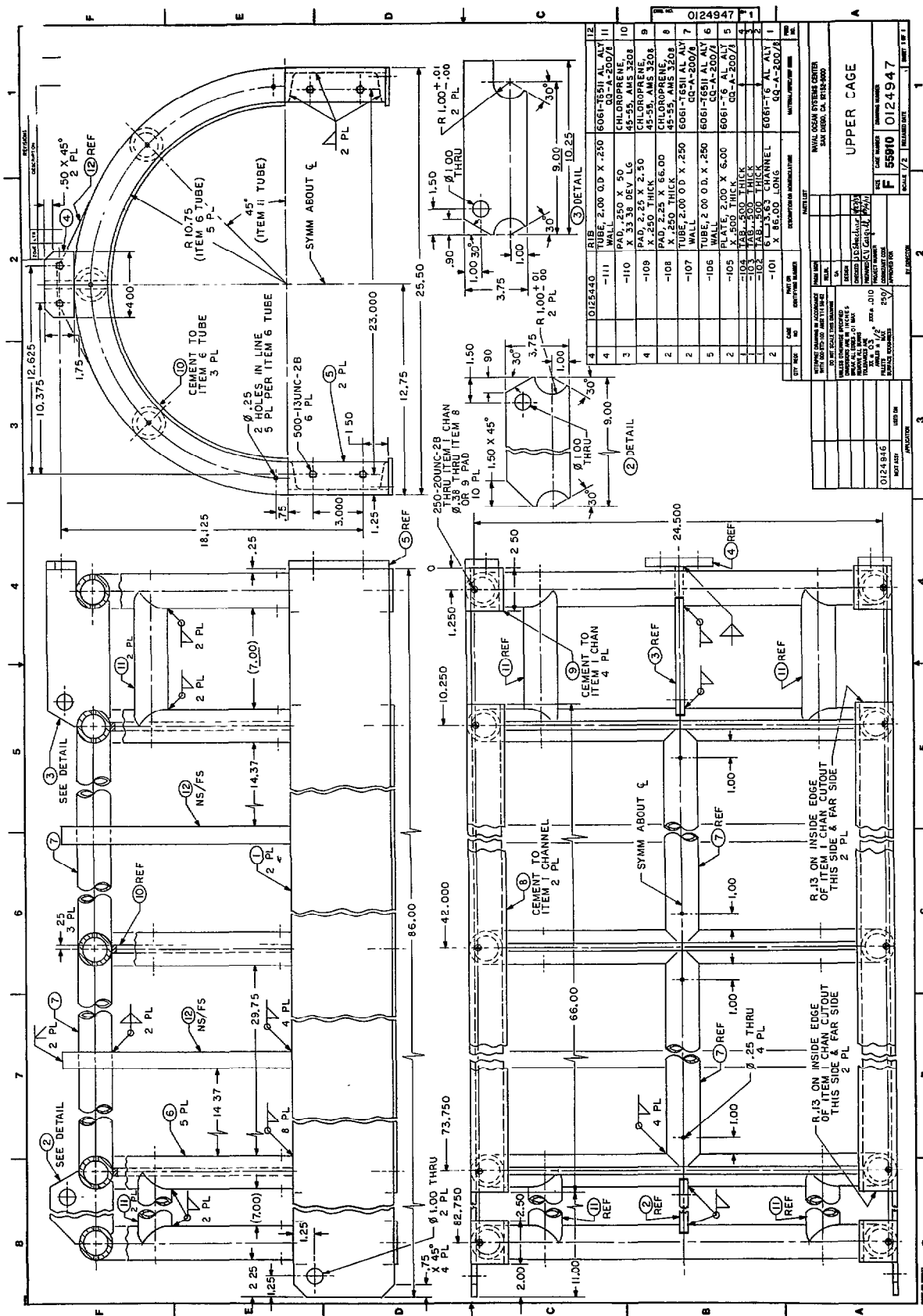
Figure A-4. Fabrication drawing of lifting cage; upper cage assembly.

A-6
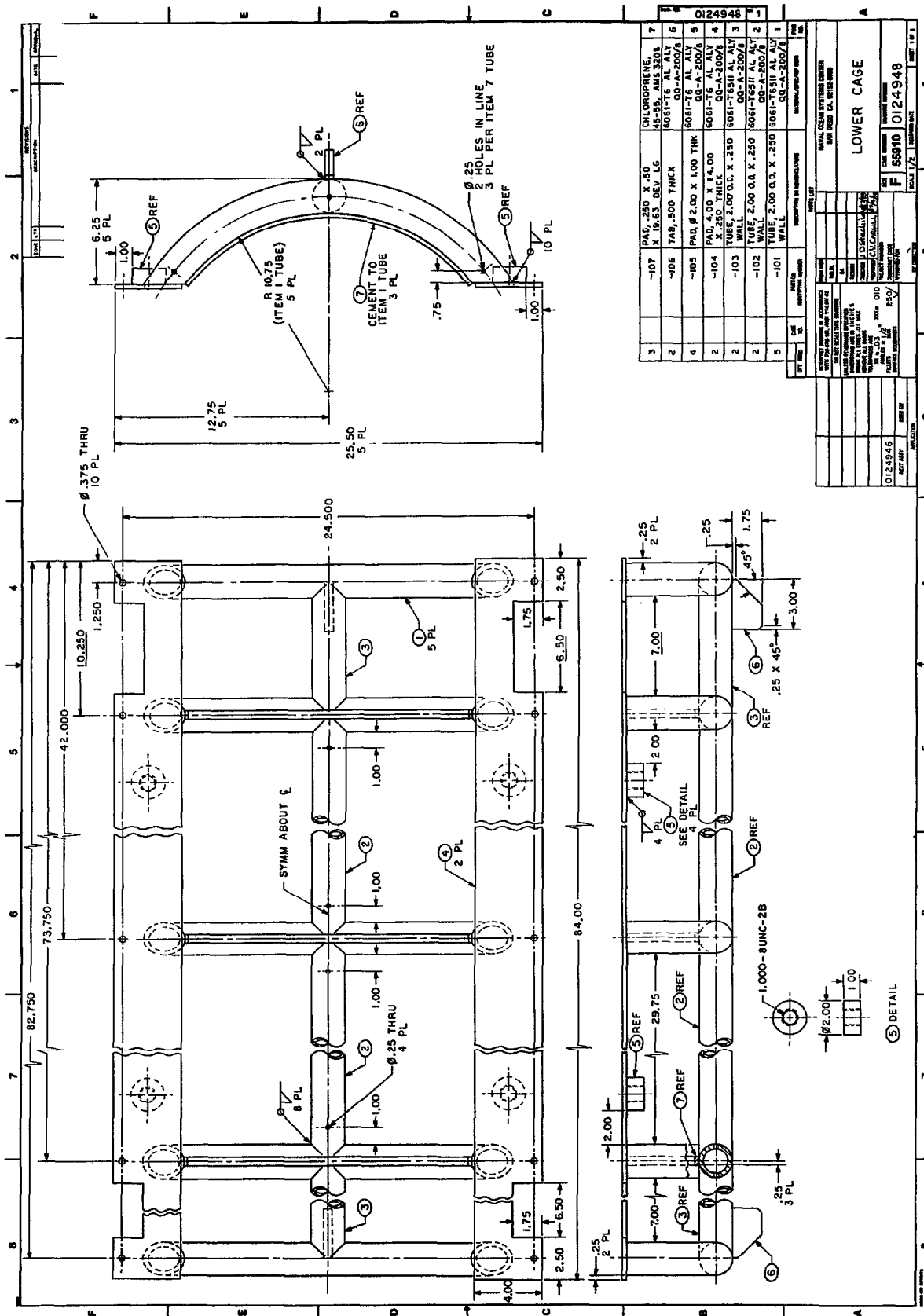
Figure A-5. Fabrication drawing of lifting cage; lower cage assembly.

A-7

NOTES:
1. MATL: 6061-T6 AL ALY
   IAW QQ-A-200/8.

1.00
STOCK

R 1.00 +.01 / -.00

1.00

.50

1.00

11.75

R 10.75

2.00
CONSTANT

DWG NO   SH

REVISIONS

ZONE | LTR | DESCRIPTION | DATE | APPROVAL

PARTS LIST

FIND NO

QTY | REQ | FSCM NO | PART NO IDENTIFYING NUMBER | DESCRIPTION OR NOMENCLATURE | MATERIAL/SPEC/REF DESG

DO NOT SCALE THIS DRAWING

UNLESS OTHERWISE SPECIFIED
DIMENSIONS ARE IN INCHES
BREAK ALL EDGES
REMOVE ALL BURRS MAX
TOLERANCES ARE
XX ±.03   XXX ±
ANGLES ± 1/2°
FILLETS 1/2 MAX
SURFACE ROUGHNESS 250/

INTERPRET DRAWING
IN ACCORDANCE WITH
DOD STD 100

APVD J.O. Stevens
CHKD J.D. Shotwell
PREP   9/9/27

PROJ NO
COG CODE
RLSE DATE

APPROVED FOR

BY DIRECTION

NAVAL OCEAN SYSTEMS CENTER
SAN DIEGO, CA 92152

RIB,
UPPER CAGE

SIZE | FSCM NUMBER | DRAWING NUMBER
C | 55910 | 0125440

SCALE 1/2 | UNIT WT | SHEET 1 OF 1

0124947

NEXT ASSY | USED ON

APPLICATION

☆U.S. GOVERNMENT PRINTING OFFICE
1984-784-428

NOSC-SD 3910/81(REV 12-83)

A-8
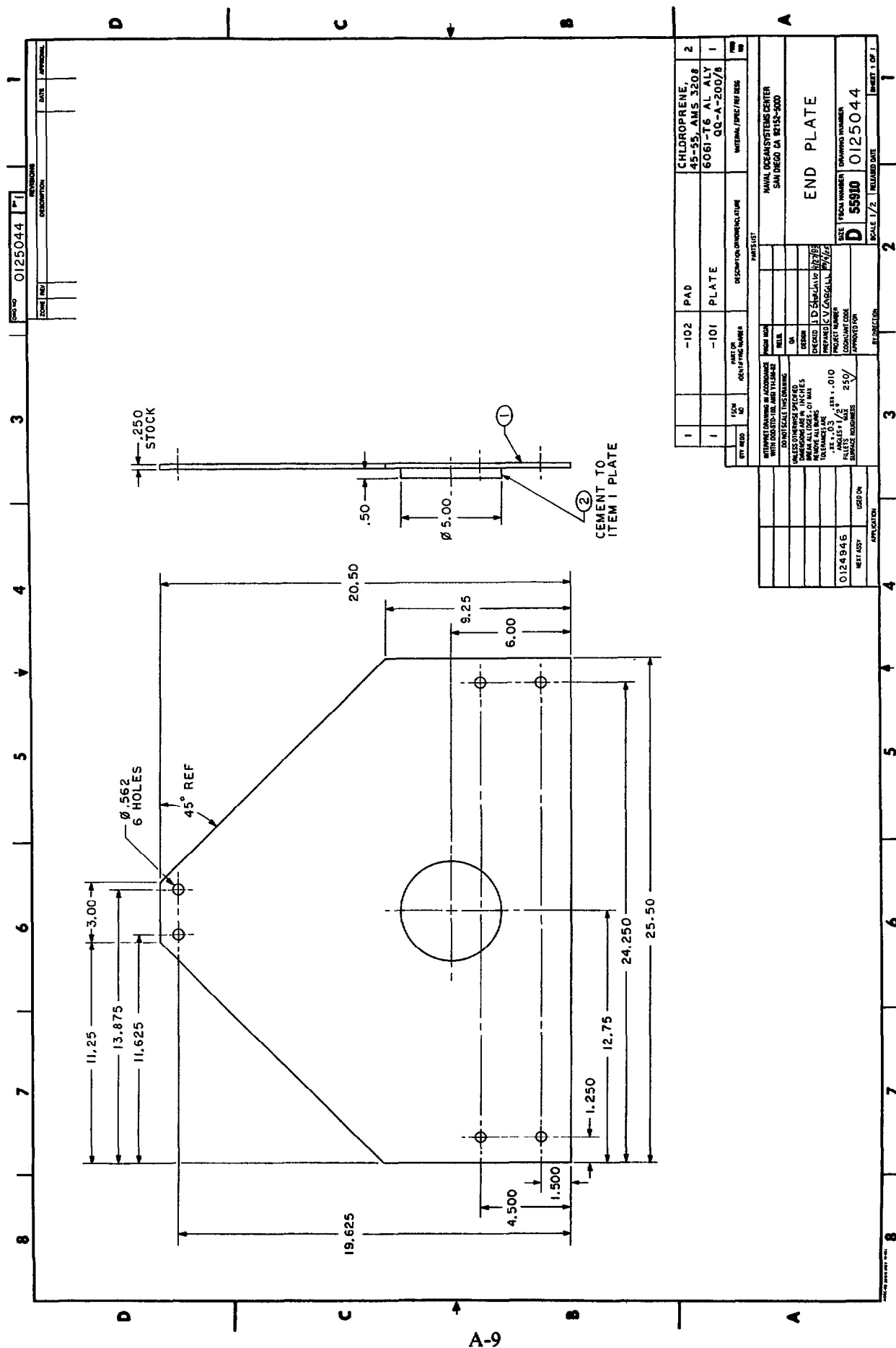
Figure A-7. Fabrication drawing of lifting cage; end plate detail.

.250
STOCK

CEMENT TO
ITEM 1 PLATE

.50

Ø 5.00

20.50
9.25
6.00

Ø .562
6 HOLES

45° REF

3.00
11.25
13.875
11.625

25.50
24.250
12.75

1.250
1.500
4.500
1.500

19.625

NAVAL OCEAN SYSTEMS CENTER
SAN DIEGO CA 92152-5000

END PLATE

SIZE D   FSCM NUMBER 55910   DRAWING NUMBER 0125044

SCALE 1/2   SHEET 1 OF 1

CHLOROPRENE,
45-55, AMS 3208

6061-T6 AL ALY
QQ-A-200/8

-102   PAD
-101   PLATE

0124946

0125044   REV 1

REVISIONS

APPENDIX B

IMPACT TESTING OF CERAMIC HOUSING

INTRODUCTION

Because of its perfectly elastic behavior and low tensile strength, alumina ceramic is very sensitive to point impacts. Point impacts that would generate local yielding in aluminum or titanium housings induce in alumina ceramic a family of cracks radiating from the point of impact. With increase in the thickness of ceramic shells comes increased resistance to fracture initiations by point impacts. Since the ceramic cylinders are twice as thick as ceramic hemispheres, their impact resistance is significantly higher, but still not high enough to withstand all the point impacts to which the housing may be subjected during assembly and subsequent handling during sea operations. For this reason, it is necessary to enclose the ceramic components of the housing with some protective cover that will decrease the effect of point impact.

There are basically two approaches to protect the ceramic shells from fractures initiated by point impacts. One approach relies on an elastomeric coating that not only absorbs some of the kinetic energy of the impacting body, but also distributes the pressure under the pointed object over a larger area. In this approach, the magnitude of tensile stresses in ceramic under the point of contact with an impacting object appears to vary inversely with the thickness of the elastomeric coating.

The other approach to reducing the effect of point impact on ceramic shells relies on a stiff, over-sized enclosure separated from the ceramic shell by air space and supported only by metallic components of the housing. Thus, for example, in the case of cylindrical shells the cylindrical enclosure would be supported readily by metallic end caps providing it with a 0.375-inch standoff from the ceramic surface. In the case of a hemisphere, the enclosure would be supported by the equatorial end cap and penetration inserts at the penetrations. The preferable materials for such enclosures are plastic composites because of their low weight, elastic behavior, resistance to seawater, and low hardness. An outstanding choice for this application is plastic composite reinforced with SPECTRA 2000 polyethylene fibers or cloth, whose density approaches seawater (i.e., it does not contribute any weight to the housing when it is submerged in seawater).

The approach using rigid enclosures for protecting ceramic shells against point impacts was not applied to NOSC housings because of the high cost of such enclosures and the lack of operational requirement for such enclosures on housing serving only as laboratory test specimens. If the NOSC 20-inch-diameter ceramic housings are applied in the future to an operational deep submergence system, the elastomeric jackets should be replaced with the lighter, more impact-resistant plastic composite enclosures laminated from resin impregnated SPECTRA 2000 cloth.

SCOPE OF TEST PROGRAM

The testing program consisted of impact testing of an alumina ceramic cylinder with an 0.680-inch wall thickness covered with a protective elastomeric jacket of 0.375-inch thickness. The jacket was a seamless, snug fitting, cylindrical shell molded by Gallagher Corporation of Gurnee, Illinois, from a polyether urethane compound. The physical properties of the jacket material are shown below:

> Harness 65A
> 100% Modulus, 415 psi
> 300% Modulus, 795 psi
> Tensile Strength, 4200 psi
> Elongation at Break, 670%
> Tear Strength, Die C. 250 pli
> Tear Strength, D470, 55 pli
> Bashore Resilience, 55%
> Compression Set, 5%
> (Method B, 22 hrs. @ 158°

No testing was performed on 0.375-inch-thick segmented construction, neoprene jackets bonded to ceramic hemisphere, since there were no spare hemispheres that could be tested to destruction.

TEST ARRANGEMENT

The test arrangement consisted of a weight at the end of pendulum striking a cylinder held in place by a wooden cradle fastened to the base of the pendulum impactor. The kinetic energy of the impactor was varied by (1) raising the pendulum from 0 to 90 degrees elevation in 5-degree increments, and (2) increasing the weight of the striker from 2 to 24 pounds in three steps. The nose of the strikers was configured to a 1.0-inch spherical radius, so that regardless of the striker size the footprint of the hose upon the elastomeric jacket was always the same.

The cylinder was rotated 10 degrees after every impact to insure that any local tearing of the elastomeric jacket produced by prior impact would not decrease the impact protection afforded by the jacket for the next impact test.

TEST PROCEDURE

Phase 1—Cylinder with 1/4-inch-thick jacket.

    a. Impact with 2-pound striker from 5-, 10-, 15-, 20-, and 25-degree elevations.

    b. Impact with 12-pound striker from 5-, 10-, 15-, 20-, and 25-degree elevations.

Phase 2—Cylinder with 1/8-inch-thick elastomeric jacket.

    a. Impact with 2-pound striker from 5-, 10-, 15-, 20-, and 25-degree elevations.

    b. Impact with 12-pound striker from 5-, 10-, 15-, 20-, and 25-degree elevations.

Phase 3—Cylinder without jacket.

    a. Impact with 2-pound striker from 5-, 10-, 15-, 20-, and 25-degree elevations.

    b. Impact with 12-pound striker from 5-, 10-, 15-, 20-, and 25-degree elevations.

Phase 4—Cylinder with 3/8-inch thick jacket.

    a. Impact with 12-pound striker at 5-degree intervals from 0 to 90-degree elevations.

    b. Impact with 24-pound striker at 5-degree intervals from 0 to 90-degree elevations.

TEST OBSERVATION

1. The bare ceramic cylinder with 0.68-inch thickness withstands repeatedly point impacts with kinetic energies less than 67-pound inches.

2. The ceramic cylinder jacketed with 0.375-inch-thick polyurethane cover withstands repeatedly point impacts with kinetic energies less than 1000-pound-inches.

3. It requires a point impact with over 1180-pound-inch kinetic energy to fracture a 94-percent alumina ceramic cylinder with 0.68-inch wall thickness protected by 0.375-inch-thick polyurethane jacket.

4. The fracture of the jacketed cylinder appeared to have been originated by the tearing of the elastomeric jacket directly under the point of the 1310-pound-inch impact, which allowed the striker to contact the bare ceramic directly. The tearing apart of the elastomeric jacket was due to high tensile strains extending laterally from under the point of contact with the striker where very high compressive strains are generated during impact. It can be postulated that the tearing apart of the jacket was facilitated by the loose fit between the jacket and the ceramic cylinder, which permitted the elastomeric jacket to displace laterally, freely. Bonding of the elastomeric jacket to the ceramic surface would mechanically restrain the lateral displacement of the elastomer, thus increasing its resistance to tearing and the impact protection that it provides to the ceramic housing.

DISCUSSION

It appears that the 0.375-inch-thick polyurethane jacket is more than adequate to protect the ceramic housings from casual point impacts encountered during shop assembly and handling in a test facility environment. It is hard to imagine that during assembly and pressure testing the ceramic housing would encounter a point impact of over 100-pound-foot energy, equivalent to the kinetic energy of an 18-inch pipe wrench accidentally dropped from an overhead walkway upon the housing resting on the floor below.

CONCLUSION

Elastomeric coatings/jackets provide economically acceptable protection against point impacts that a ceramic housing may encounter during its assembly and handling in a machine shop environment.

Figure B-1 Impact tester with interchangeable strikers of different weights
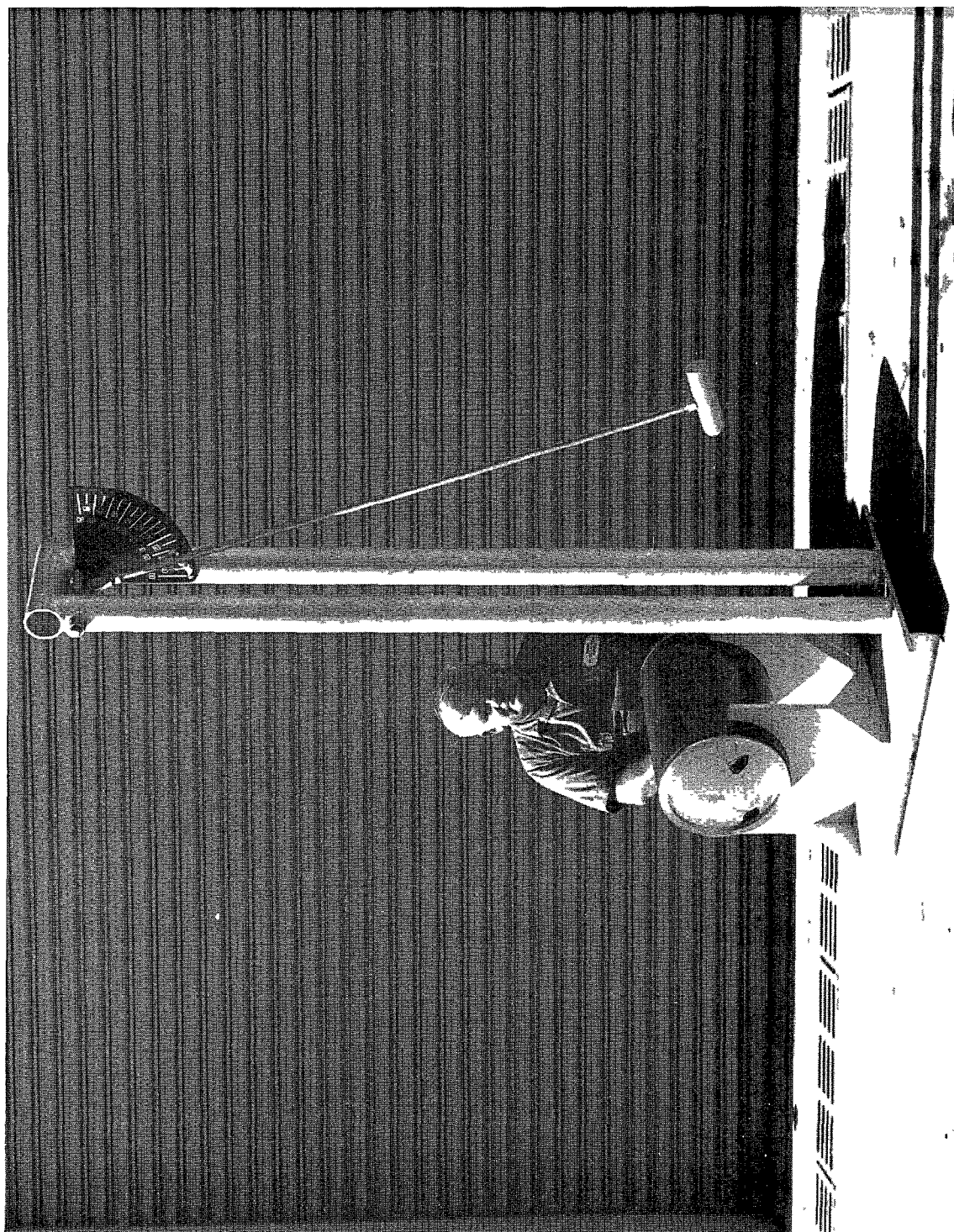
Figure B-2. Impact testing of ceramic cylinder with 12-pound striker

Figure B-3. Failed ceramic cylinder after impact testing.